DISPERSED AIR FLOTATION OF FINE PARTICLES

A Thesis submitted to the

University of London

for the degree of

DOCTOR OF PHILOSOPHY

by

GEORGE LEONARD COLLINS, B.Sc.

Department of Chemical Engineering and Chemical Technology,
Imperial College of Science and Technology,
London.

September, 1975

ABSTRACT

In this work the flotation of small polystyrene particles by small bubbles was investigated. The purpose of the investigation was to help obtain information on the physical variables which control the kinetics of the flotation of fine particles in effluent treatment cells.

Experimentally it was found that the rate of flotation was proportional to the 1.5 power of the particle size. This was for particles with diameters between 6 and 20 microns, floated by bubbles with diameters less than 100 microns. The double layer repulsion between particle and bubble was found to be an important rate-controlling variable. The rate constant, which was used as a measure of the rate of flotation, varied with the magnitude of the repulsion, in a similar way to the filter coefficient used by another investigator to characterise deep-bed filter efficiency. The two processes, flotation and filtration, appear to be analogous over the range of variables studied.

A theoretical investigation based on a model used in a filtration study was found useful for predicting the dependence of flotation rate on particle size. The theoretical work done by workers in the filtration field should be studied by workers interested in the flotation of fine particles by small bubbles.

ACKNOWLEDGEMENTS

I would like to express my thanks to:

Dr. G.J. Jameson for his guidance and encouragement during the last three years.

Dr. J.A. Kitchener for the invaluable discussions we had.

Dr. A.L. Halmos for his assistance during the theoretical part of this investigation.

CSR Limited of Sydney, Australia for their generous sponsorship.

TABLE OF CONTENTS PAGE

LIST OF FIGURES

LIST OF TABLES

CHAPTER 1

INTRODUCTION

In this chapter the field of flotation is introduced, then the general aims of the thesis are presented. Details of the organisation of the thesis are then given.

Lemlich (1966) coined the term "adsorptive bubble separation methods" for separation processes which depend on material being adsorbed on or attached to the surface of bubbles rising in a liquid. Minerals, colloid particles, ionic species, detergents etc. have been separated from liquid by this technique. Reviews by Lemlich (1972) and Somasundaran (1972) contain lists of substances that may be separated. When the substance to be separated is a solid, the process is commonly called "particulate flotation" or more simply "flotation".

In general, particles suspended in water, which is almost without exception the suspending medium, need to have naturally hydrophobic surfaces or to have their surfaces rendered hydrophobic by chemical means. Bubbles of gas are generated and as these rise they collide with the particles suspended in the water. Those particles which have hydrophobic surfaces have the chance to become attached to the bubbles and to rise with them to the surface. If a stable froth is present the particles will concentrate there.

Bubbles can be produced by dispersing air in the suspension of particles (often called the "pulp") and the process is called "dispersed air flotation" which is the method of bubble generation studied in this investigation. Bubbles can also be produced by saturating water with air under pressure and then releasing the pressure. This technique produces tiny bubbles which form on the hydrophobic surfaces of the particles. The same effect can be obtained by reducing the pressure above water. When air is forced out of solution to form bubbles, the process is called "dissolved air flotation". The interested reader can refer to Burman (1974) who has recently studied the growth of bubbles in supersaturated solutions, and Bratby and Marais's (1974) review of dissolved air flotation. The methods of bubble production in the two types of flotation are obviously different, but once a bubble is formed in a dissolved air process it will rise and collide with particles in the same way as a bubble in a dispersed air process.

The best known and most important use of dispersed air flotation is the benefaction of minerals in the mining industry (see Taggart (1945), Sutherland and Wark (1955), Klassen and Mokrousov (1963) and Lemlich (1972)). Mineral flotation owes its beginning in modern form to the brothers Bessell (Sutherland and Wark (1955)) who in 1877 patented a device to separate graphite from gangue (waste). This illustrates the aim of mineral flotation - to remove one mineral from suspension while leaving unwanted material in suspension.

Flotation has been used to clarify effluent in the paper industry since the 1920's. Barry (1951) discussed a flotation cell for clarifying industrial effluent. In the 1960's workers such as Grieves, Karger and Rubin, studied the clarification of water. Lemlich (1972) and Somasundaran (1972) review developments in this period. Grieves and Bewley (1972) designed a continuous flotation and activated carbon filtration plant to produce small quantities of potable water. Cassell et al. (1971) studied the flotation of colloidal pollutants using aluminium salts and anionic surfactants.

In the late 1960's Saint-Gobain (French Patent 2050310) patented a flotation plant using electrolysis-bred bubbles. Although the electrode processes in an electroflotation cell have no parallel in dispersed air flotation, the predominant particle capture mechanism away from the electrodes must be the same as in a conventional dispersed air cell. Kuhn (1974) reviews electroflotation and sees a good future for the process.

Richards (1975) has recently investigated the possibility of replacing the sedimentation process used to clarify water for public supply by a dissolved air flotation process. He points to one of the major advantages of flotation over sedimentation - speed of separation. In his experiments the settling of a typical coagulating hydrolysis product (aluminium hydroxide) varied between 0.0012 - 0.003 cm/sec.

A bubble of diameter 100 microns with coagulated material of more or less neutral density attached to it, will rise at about 0.5 cm/sec. Such a difference means that a flotation unit can be considerably smaller than the equivalent sedimentation plant. His results showed that dissolved air flotation was certainly a reasonable alternative to sedimentation.

Most of the work on effluent flotation has dealt with the chemical aspects of the process and very little work has been done on the physics of bubble/particle attachment. Workers in mineral flotation have paid some attention to bubble/particle attachment but their results may not be applicable to effluent flotation for the following reasons:

a) Particles in an effluent treatment plant are usually small (less than 20 microns in diameter) and approximately of neutral buoyancy. The particles in mineral flotation are usually much larger (of the order of 50 microns in diameter) and relatively dense, although small difficult to float particles called "slimes" are sometimes present in mineral flotation cells.

b) Effluent treatment cells are usually unstirred whereas mineral flotation cells are stirred vigorously to keep the larger particles in suspension.

c) The concentration of solids in an effluent treatment plant is usually much lower than in a mineral flotation plant, 20 - 1000 ppm against 25%.

d) The bubbles in effluent treatment plants are often less than 100 microns in diameter. The flow patterns around these bubbles can be calculated using Stokes approximation for spheres. Mineral flotation cells use comparatively large bubbles (500 - 2000 microns). Stokes approximation would certainly be in error for the flow around these bubbles.

If effluent flotation is to be useful commercially the physical variables that control the kinetics of the process must be well understood. The aim of this investigation is to contribute to this understanding.

The thesis is organised as follows. In Chapter 2 double layer forces, van der Waals forces and disjoining pressure are briefly discussed. Chapter 3 deals with the background to the work and surveys some of the previously reported results of significance, both theoretical and experimental. Then the specific aims of this investigation are presented. In Chapter 4 the experimental part of the work is discussed and the details of the apparatus and techniques are given. In Chapter 5 the experimental results are given. Chapter 6 presents a theoretical study of particle collection. Chapter 7 contains final discussion and conclusions.

CHAPTER 2

SURFACE FORCES IN FLOTATION

In this Chapter electrokinetic phenomena, double layer forces and van der Waals forces are briefly reviewed. The disjoining pressure concept of films is then explained. These surface chemistry ideas are necessary for an understanding of the work in this investigation.

2.1 Electrical forces

2.1.1 Electrokinetic phenomena and the double layer

By the end of the 19th century scientists had found that in general there were charges associated with the boundary between a liquid and a solid. These charges manifested themselves in four phenomena called electro-kinetic phenomena. Each of these phenomenon has in common, relative movement between the solid and the liquid and the presence of an electric field.

The four electrokinetic phenomena

	Solid moves	Liquid moves
Motion produced by an electric field	Electrophoresis	Electro-osmosis
Electric field produced by motion	Dorn effect (sedimenting potential)	Streaming potential

To explain electrokinetic phenomena it was obviously necessary to assume that there were charges at the solid /liquid interface. It was also assumed that because the bulk of the liquid was electrically neutral, these charges would be opposed by charges of the opposite sign in the liquid. This "double layer" of charges was proposed by Helmholtz. The charge of the solid was considered to be completely neutralised by a layer of charges in the solution.

Because of the thermal motion of molecules in a liquid at room temperature it is hard to accept such a rigid structure. Gouy and later Chapman considered the problem of finding the spatial distribution of counter-ions (neutralising charges) in the liquid, given that a charged surface is present. Their result in its exact form is quite complicated, but making the assumption that the charge is not too high (see Dukhin and Derjaguin (1974) for details) the potential is given by:

$$\Psi_x = \Psi_o \exp - (\kappa x) \qquad (2.1)$$

Ψ_x is the potential at a distance x from a flat surface

Ψ_o is the potential at the surface i.e. $x = 0$

κ is a characteristic constant. The value of this constant is usually determined by the concentration of electrolyte present:

$$\kappa = \left[\frac{4\pi F^2}{\varepsilon RT} \sum_{i=1}^{n} c_{i\infty} z_i^2\right]^{\frac{1}{2}} \text{cm}^{-1} \qquad (2.2)$$

F is the Faraday

$c_{i\infty}$ is the bulk electrolyte concentration of species i

z_i is the valency of species i

ε is the dielectric constant of the liquid

R is the universal gas constant

T is the absolute temperature

For an aqueous solution of a symmetrical electrolyte at 25°C equation 2.2 becomes:

$$\kappa = 0.328 \times 10^8 (cz^2)^{\frac{1}{2}} \text{cm}^{-1} \qquad (2.3)$$

For an unsymmetrical electrolyte z is the counter ion valency. At a distance of $1/\kappa$ cm from the flat surface the potential is decreased by a factor of 1/e. The potential decays to zero a short distance further into the liquid. $1/\kappa$ is often referred to as the "double layer thickness".

The treatment of Gouy and Chapman assumes that the counter-ions are point charges. Their theory predicts physically impossible concentrations of electrolyte close to the surface under certain circumstances. Stern tried to refine the model by dividing the double layer into two. He assumed that a region of firmly bound ions existed right next to the surface, and the centres of these ions could not approach closer to the surface than half an ionic diameter. This layer, later called the Stern layer, he said would only be a few Angstroms thick. Outside this layer of

firmly bound ions he assumed a mobile diffuse layer to exist.

Figure 2.1 shows a typical representaion of the Stern - Gouy Chapman model (Shaw 1969). The surface potential Ψ_o is reduced to the Stern potential Ψ_δ. The potential then decays to zero in the diffuse double layer. At some distance from the surface the ions change from being firmly bound to being free to move in the liquid. A "plane of shear" is assumed to exist at this distance from the surface. The "plane of shear" is probably a region of rapidly changing viscosity rather than a true plane. The potential at the plane of shear is called the "zeta potential" and is the potential which manifests itself in electrokinetic phenomena. The position of this plane is not known, but it is assumed to be somewhere in the Gouy - Chapman diffuse double layer, probably close to the outside of the Stern layer. This implies of course that $|\Psi_\delta| \geq |\zeta|$. For a detailed discussion of Stern's view of the double layer see Dukhin and Derjaguin (1974).

2.1.2 Electrophoresis

When an electric field is applied to a suspension of particles of radius. a in water, the particles will tend to move towards the electrode carrying a charge opposite in sign to the charge carried by the particles.

By equating the electrical and viscous forces involved and assuming that κa was large (i.e. the double layer thickness was small compared with the radius of the

Figure 2.1 Schematic representation of an electric double layer according to Stern's theory

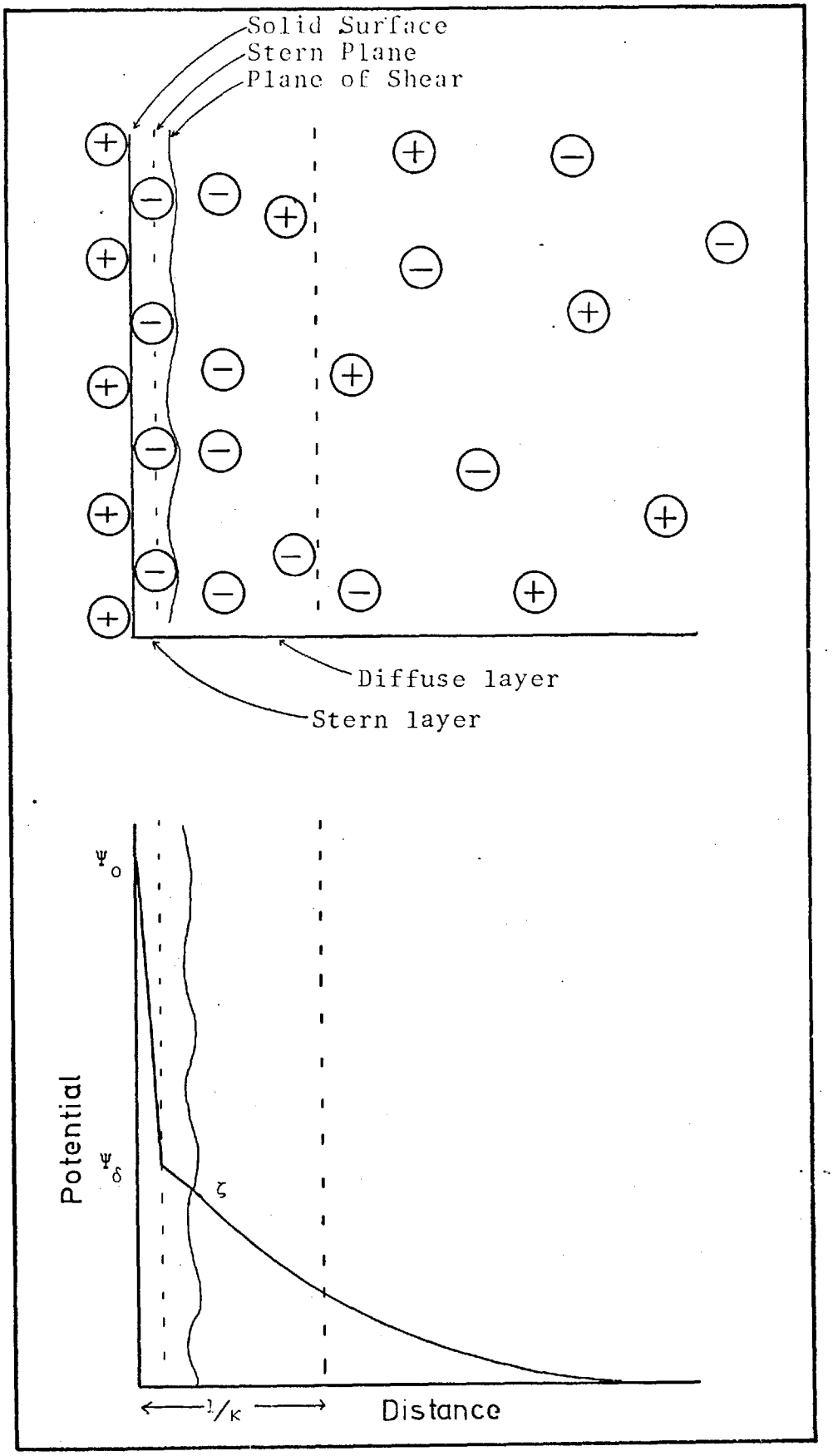

particle) Smoluchowski showed that the velocity of the particle per unit of electric field was given by:

$$U_E = \frac{\zeta\varepsilon}{4\pi\eta} \qquad (2.4)$$

Where U_E is the mobility of the particle

ζ is the zeta potential

ε is the dielectric constant

η is the viscosity

at 25^oC $\zeta = 12.85U_E$ millivolts. In practice if $\kappa a \geqslant 300$ equation 2.4 holds. For particles of radius 5 microns in 10^{-4}M Na_2SO_4, $\kappa a = 325$.

If $\kappa a << 1$ Hückel showed that:

$$U_E = \frac{\zeta\varepsilon}{6\pi\eta} \qquad (2.5)$$

Hückel's equation 2.5 is not applicable to particles in aqueous media but does have possible application to electrophoresis in non-aqueous media of low conductance.

Between these two extremes of κa, U_E becomes a function of κa. Wiersema, Loeb and Overbeek (1966) have shown how to calculate ζ from U_E in this region.

2.1.3 The potential of the double layer

The potential due to double layer forces can be calculated from a knowledge of the surface potential. As two spherical particles approach one another, the surface

charge or potential may remain constant or may change. Three situations are considered possible according to Kar et al. (1973).

a) Constant surface potential on both

$$V_{DL} = \frac{\varepsilon a_1 a_2}{4(a_1 + a_2)} \left\{ 2\Psi_1 \Psi_2 \ln \left[\frac{1 + \exp(-\kappa h)}{1 - \exp(-\kappa h)} \right] + (\Psi_1^2 + \Psi_2^2) \ln [1 - \exp(-2\kappa h)] \right\} \qquad (2.6)$$

Where V_{DL} is the potential of the double layer

a_1 and a_2 are the particle radii

h is the distance separating the two surfaces of the spheres

For identical spheres equation 2.6 approaches a limit of $\frac{\varepsilon_o \Psi^2 \ln 2}{2}$ as h approaches O

The other two situations are, b) Constant surface charge on both and c) Constant surface potential on one and constant surface charge on the other. For details see Kar et al. (1973).

2.2 van der Waals forces

Attractive forces exist between atoms and molecules; this is a necessary assumption when dealing with anything except an ideal gas. van der Waals derived his famous equation by assuming that attractive forces exist between molecules in a gas.

The van der Waals forces can be separated into orientation, induction and dispersion forces according to Israelachvili and Tabor (1973). Orientation and induction forces occur between molecules possessing a strong permanent dipole moment. Dispersion forces predominate for all but the most polar molecules. A considerable amount of work

has been done to understand dispersion forces, assuming them to be predominant. Unfortunately water, which figures in many important systems, possesses a strong permanent dipole moment.

2.2.1 Attractive dispersion forces between atoms and molecules

The general form of the attractive potential between atoms is:

$$V_v = \frac{-K}{d^6} \qquad (2.7)$$

V_v is the van der Waals dispersion potential
K is a constant
d is the distance between atoms

The attractive potential is due to instantaneous dipole moments in molecules that may have no permanent dipole moment (e.g. methane). The existence of these instantaneous dipole moments is explained in classical terms by the electrons being on one "side" of the molecule at a particular instant. The forces produced are called dispersion forces as they are closely related to optical dispersion effects.

Equation 2.7 is valid if $d \leqslant \lambda_i/2\pi$ where λ_i are the characteristic absorption wavelengths of the atoms. At larger distances the time taken for the electromagnetic field of the first atom to reach the second may be comparable with the fluctuating period of the dipole itself. In this case the dipole of the first atom is no longer in phase with its neighbour's. For $d \gg \lambda_i/2\pi$ the potential is called the

retarded van der Waals potential and is given by:

$$V_v = \frac{-K'}{d^7} \qquad (2.8)$$

Where K' is a constant

Thus as d increases above $\lambda_i/2\pi$ the nonretarded $1/d^6$ power law changes to the retarded $1/d^7$ power law. The transition is gradual and may extend over several hundred Angstroms.

The attractive dispersion interactions between two atoms or molecules has received considerable attention. The theory developed is very important, but in this investigation it is the interaction between large bodies which is important. The interested reader can refer to the review by Israelachvili and Tabor.

2.2.2 Dispersion forces between macroscopic bodies

The Derjaguin, Landau, Verwey and Overbeek (D.L.V.O) theory of colloid stability recognises the existence of two forces. Double layer forces which are repulsive between similar particles, and dispersion forces which are generally attractive. The stability of colloids can be explained by the interplay between these two forces. Napper (1970) presents an easy to read review of colloid stability.

Assuming that the dispersion energies are additive, the potential energy and hence the force between bodies can be derived for different geometries. It is common

practice to use "Hamaker constants" A and B when dealing with the nonretarded and retarded force between large bodies. These constants (also called van der Waals constants) are related to K and K' of equations 2.7 and 2.8 by:

$$A_{12} = \pi^2 N_1 N_2 K_{12} \tag{2.9}$$

$$B_{12} = \pi^2 N_1 N_2 K_{12}/10 \tag{2.10}$$

Where A_{12} is the nonretarded Hamaker constant for substance 1 and substance 2 separated by vacuum

B_{12} is the retarded Hamaker constant for substance 1 and substance 2 separated by vacuum

N_1 and N_2 are the number of polarizable atoms per unit volume in each of the substances

Israelachvili and Tabor list expressions for the force of interaction between macroscopic bodies of different geometries. For two spheres for example, separated by a distance h where h is much smaller than the radii of either sphere, the nonretarded potential energy of interaction is:

$$V_V = \frac{-A}{6h} \frac{a_1 a_2}{(a_1+a_2)} \tag{2.11}$$

Where A is the nonretarded Hamaker constant for the interaction

The corresponding expression for the retarded potential is:

$$V_V = \frac{-\pi B}{3h^2} \frac{a_1 a_2}{(a_1 + a_2)} \qquad (2.12)$$

Where B is the retarded Hamaker constant for the interaction

The retarded Hamaker constant B is difficult to estimate. In this work only nonretarded interactions are considered.

2.2.3 Determination of the Hamaker constants from macroscopic data

According to Lifshitz's theory (see Lifshitz (1956)) the Hamaker constant should be calculated from the optical data of the media concerned. The Lifshitz general expression for the Hamaker constant for two bodies 1 and 2 separated by a third 3 is, according to Krupp et al. (1972):

$$A_{132} = \frac{3\hbar}{4\pi} \int_0^\infty \frac{\varepsilon_1(i\xi) - \varepsilon_3(i\xi)}{\varepsilon_1(i\xi) + \varepsilon_3(i\xi)} \cdot \frac{\varepsilon_2(i\xi) - \varepsilon_3(i\xi)}{\varepsilon_2(i\xi) + \varepsilon_3(i\xi)} \, d\xi \qquad (2.13)$$

Where $\hbar = \frac{h}{2\pi}$: h is the Plank constant

$\varepsilon i(i\xi)$ is the dielectric permittivity of the interacting bodies at the imaginary frequency $i\xi$

In principle the determination of $\varepsilon i(i\xi)$ requires a thorough knowledge of the absorption spectrum of medium i which is not available for most substances. Approximations can be made and Israelachvili and Tabor discuss these

approximations.

Dispersion forces are often thought of as purely attractive. Equation 2.13 shows that the interaction can be repulsive if:

$$[\varepsilon_1(i\xi) - \varepsilon_3(i\xi)] \times [\varepsilon_2(i\xi) - \varepsilon_3(i\xi)] < 0$$

that is if $\varepsilon_1(i\xi) > \varepsilon_3(i\xi) > \varepsilon_2(i\xi)$

2.2.4 Temperature dependent van der Waals forces

Equation 2.13 is strictly only valid for media at zero temperature, above absolute zero there is an additional temperature dependent term. Israelachvili and Tabor say this term increases the nonretarded Hamaker constant by approximately :

$$3 \times 10^{-14} \left[\frac{\varepsilon_1(0) - \varepsilon_3(0)}{\varepsilon_1(0) + \varepsilon_3(0)}\right] \cdot \left[\frac{\varepsilon_2(0) - \varepsilon_3(0)}{\varepsilon_2(0) + \varepsilon_3(0)}\right] \text{ ergs}$$

Where $\varepsilon_1(0)$ is the dielectric constant of medium i at zero frequency

at room temperature. The additional term is usually quite small for interacting bodies with Hamaker constants of about 10^{-12} ergs. If the bodies are separated by water however, as they are in flotation, the additional term can be very significant. For example, Parsegian and Ninham (1970) have shown that the temperature dependent term is about half of the total Hamaker constant for two water phases separated by a hydrocarbon film.

2.2.5 Combining laws

Combining laws are frequently used for obtaining approximate values of unknown Hamaker constants in terms of known ones.

Kitchener (1974) has discussed the dangers of using some combining laws particularly if these laws are given the status of equations. Churaev (1972) has shown that Hamaker's (1937) expression for the net interaction between two bodies 1 and 2 immersed in a liquid medium 3 namely:

$$A_{132} \simeq A_{12} + A_{33} - A_{13} - A_{23} \qquad (2.14)$$

is not correct, because it implies that interaction between bodies does not depend on the medium through which the electromagnetic forces are transmitted. Visser (1972) presents a corrected version of 2.14 which will be discussed in Chapter 5. Two useful combining laws, according to Israelachvili and Tabor are:

$$A_{132} \simeq \pm (A_{131} \cdot A_{232})^{\frac{1}{2}} \qquad (2.15)$$

$$\left.\begin{aligned} A_{121} &\simeq A_{131} + A_{232} - 2A_{132} \\ &= (A_{131}^{\frac{1}{2}} \pm A_{232}^{\frac{1}{2}})^2 \end{aligned}\right| \qquad (2.16)$$

2.2.6 Dispersion forces between bodies with surface layers

In the last five years much interest has been shown in the estimation of the forces between two bodies with thin surface layers. Langbein (1969) and Parsegian and Ninham (1971) determined the potential between two bodies with surface layers. The subject is of considerable importance

in biological systems. Their results showed that surface layers have a significant effect when the distance of separation between two bodies is of the same order as the thickness of the layers but the effect of the surface layers decreases as the distance of separation increases.

2.3 The disjoining pressure concept

During flotation the liquid film between an air bubble and a particle must thin then rupture if a contact angle is to form. Surface forces decide the rate at which this film will thin, and if in fact it will rupture.

Derjaguin and his co-workers have evolved the concept of disjoining pressure to explain the film thinning process. The concept is best illustrated by an example. Studies by Read and Kitchener (1967) and (1969) showed that thin wetting films formed between a bubble and a hydrophilic* silica plate, behaved as though there was an excess pressure Π, acting normal to the film. The pressure acted on the film to oppose further thinning. This excess pressure is the disjoining pressure. It is equal to the difference between the pressure in the bubble, P in Figure 2.2, and the pressure in the bulk liquid adjacent to the silica/water interface P^0.

Figure 2.3 is a schematic representation of disjoining pressure versus distance of separation h. Films are stable

* *A surface is described as hydrophilic or hydrophobic according to whether the contact angle is zero or non-zero respectively.*

Figure 2.2 A film between a bubble and a flat plate. After Blake and Kitchener (1972)

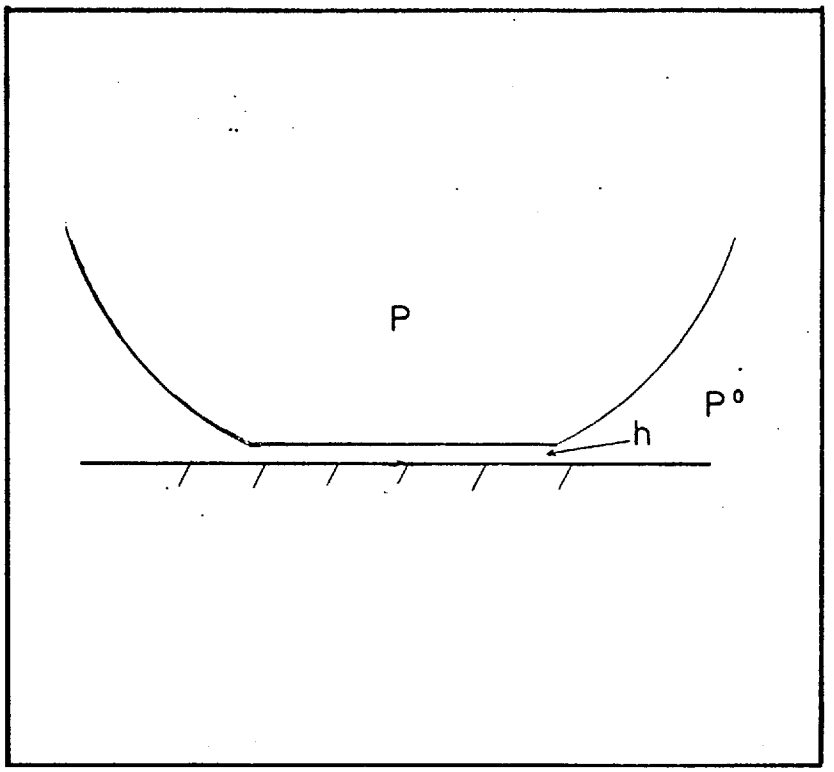

Figure 2.3 Schematic representation of disjoining pressure vs distance h . After Blake and Kitchener

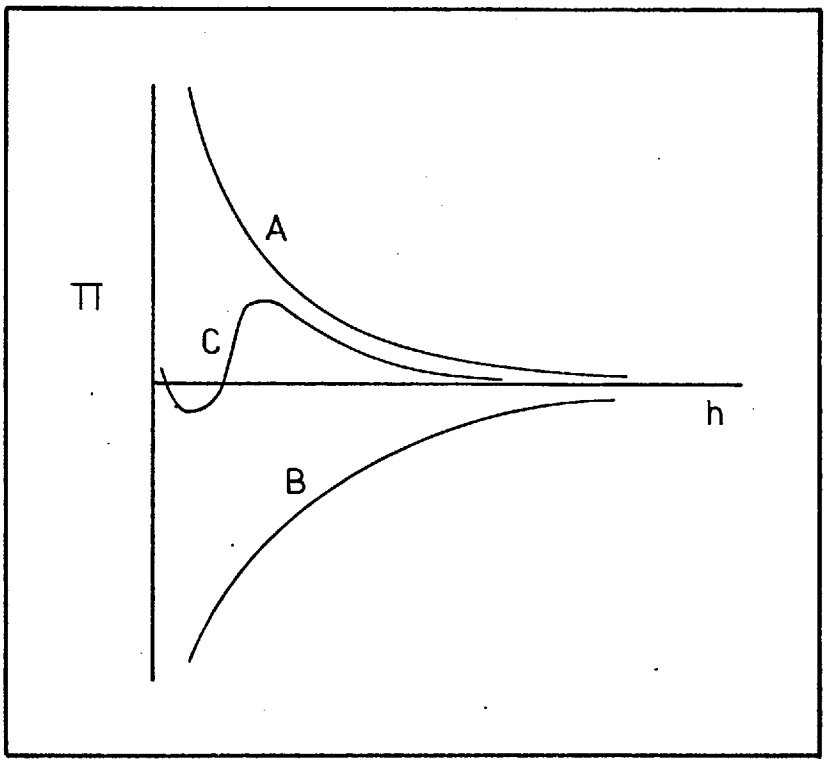

if $(\frac{d\Pi}{dh}) < 0$ (curve A), unstable if $(\frac{d\Pi}{dh}) > 0$ (curve B). Curve C can result if the film stability varies with distance.

The disjoining pressure is conveniently considered to be made up of three terms:

$$\Pi = \Pi_{DL} + \Pi_V + \Pi_S \qquad (2.17)$$

Where Π_{DL} and Π_V are the double layer and van der Waals dispersion contributions respectively

Π_S we shall call the specific surface term

The specific surface term contains all the other surface effects not included in Π_{DL} and Π_V such as hydrogen bonding, dipole-dipole interactions, etc. These effects are very important in flotation because of the special nature of water. The overriding importance of the specific surface term for water is illustrated by the observation that many solids are hydrophobic and yet oleophilic, in spite of the fact that the dispersion energy for water is low. On dispersion energies alone, according to Read and Kitchener, water should spread on paraffin wax, graphite, sulphur and mercury. It does not spread because its cohesive energy is mainly due to hydrogen bonding.

Fowkes (1964) and Kitchener (1975) agree that the term which decides if a substance is hydrophobic or hydrophilic is not the van der Waals dispersion term, but the specific surface term. Laskowski and Kitchener (1969) found strong

circumstantial evidence for this belief. They studied the hydrophilic-hydrophobic transition on silica. Silica is considered to be naturally hydrophilic because of hydrogen bonds between silol groups at the surface, and adjacent water molecules. If enough silol groups are removed by methylation or even strong heating, silica becomes hydrophobic. Laskowski and Kitchener found that the zeta potential of the methylated silica was essentially the same as the zeta potential of the unmethylated silica. They assumed that van der Waals dispersion forces were unaltered by addition of methyl groups on as little as 60% of the available sites. They explained their results by considering the change in the specific surface term of the disjoining pressure. They suggested that when enough of the silol groups were removed the surface would become hydrophobic, because there would exist at the junction of the non-polar methyl groups and the water phase, a boundary plane across which there would be fewer hydrogen bonds per unit area than across any plane in bulk water. The water would try to avoid this plane and so a non-zero contact angle would be formed after film rupture.

According to Kitchener (1975) there is no way at present to estimate the magnitude or distance dependence of the specific surface term. Russian workers apparently believe that the effect could be quite long range (1000Å) while Western surface scientists believe the effect is of a much shorter range, perhaps a few molecular diameters.

The thick fog of confusion which still surrounds the subject of hydrophobicity has been well illustrated in an

article by Rao (1974) and the discussion of his article by Lovell (1974). Rao quickly dismisses specific surface forces, or hydration forces as he calls them, as being unimportant. He then starts discussing the role of the dispersion forces and their attendant Hamaker constants in a confused manner. Lovell challenges Rao's assumption on specific surface forces and corrects some of Rao's statements on Hamaker constants as measures of hydrophobicity. Both authors make the mistake of using combining law approximations as actual equalities. In a timely paper Kitchener (1974) discusses both articles. He corrects the confused terminology used and discusses the dominance of specific surface forces in determining the hydrophobicity of minerals.

CHAPTER 3

THEORETICAL AND EXPERIMENTAL BACKGROUND

In this chapter the background to the work is presented. Special attention is given to some articles which are of particular interest. A number of relevant papers which are not directly concerned with flotation will also be discussed.

The kinetics of flotation has been studied mainly by workers concerned with mineral flotation. Their work is relevant to the flotation of fine particles in effluent treatment cells as long as the results are viewed in the light of the differences between the two processes.

One of the first studies was undertaken by Gaudin et al. (1942). They used a steady state technique to measure the rate of flotation of galena crystals in a mechanical cell. They found that the rate of flotation was independent of particle size up to four microns in diameter, then it became proportional to the particle diameter between four and twenty microns. They made no mention of bubble diameter in their experiments, but it was probably 0.02 - 0.20cm which is a typical figure for a mechanical cell.

Sutherland (1948) examined the formal mathematics of collision theory with regard to flotation. Using a Potential flow model description of the fluid field around

a bubble of radius a_b, Sutherland considered the motion of an "inertialess" particle of radius a_p. The particle was confined to motion along a liquid streamline and the only way collisions could result was by interception of the particle and bubble surfaces, i.e. when the centre of the particle was within a distance of $(a_b + a_p)$ from the bubble centre. Sutherland proceeded to show that n the number of collisions occurring per unit time was:

$$n = 3\pi a_b a_p N_o N' U \qquad (3.1)$$

Where U is the bubble rise velocity

N' is the number of bubbles per cm^3

N_o is the number of particles per cm^3

Equation 3.1 is often expressed as collision efficiency E_c :

$$E_c = \frac{\text{No. of particles colliding with the bubble}}{\text{No. of particles which pass through the bubble's cross sectional area}} \qquad (3.2)$$

Equation 3.1 becomes:

$$E_c = 3a_p / a_b$$

The overall efficiency of particle capture E is given by:

$$E = E_c \cdot E_a \qquad (3.3)$$

Where E_a is the adhesion efficiency

E_a is the fraction of particles which actually adhere to the bubble after collision. If froth processes such as

redispersion etc. can be ignored, the rate of flotation as measured in an actual experiment will be proportional to E.

Only limited experimental information on adhesion efficiency is available. Brown (1960) and Flint (1971) found, not unexpectedly, that the probability of adhesion decreased as the angle formed between the particle point of contact and the vertical axis of the bubble increased. Adhesion efficiency must be a function of the hydrodynamic and surface forces involved in the particle/bubble interaction.

If E_a is constant as a number of authors have assumed, the rate of flotation is a function of particle size and bubble size. We can see this by taking Sutherland's result as an example. The volume swept out by the bubble is proportional to a_b^2, so the number of particles picked up by Sutherland's bubble should be proportional to the bubble radius a_b. For a fixed gas flow rate the number of bubbles in the flotation cell will be proportional to $1/a_b^3$. Therefore, the rate of flotation will be proportional to a_p/a_b^2 in Sutherland's case. The dependence of the rate of flotation on particle size derived by Sutherland agrees with the dependence found by Gaudin et al. for particles larger than 4 microns in diameter.

Morris (1952) studied the flotation of copper pyrite in a batch cell, and found that the rate of flotation was proportional to $\ln(a_p)$. He made no mention of the size of the bubbles in his experiments. Bushell (1962) found in his experiments that the rate of flotation was independent of

particle size. Again there was no mention of bubble size. These two results are obviously at odds with each other and also with Gaudin et al.

Tomlinson and Fleming (1963) conducted careful batch experiments on flotation, their apparatus was specially designed to remove the effect of redispersion of particles from the foam layer. They found that provided the concentration of particles was not too high, the rate of flotation for easily floated particles was proportional to a_p^2 . For less easily floated particles the rate was less dependent on particle size. The mean bubble size in their experiments was 0.08cm and the size range of particles was 14 - 400 microns in diameter.

Two years before Tomlinson and Fleming's paper, Derjaguin and Dukhin (1961) published their *"Theory of Flotation of Small and Medium-size Particles"*, which was the first attempt to present a unified picture of mineral flotation kinetics. Derjaguin and Dukhin regarded the approach of a particle to a bubble surface as taking place in three stages. They called these stages zones 1, 2 and 3. In zone 3 the disjoining pressure alone affected the precipitation of particles. Zone 3 was a film with thickness of some thousands, or tens of thousands of Angstroms. Zone 2 was the diffusional boundary layer of the bubble. The mean thickness of zone 2 was about 10 microns. Derjaguin and Dukhin showed that a strong electric field existed in zone 2, because of transport of ionic surfactant to the surface of the bubble. The field is a result of the diffusion potential that must exist in any

electrolyte, in the presence of a concentration gradient, when the cation and anion diffusivities are unequal. Particles passing through zone 2 would "feel" the field and would be acted on by an electrophoretic force in the same way as they are in an electrophoresis cell. Derjaguin and Dukhin called this force the "diffusiophoretic force". Lyman (1974) while acknowledging the existence of this force, criticised the way Derjaguin and Dukhin had estimated its magnitude. He showed that if the bubble had a double layer the diffusiophoretic force as expressed by Derjaguin and Dukhin disappeared.

In zone 1 which comprises the entire liquid outside zone 2 the particles were acted on by purely hydrodynamic forces. Hydrodynamic drag tended to sweep the particles around the bubble following the liquid streamlines, but particle inertia and gravity tended to force the particles towards the bubble.

Particles approaching the bubble would have to pass through zones 1 and 2 successfully before they could enter zone 3. In zone 3 their fate would be decided by the form of the disjoining pressure curve, Figure 2.3 .

From their analysis Derjaguin and Dukhin concluded that the efficiency with which inertialess particles would enter zone 3 would be independent of the size of the particles. They also concluded that there would be a size below which the particles could not reach zone 3.

Taking galena as an example, the critical particle diameter for 0.1cm diameter bubbles would be about 30 microns, but Gaudin et al. (1942) were apparently able to float discrete particles of galena with diameters of four microns.

Because of the great difficulties in dealing quantitatively with the forces acting in zones 2 and 3, research has been mainly concentrated on the hydrodynamic processes in zone 1. In the 1950's and early 60's theories of particle collisions were applied to studies of raindrop coalescence and dust collection. Hocking (1960) and Shafrir and Neiburger (1964) included the effects of asymmetrical low Reynolds number flow around a target sphere, and the finite size of the impinging sphere. Fonda and Herne (1957) estimated the efficiency of collision for Stokes and Potential flow around a target sphere.

Flint and Howarth (1971) summarised the theoretical work on the collision efficiency of bubbles and particles, in three statements, and pointed out that some were contradicted by experience:

a) The collision efficiency for Potential flow around a bubble is greater than that for Stokes flow. This is a consequence of the considerable curvature of the streamlines even at large distances from a sphere for Stokes flow.

b) A critical value of particle diameter exists

below which no collisions can occur. The experimental results of Gaudin et al. (1942) challenge this statement as we have seen.

c) For bubble/particle systems an increase in bubble size increases the collision efficiency; as Flint and Howarth say, this statement is doubtful, because it is known that flotation of very fine particles can be improved by using smaller bubbles not larger ones.

They concluded that collision theory in flotation was not well understood. They were particularly critical of the equation of motion with which Derjaguin and Dukhin (1961) had started their analysis. Flint and Howarth wrote down the equation of motion for a particle approaching a stationary sphere as:

$$4/3\ \pi a_p^3\ \rho_p \frac{\partial v'_j}{\partial t} = G_j + C_d(u'_j - v'_j) \qquad (3.4)$$

Where G_j is the body force acting on a particle
C_d is the drag coefficient of the particle
v'_j is the particle velocity
u'_j is the fluid velocity with no particle present
ρ_p is the particle density

Derjaguin and Dukhin had written the term on the left hand side of equation 3.4 as: $4/3\ \pi a_p^3\ (\rho_p - \rho_f)$ where ρ_f is the fluid density. As Flint and Howarth pointed out this led Derjaguin and Dukhin to find that the particles did not deviate from the fluid streamlines,

and led them to make the assertion that a critical size of particle would exist.

Flint and Howarth solved the corrected equation and found that:

a) There were two regions of particle behaviour characterised by a parameter Fonda and Herne had called K :

$$K = \frac{2\ \rho_p\ a_p^2\ U}{9\ \eta_f\ a_b} \qquad (3.5)$$

Where U is the bubble rise velocity

η_f is the fluid viscosity

If K was greater than about one (fairly large particles), collision efficiency was dependent on inertial forces, and was increased by enlarging the bubble size. For fine particles (K less than about 0.1) collision efficiency was almost independent of K but was strongly dependent on another parameter G :

$$G = \frac{2(\rho_p - \rho_f)a_p^2\ g}{9\ \eta_f\ U} \qquad (3.6)$$

Where g is the acceleration due to gravity

Since G decreases with increasing bubble size the collision efficiency for small particles would be increased by reducing the bubble size.

b) Collision efficiencies were only zero in flotation systems if G equalled zero i.e. $\rho_p = \rho_f$

c) For values of K less than about 0.1, particle inertia may be neglected and collision efficiency could be calculated from:

$$E_c = \frac{G}{1+G} \qquad (3.7)$$

This result applied to Potential and Stokes flow.

Reay and Ratcliff (1973) studied as Flint and Howarth had done, the collision efficiency in flotation. They were specifically interested in effluent treatment and were probably the first investigators to consider its special problems. They investigated the case of bubbles less than 100 microns, and particles less than 20 microns in diameter; typical sizes for an effluent treatment plant. They made a number of important assumptions at the start of their investigation.

a) The flow pattern around the front of the bubble is given by Stokes flow for creeping flow around a rigid sphere. This assumption of a rigid sphere is reasonable in a solution containing a surfactant.

b) Electrical interactions between particle and bubble have a negligible effect on particle trajectory.

c) All particles collected are immediately swept to the back of the bubble so that the full front surface is always clear. Photographic evidence collected by Tomlinson and Fleming (1963) and Reay (1973) supports this.

d) The motion of the bubble is not affected by the

presence of the particles. A valid assumption if the particle concentration is small.

e) The fluid velocity used in computing the drag on the particle is the velocity which would have existed at a point occupied by the centre of the particle if the particle were absent. This last assumption is only valid as: $a_p \to 0$.

Reay and Ratcliff wrote the equations in the same form as Flint and Howarth had done. They then considered the conditions under which the unsteady term in equation 3.4 was important and found that the term could be ignored for bubbles up to 100 microns in diameter, rising in water through a suspension of particles with diameters up to 20 microns. They concluded that gravity was the only factor causing the particles to deviate from the fluid streamlines. They calculated the flux of particles onto the bubble and hence the collision efficiency. The important result they obtained was:

$$E_c \propto \left(\frac{a_p}{a_b}\right)^N \qquad (3.8)$$

The exponent N was 1.9 for particles with $\rho_p/\rho_f = 1.0$ and 2.05 for $\rho_p/\rho_f = 2.5$ If we consider Flint and Howarth's results for small K and small G we find:

$$E_c \propto \left(\frac{a_p}{a_b}\right)^2 \qquad (3.9)$$

Which is essentially Reay and Ratcliff's result. The two approaches differ mainly in the definition of grazing

trajectory. Flint and Howarth defined a grazing trajectory as one which would cause the centre of the particle to just touch the surface of the bubble. Reay and Ratcliff considered a grazing trajectory to be one in which the particle surface just touches the bubble surface. As a consequence of these two different definitions Reay and Ratcliff's results are slightly higher than Flint and Howarth's under the same conditions. Reay and Ratcliff's analysis also allows a non-zero rate of flotation for particles of neutral density.

Reay and Ratcliff also investigated the collection efficiency of particles so small that Brownian diffusion becomes the predominant mechanism of particle transport to the bubble surface. They deduced that:

$$E_c \propto \frac{1}{a_p^{2/3}\, a_b^2} \qquad (3.10)$$

They were able to test experimentally the correctness of their theoretical predictions for large particles. They found that the collection efficiency of individual bubbles rising through a suspension of small glass spheres was proportional to $1/a_b^2$ as expected, and proportional to a_p^2 up to about 15 microns. After this microscopic study Reay and Ratcliff (1974) investigated the rate of flotation of glass spheres and polystyrene particles in batch experiments. The rate of flotation would be expected to be proportional to a_p^2 but inversely proportional to a_b^3 . Only two data points were available to test the dependence on bubble size

but they were consistent with the expected result. The experimental dependence on particle size was more complex. It was found that the rate of flotation was proportional to a_p^N, where N was about 1.5 for glass spheres, in reasonable agreement with theory. For polystyrene particles however, N was about 0.5, completely at odds with theory. Reay (1973) tried to quantitatively explain the anomalous behaviour of the polystyrene particles by considering the effect of electrical forces, which he had originally assumed could be ignored. The zeta potential of the glass spheres was essentially zero, but the zeta potential of the polystyrene particles was about 11mV. He guessed that the bubble would be negatively charged for most of its life despite the presence of a cationic surfactant which would be expected to render it positive. He assumed that the large quantity of alcohol he had used as a frother would retard the adsorption of the cationic surfactant. Later he found that his explanation was incorrect. Reay and Ratcliff (1974) then suggested that Derjaguin and Dukhin's analysis of flotation rate, which had shown that the flotation rate should be independent of particle size, could be applied to the polystyrene results. They realised that the conditions to which the analysis applied were very different from their experimental conditions, but were faced with an unexpected experimental result and so hoped Derjaguin and Dukhin's analysis could be stretched a little.

We have mainly discussed hydrodynamic forces up to this point. Now we turn to the effect of double layer forces on the rate of flotation.

Derjaguin and Dukhin (1961) as part of their analysis of flotation discussed the forces acting in zone 3. These were the forces making up the disjoining pressure:

$$\Pi = \Pi_{DL} + \Pi_V + \Pi_S \qquad (2.17)$$

They set the specific surface term to zero because of difficulties in estimating its value. The only terms left in equation 2.17 were the contributions from double layer and van der Waals dispersion forces. The authors discussed what they called "bulk hydrophobicity" characterised by a positive Hamaker constant for the bubble/particle interaction, and developed a criterion (based on colloid theory) for fast flotation:

$$\frac{1}{\kappa} \frac{\varepsilon \psi_o^2}{A} < K_c \qquad (3.11)$$

Where ε is the dielectric constant

$1/\kappa$ is the double layer thickness

ψ_o is the surface potential of the particle

A is the Hamaker constant for the interaction

K_c is a constant of order 1

The criterion was tested by Derjaguin and Shukakidse (1961) by studying the flotation of antimonite, a

naturally hydrophobic mineral. The criterion is almost certainly useless according to Lovell (1974) and Kitchener (1975), because of its neglect of the important specific surface term in equation 2.17 . The experimental results presented by Derjaguin and Shukakidse however are interesting. They used fairly large particles 43 - 150 microns in diameter and measured a variable proportional to the rate of flotation. The surface potential Ψ_o they assumed to be equal to the zeta potential of the particles, a fairly common assumption. Their results showed that the rate of flotation dropped sharply as the zeta potential of the particles was increased beyond a critical value.

Some later workers also discussed the effect of particle zeta potential on flotation rate. Jaycock and Ottewill (1963) studied the adsorption of a cationic surfactant onto negatively charged silver iodide crystals. They found that the flotation rate measured in a Hallimond tube was highest when the zeta potential of the particle was zero. DeVivo and Karger (1970) investigated the flotation of clay particles. They found that for bubbles with diameters of about 200 microns the maximum flotation rate occurred when the zeta potential of the clay was zero, in agreement with Jaycock and Ottewill. Coagulation may have taken place in both experiments because the zeta potential was zero, if it had, the increase in particle size could have

caused the increased rate. DeVivo and Karger also found that if the bubbles were larger, the clay particles floated best when their zeta potential was quite high. A strange result that has never been satisfactorily explained.

When discussing the correlation between zeta potential and flotation rate we are really discussing the effect of double layer interaction between particle and bubble. Only a few investigators have studied both particle and bubble zeta potential and their effects on flotation rate. Dibbs et al. (1972) studied the effect of particle zeta potential and the streaming current of rising bubbles on flotation rate. They concluded that the double layer interactions between the particle and the bubble played a significant role in the flotation of quartz in a solution of dodecylamine hydrochloride. Their results are impossible to interpret in terms of bubble zeta potential because like Samygin et al. (1964) they used bubbles in a Reynolds number regime that defies analysis. Lyman (1974) investigated theoretically the Dorn potential of rising bubbles, the Dorn potential being the potential giving rise to the streaming current measured by Dibbs et al. He presents an analysis of the Dorn potential which should make future experimental work easier to plan. In his thesis Lyman expands the work of Harper (1972) on the motion of bubbles in surfactant solutions, and makes a significant contribution

to understanding the adsorption of surfactant onto the surface of bubbles.

Cichos (1973) investigated the influence of the zeta potential of bubbles and particles on flotation rate. He used the technique of McTaggart (1922) to measure the zeta potential of the bubbles. From his results he was unable to say if double layer forces affected the rate of flotation. In some experiments they did, and in some they did not.

The theory of film thinning presents considerable difficulty because of the uncertainty surrounding the specific surface forces. A number of experimental studies however, have yielded some interesting results for workers in flotation.

Evans (1954) studied the thinning of the film between a rotating silica disk and a captive air bubble. The film could be kept at constant thickness by adjusting the angular speed of the disk. He rendered one half of the disk hydrophobic and found no variation in the thickness of the film when the bubble passed the line separating the hydrophobic and hydrophilic sections, as long as the film was thick. If the film was allowed to thin to below about 1500Å it ruptured spontaneously. The "rupture thickness" as he called it, was dependent on the contact angle but was independent of the nature of the solution. Sutherland and Wark (1955) when they discussed Evans's experiments wrote:

"It is not possible to set down a well-proven explanation of all these facts. How is it that air suddenly takes the place of the water over the hydrophobic spot? It seems certain that the air itself is not the dominating factor nor the water close to the air/water interface. It is to the water-solid interface that we must look for the first change which leads finally to the air-solid contact."

Read and Kitchener (1967) and (1969) investigated the thinning of wetting films on a hydrophilic silica plate. Under their experimental conditions stable wetting films were easily formed, the thickness of these films depended on the ionic strength of the solution and the ionic strength controlled the zeta potential of the silica. The double layer forces which in their experiments opposed film thinning, were much stronger than the dispersion forces which also opposed thinning. They discounted specific surface forces as being unimportant at the film thickness of 800Å. They had shown in effect, that the most important contribution to disjoining pressure of their films was the double layer contribution.

Blake and Kitchener (1972) followed on from Read and Kitchener's work, and studied the stability of aqueous films on hydrophobic methylated silica. Using a similar technique they were able to sustain metastable films as thin as 600Å. Again the thickness of films depended on the ionic strength of the solution. Blake

and Kitchener showed that a sufficiently high double layer repulsion could stop a contact angle being formed on a hydrophobic surface. The authors had demonstrated that the electrical double layer could be of particular importance in the kinetics of bubble-particle contact. Their results explain why weakly hydrophobic solids such as coal can be floated faster in brine than in ordinary water.

During this investigation it became apparent that there were similarities between the flotation of fine particles found in effluent treatment cells and deep-bed filtration.

At first glance the two processes, filtration and flotation may seem quite different. In fact there are many differences but also a number of similarities. Consider a spherical filter grain (collector) in a filter bed, fluid flows past with the particles to be removed suspended in the fluid. Depending on the chemical and physical conditions, the particles will become attached to the collector or will remain in suspension. In flotation the bubble rises through a stationary fluid but to an observer on the collecting sphere the hydrodynamics are the same. Of course there are considerable differences, some of the major ones being:

a) The collector in filtration is a solid.
b) The packing of collectors is much closer in a filter bed.

c) Surface active agents need not be added in filtration so the diffusiophoretic effect is absent.

d) Once the particles adhere to the surface of the filtration collector they stay fixed, so the character of the leading surface changes with time.

e) The removal of particles is governed by the depth of a filter. In flotation, time is the analogous variable.

f) Experimentally there are more variables under control in filtration. For example, one can vary the collector size and the fluid velocity independently, this is not possible in flotation experiments.

Because of the similarities and some of the differences it is interesting to examine the results of workers in the filtration field.

On the subject of double layer forces, Ives and Gregory (1966) examined the role of surface forces in filtration. They found that double layer forces certainly lowered the filtration efficiency, which agrees with some flotation studies.

Not surprisingly the trajectory approach has been adopted by most workers to calculate the collection efficiency in filtration. Spielman and Goren (1970) considered the efficiency of particle capture by van der Waals dispersion forces from low speed flows. They included in their analysis the extra resistance felt by a particle as it nears another object. Their analysis

showed that if only viscous and van der Waals dispersion forces were acting the collector efficiency was a function of a dimensionless group, N_{ad} .

$$N_{ad} = \frac{A\, a_c^2}{9\pi\, \eta a_p^4 A_s\, U} \qquad (3.12)$$

Where A is the Hamaker constant

a_c is the collector radius

A_s corrects the flow for the close packing of the filter grains

U is the fluid velocity far from the collector

If N_{ad} was very small $E_c \propto a_p^2 / a_c^2$, the same result obtained by Flint and Howarth (1971) and Reay and Ratcliff (1973). If however, N_{ad} was large $E_c \propto a_p^{2/3} / a_c^{4/3}$.

Yao, Habibian and O'Melia (1971) extended the work of Spielman and Goren by including Brownian particles in their analysis and found that $E_c \propto 1/(a_p \cdot a_c U)^{2/3}$ which is equivalent to $E_c \propto 1/a_p^{2/3} a_c^2$ as Reay and Ratcliff later found. Experimental work was in fair agreement with the results for Brownian particles, but for larger particles E_c was simply proportional to a_p . To explain this disagreement with theory they invoced Spielman and Goren's result i.e. the presence of an attractive van der Waals dispersion force.

In the next three years, Spielman and his collaborators investigated different aspects of filtration. Spielman

and Fitzpatrick (1973) developed a theory to predict filter efficiency under van der Waals dispersion forces and gravity. Fitzpatrick and Spielman (1973) presented experiments in reasonable agreement with the theory. During these experiments they found that the filter coefficient suddenly dropped as the zeta potential of the collector and particle (which were both negatively charged), increased beyond a certain value. They guessed this drop was due to double layer repulsion becoming dominant and stopping capture. In a subsequent paper Spielman and Cukor (1973) showed theoretically that such behaviour could be expected. The results presented in these two papers immediately recall the flotation results of Derjaguin and Shukakidse for the flotation of antimonite.

Prieve and Ruckenstein (1974) approached collection efficiency in a different way. Instead of using a trajectory method they started with the equation of continuity for mass diffusion. The particle velocities were determined by van der Waals dispersion and viscous forces. The rate of deposition was determined by integrating the flux of particles over the collector surface. Their results as presented are difficult to use.

After reviewing the background to flotation kinetics we can conclude:

a) The theoretical work of Flint and Howarth (1971)

Reay and Ratcliff (1973) and Reay (1973) for small particles is reasonably consistent. There seems no point in pursuing their purely hydrodynamic approach any further.

b) There is a lack of carefully planned experimental investigations. There are a number of anomalous results (DeVivo and Karger (1970), Reay and Ratcliff (1974)) which have not been explained or properly investigated.

c) The effect of double layer interaction between a bubble and a particle is not understood.

d) Specific surface forces remain an unsolved problem.

According to Flint (1973) the designer of mineral flotation cells must rely entirely on empiricism and "experience", since the basic design procedures for flotation have not been established. The same can be said of the flotation of fine particles in effluent treatment cells. The dependence of flotation rate on particle size is an important design factor, so is the dependence of flotation rate on double layer interaction. This investigation grew from the need to gain a better understanding of these two factors.

The specific aims of this thesis were to investigate the flotation rate of fine particles up to about 20 microns in diameter; then to determine the effect of double layer interaction on the flotation rate of these particles. Polystyrene particles seemed ideal material

for the study, for a number of reasons:

a) They are almost of neutral buoyancy, typical of many materials that are difficult to remove from suspension.

b) They are inert in water

c) They are uniformly spherical, which means that the "shape" factor discussed by Sutherland and Wark (1955) is not important.

d) The size range is typical of the larger particles found in effluent treatment cells and is within the range of a number of theoretical analyses.

Polystyrene particles which are negatively charged in water would be best floated by a cationic surfactant. The magnitude of the double layer interaction could be varied by adding an inorganic salt such as sodium sulphate to the flotation solution. The interested reader can refer to a paper by Connor and Ottewill (1971) for a study of the adsorption of cationic surfactants on polystyrene surfaces.

CHAPTER 4

EXPERIMENTAL - APPARATUS AND TECHNIQUES

In this chapter the details of the experimental method are presented. To obtain the necessary kinetic data the polystyrene particles were suspended in a surfactant solution, the particles were then floated in a suitable cell. The change in particle concentration with time was followed with a Coulter Counter. Various tests were necessary to ensure that subsidiary processes were not important.

A great deal of pre-planning and practice was necessary to ensure that each kinetic experiment was completed in one working day.

4.1 The flotation apparatus

A batch system was chosen for the experiments. The limitations of this system were considered and compared with the difficulties involved in developing a steady-state continuous system. None of the continuous systems mentioned in the literature seemed suitable. Perhaps the one that appealed most was a steady-state technique described recently by Watson and Grainger-Allen (1973). Even this system was thought unsuitable because of the low density of the polystyrene particles (1.05 grams/cc) and the proposed low particle concentration (0.5 grams/litre).

Three designs of batch flotation cells were tried. The first one was based on the cell used by Sheiham and Pinfold (1972). This cell proved unsatisfactory because the sparger area was too small compared with the column area. The second type of cell was a large version of a Hallimond tube similar to a cell described by Tomlinson and Fleming (1963). This cell was designed to isolate the foam produced during flotation from the pulp. The cell was unsuitable because severe back-mixing brought the light polystyrene particles back into the main flotation chamber.

The best and most convenient cell was found to be a 1000ml porosity 4 sintered glass filter funnel. Figure 4.1 shows the flotation cell used.

What might be described as a conventional gas control system was used, the essential details are shown schematically in Figure 4.2. The gas from the nitrogen cylinder was first passed through a rough control valve then through a gas washing bottle filled with distilled water to pre-saturate the gas. An Edwards needle valve was used to regulate the gas flow. The volume of gas was measured with a soap bubble flow meter (with an attached calibrated thermometer) and a mercury manometer. A rotameter monitored the flow of gas before and during an experiment.

A wet type gas meter manufactured by Alexander Wreight & Co. with a certified error of ±0.25% was used

Figure 4.1 Flotation cell

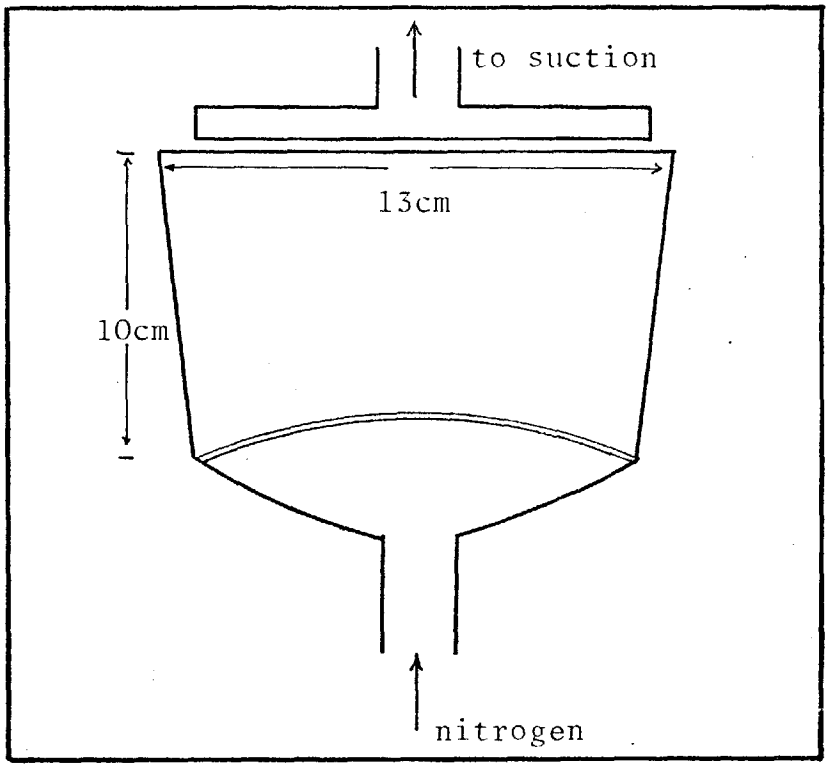

Figure 4.2 Flotation equipment

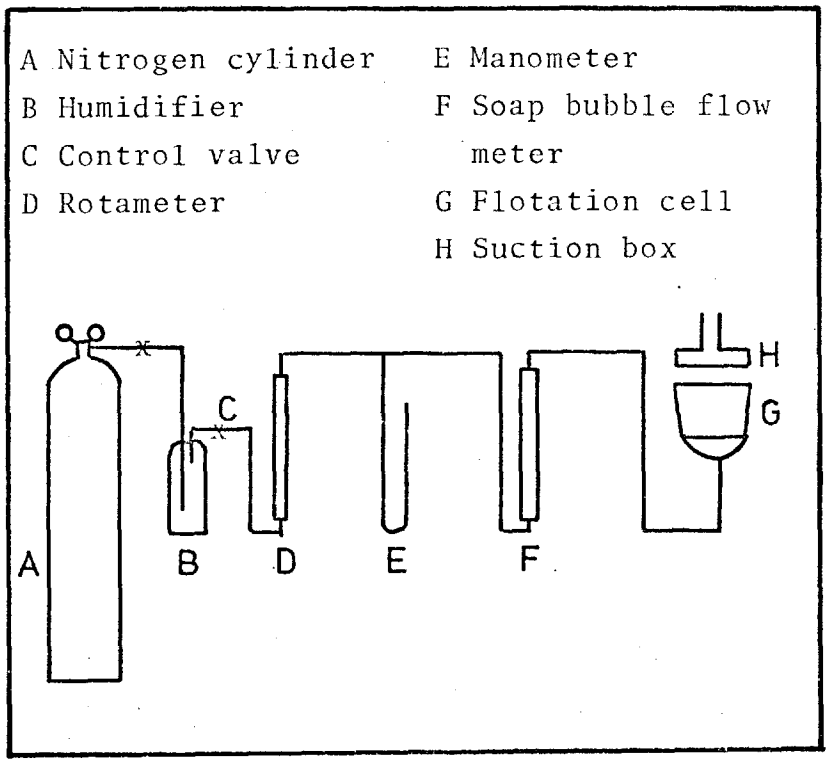

to check the accuracy of the gas measuring system. Ideally of course, the gas meter should have been incorporated in the gas train, but this was not possible because of the relatively low working pressure of the meter. To simulate actual running conditions a pressure reducing restriction was placed between the end of the gas train and the meter, the cell was not connected during the calibration run. A difference of 1.4% was found in the volume of gas measured by the meter and the volume estimated from reading the soap bubble flow meter and the manometer. The calibration run lasted for 45 minutes and an actual flotation run lasted for less than 10 minutes. This result and the steadiness of the rotameter during the calibration run proved that the gas train was suitable for controlling and measuring the flow of gas during a flotation experiment.

A suction box was placed just above the cell during a flotation run to remove the foam produced as soon as it was formed. In practice a maximum of about 0.1cm of foam was present at any time during a flotation run.

Flotation systems very similar to the one described above have been used by Almond (1955) and more recently by Reay and Ratcliff (1974) and Rubin and Johnson (1967).

4.2 The main analysing instruments

4.2.1 Electromobility apparatus

A Rank Brothers Particle Micro-Electrophoresis apparatus was used for electromobility determinations on the polystyrene particles. The instrument was set up for use with a 0.1 x 1cm flat quartz cell. The flat cell was necessary because the polystyrene particles, although small and light settled at appreciable velocities.

The apparatus was calibrated as described in the instructions. The cell resistance with 0.100M KCl at 25°C was 5.92K Ω determined using an Autobalance Precision Bridge B331 operating at 10^4 radians/sec. The resulting electrical cell length was 7.63cm.

A calibrated thermometer was used to measure the temperature of the water bath surrounding the cell. The temperature for all determinations was 25°C ± 0.5°C. The instrument voltmeter was checked against a D.V.M. and was found to be reading 0.5V high. The microscope was calibrated using a standard engraved microscope gradicule.

To check the calibration parameters, the mobility of human erythrocytes was determined in M/15 phosphate buffer. The value obtained was -1.32 ± 0.09 microns/sec/Volt/cm. This agreed with the value quoted by Shaw (1969) of -1.31 ± 0.03.

Before a mobility determination the cell was soaked in chromic acid, then washed several times in distilled water and soaked in distilled water for at least two hours. It was then rinsed with 0.1N NaOH, rinsed with distilled water again and left to soak in distilled water for about 40 minutes. The cell was finally rinsed and filled with the solution to be analysed.

At least ten transit times were taken at each stationary level. If there was not reasonable agreement between the readings at the two stationary levels the cell was refilled with a fresh sample.

A small computer programme was written to convert the transit times into mobility in units of microns/sec/Volt/cm. The programme printed the mean mobility and the standard deviation, which was typically about 10% of the mean value.

4.2.2 The Coulter Counter

The Coulter Counter is a particle counting device which can count particles larger than a selected size and ignore smaller particles. By altering the counting threshold it is possible to determine the particle size distribution of a sample. The sample must have a relatively narrow size range for convenience and a suitable suspending medium needs to be chosen. The Coulter Counter is a common laboratory instrument so no further details will be given here, however for

completeness a brief description of the Counter's operation is given in Appendix A.1. For most flotation experiments a model ZB was used, in some earlier experiments a model A was used.

4.3 Materials used

4.3.1 Water

The distilled water used in all flotation experiments was obtained from the Mining and Mineral Technology Department at Imperial College. It was prepared by passing once-distilled water through an ion-exchange column, an activated charcoal column and then distilling it again in an all glass still. The water produced from this still had a conductivity of $1 \times 10^{-6} \Omega^{-1}$ or less, and a pH of about 5.6 . Bubble persistence tests showed no evidence of surfactant contamination.

4.3.2 The surfactant

The surfactant used was hexadecyltrimethylammonium bromide, often called CTAB (cetyltrimethylammonium bromide). It is a quaternary ammonium salt yielding a positively charged surface active ion ($CTAB^+$) when dissolved in water. The surfactant was obtained from BDH as a general laboratory reagent. The material smelt strongly of amine so it was recrystallised from acetone and water. The recrystallised material melted with decomposition at 234 - 242^{o}C, this is in good agreement with the melting point quoted by Shelton et al.

(1946). A plot of surface tension versus log of the concentration of CTAB (Figure 4.3) shows no distinct miminum, which is usually taken as meaning the material contained no impurities that were more surface active than CTAB. The values of surface tension were slightly higher than values obtained by Hauser and Niles (1941).

The critical micelle concentration (C.M.C.) was determined from conductivity measurements (see Figure 4.4). The value of 8.8 ± 0.1 x 10^{-4}moles/litre agreed with the value of 9.1 x 10^{-4}moles/litre quoted by Scott and Tatar (1943).

4.3.3 Sodium sulphate

BDH Analar grade reagent was used without further purification.

4.3.4 Ethyl alcohol

The ethyl alcohol was analytical reagent quality supplied by James Burrough and was used without further purification.

4.3.5 Polystyrene particles

The particles were kindly donated by Pontyclun Chemical Company Limited. The type of particles chosen for this investigation were code named 3001 microspheres. In bulk these spheres form a smooth flowing white powder. Chemically they are composed of a 94% styrene, 6% divinylbenzene copolymer. The mean particle diameter of the particles was quoted as 15 microns on a weight

Figure 4.3 Surface tension vs log (concentration of CTAB)

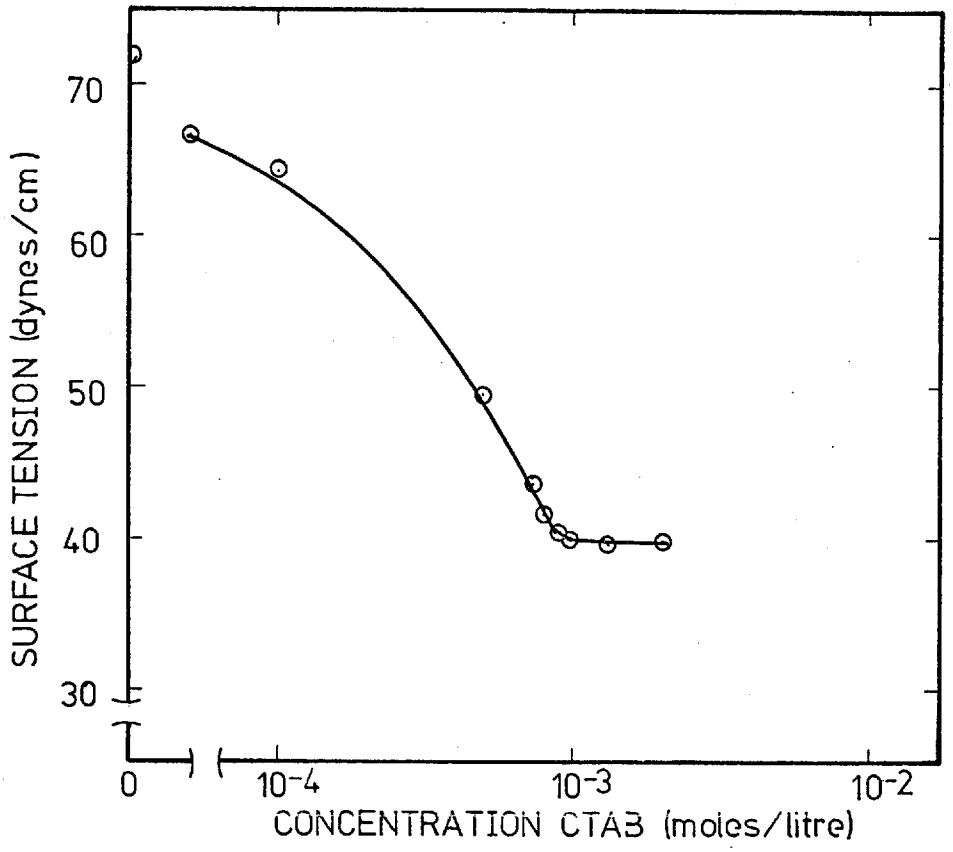

Figure 4.4 Determination of the C.M.C. for CTAB - equivalent conductance vs concentration

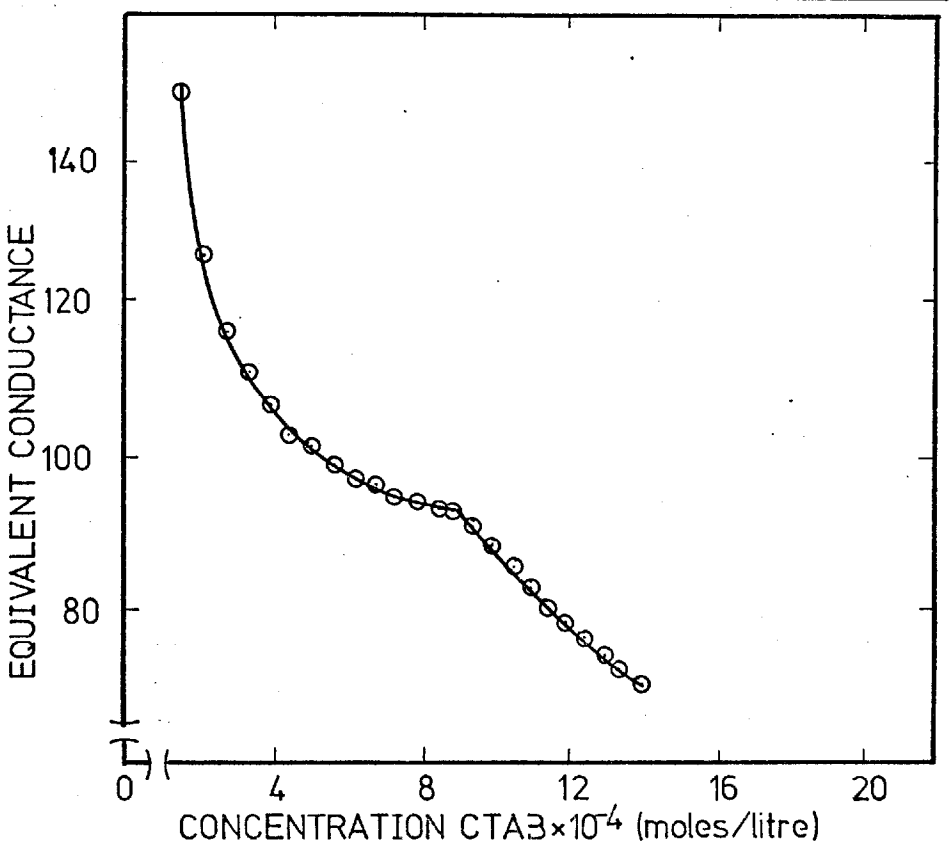

basis and 10 microns on a number basis. An actual size distribution is shown in Figure 4.5 . A number of tests were necessary to check the suitability of these particles for flotation studies.

a) Ionic contaminants

One gram of 3001 microspheres was added to 500mls of singly distilled water containing 3 drops of Shell Nonidet LE nonionic surfactant. The concentration of the microspheres in this test was three times that used in a normal flotation experiment. The conductivity of the solution before the microspheres were added was $4.6 \times 10^{-6} \Omega^{-1}$ measured on a Phillips PR9501 direct reading conductivity bridge. An hour later the reading was $4.3 \times 10^{-6} \Omega^{-1}$. This experiment showed that the particles were free from soluble ionic material.

b) Soluble pH determining contaminants

The pH of 100mls of distilled water was not affected by the addition of 1.5gms of microspheres.

c) Surface active contaminants

It is very difficult to be sure that a material is free from contamination by surface active material. A suspension of the spheres in distilled water produced no bubble persistence, so it was assumed that the microspheres were free of surfactant contamination.

d) Insoluble contaminants and the shape of the spheres

A microscopic examination of a suspension of the spheres showed that there was no insoluble foreign material present. Figure 4.6 is a photomicrograph of the 3001 microspheres, Figure 4.7 is a scanning electron

Figure 4.5 Particle size distribution.

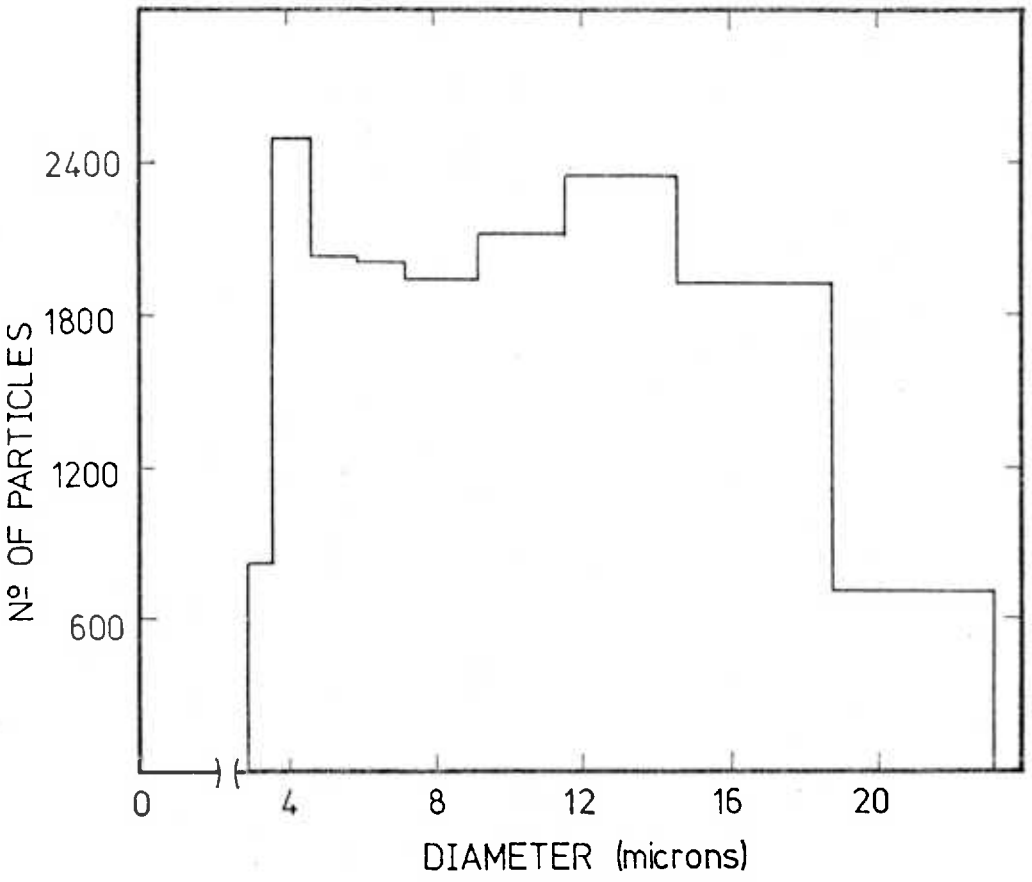

Figure 4.6 Photomicrograph of particles

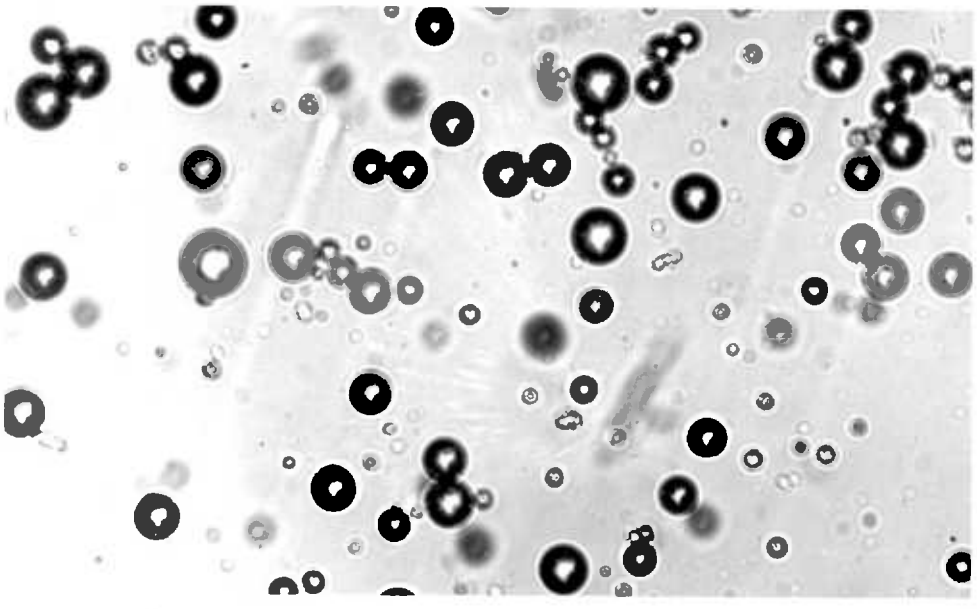

100 microns

Figure 4.7 Scanning electron micrograph of polystyrene particles

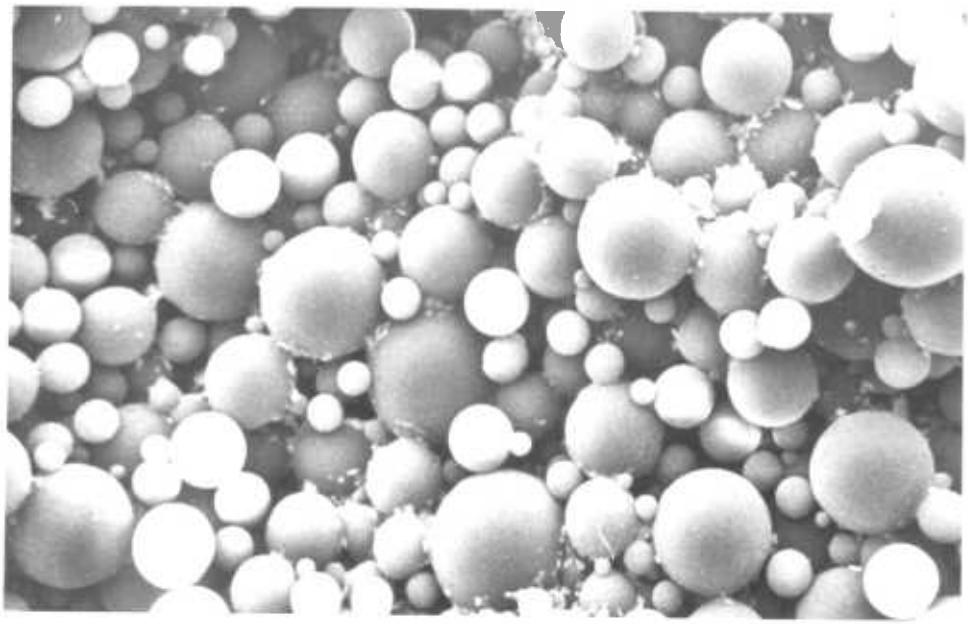

Foreign material is the remains of the dispersing agent.

micrograph of the spheres. These photographs show that the spheres are in fact spherical and relatively smooth.

e) Constancy of electromobility results

A suspension of 3001 particles was made up and the electromobility was measured at various time intervals.

Time (hours)	Mobility microns/sec/V/cm
0	-4.60
17	-4.54
89	-4.56

The unchanged mobility showed that the surface properties of the particles remained constant.

This series of tests showed that the 3001 microspheres were free from contamination and so they were judged suitable for flotation experiments.

4.4 Counting the particles

4.4.1 The suspending medium

One of the main tasks required during an experiment was to determine the size and number of particles in a sample. The Coulter Counter requires particles to be suspended in a filtered solution of electrolyte. Coulter Electronics provide a general purpose suspending solution called "Isoton". From its name and from the results of a few tests it seems to be basically a solution of 1% NaCl, in water buffered at about pH 7.4 . It also contains sodium azide as a preservative.

Isoton because of its high salt content (0.17M) caused coagulation of the polystyrene particles. This was obvious in the change in the particle count over about 10 minutes, which was the average time needed for a complete particle size analysis. The coagulating particles could sometimes be seen attached to the orifice tube in the instrument's microscope.

A number of adjustments were tried to modify the Isoton so it could be used. The pH was changed to 9.4 without any improvement in suspension stability. Agar agar acting as a protective colloid was tried, again without success. Fortunately 0.35mls of 50% BDH Nonidet P42, a nonionic surfactant, in 150mls of Isoton stabilised the suspension. The Nonidet was pre-filtered through a millipore 0.45 micron membrane immediately before use. Adding a large amount of surfactant to the bulk container of Isoton was not successful as it increased the background count after a time.

Extra care had to be taken to ensure that glassware was perfectly clean, because the detergent action of the modified Isoton brought any dirt particles into suspension causing random high background counts.

The action of nonionic surfactants as stabilising agents for polystyrene particles has been recently discussed by Ottewill and Walker (1974).

4.4.2 The calibration of the Coulter Counter

The Coulter Counter must be calibrated with

monodispersed particles of a known size. Coulter Electronics supply suspensions of polystyrene-divinyl-benzene copolymer particles suspended in a surfactant solution. Two sizes of calibrating particles with diameters of 9.09 and 19.4 microns were used for calibration. The calibrating solution contained all the material usually present, with the experimental particles replaced by the calibrating particles. The calibration factor for the Model ZB, fitted with a 100 micron orifice tube which has a resistance of 20KΩ was 2.14 . This was a mean value calculated from calibration factors for the two different sized particles. The calibration factor was checked for each new batch of Isoton.

4.5 Flotation conditions

A series of experiments were carried out to determine the best conditions for flotation. The rate of flotation should be fast enough to ensure reasonable sensitivity in the determination of the rate constant, but not so fast that taking samples becomes difficult. The conditions chosen should be reasonably close to ambient conditions.

The rates of flotation were determined for the polystyrene particles under different conditions. The particles were suspended in the solution to be tested and samples were taken at various intervals after the beginning of the experiment and their optical densities

were determined. Turbidimetric measurements were used in these preliminary experiments simply for speed. A plot of optical density against concentration of particles was linear. The gas flow rate was fixed at 3.5 litres/hour, the rate of flotation was determined by assuming first order kinetics (this assumption will be discussed fully in Chapter 5). The initial particle concentration was 0.5gms/litre.

Five of the more interesting results from a set of eleven experiments are presented in Table 4.1

Table 4.1 Flotation rates

Experiment number	Rate constant (min^{-1})	pH	Surfactant concentration	% Frother V/V
1	0.023	6	CTAB $5x10^{-5}$M	0.5% IPA†
2	0.041	6	CTAB $5x10^{-5}$M	0.5% EtOH
3	0.077	8	CTAB $5x10^{-5}$M	0.5% EtOH
4	0.041	6	H-10-x* $5x10^{-5}$M	0.5% EtOH
5	0.015	6	CTAB $1x10^{-4}$M	0.5% EtOH

† IPA is isopropyl alcohol

* Hyamine 10-x is a cationic surfactant ($C_{28}H_{44}ONCl \cdot H_2O$)

A comparison of the rate constants in experiments 2 and 5 shows that increased surfactant concentration reduced the rate constant. Jaycock and Ottewill (1963) found the same effect when floating negatively charged

silver iodide crystals with a cationic surfactant. They suggested that above a certain concentration a second layer of surfactant adsorbs onto the silver iodide particles. The molecules in this second layer are held with their charged heads in the solution and their hydrocarbon tails associated with the hydrocarbon tails of the first layer. This arrangement of molecules they said, makes the particles more hydrophilic and hinders flotation.

The conditions of experiment 3 were chosen as the most suitable. Most subsequent experiments were conducted under these conditions.

4.6 Bubble production and bubble size

The investigator has only a few methods of producing small bubbles in dispersed air flotation. In this investigation a porous glass frit blowing air into a solution containing a surfactant and a frother was chosen. Some other methods for producing small bubbles were considered and rejected, as detailed in 4.6.1 and 4.6.2 .

4.6.1 Electrolysis

Electrolysis is a method that has raised a lot of interest in recent years. Kuhn (1974) has reviewed some of the recent literature in this field. While electrolysis is undoubtedly a method to consider in a large scale plant, on a laboratory scale not enough is

known about the bubble size distribution. Reay (1974) tried electrolysis and found that he could not obtain reproducible results from day to day. A study of the bubble sizes produced by actual effluent treatment electrodes may be very rewarding, but in this investigation electrolysis, as a method for producing bubbles was not considered further.

4.6.2 Impellors

The impellor is used extensively in the mineral industry to produce bubbles. Sutherland and Wark (1955) have shown that the majority of bubbles produced by impellors are considerably larger than the 100 micron diameter limit needed in this study. Even if surfactant/frother conditions were devised to produce small bubbles (diameters less than 100 microns), considerable agitation would be produced in the cell. Most effluent treatment plants are unstirred because violent stirring breaks up the fragile flocs which are desirable in flotation plants.

4.6.3 The glass frit

To produce small bubbles on a frit, a frother must be added to a solution having such a low surfactant concentration as used in this investigation. A short chain aliphatic alcohol has been used as a frother by a number of investigators; Sheiham and Pinfold (1972), and Rubin and Johnson (1967) used ethanol, Reay and Ratcliff (1974) quote two previous investigators,

Kalman (1974) and Kaufmann (1974) who studied bubble size distributions produced by a glass frit in water containing 0.1 - 0.5% V/V of a short chain alcohol. They found that reproducible bubble size distributions could be obtained in this way.

This method of producing bubbles is fine in a laboratory but it is not practical for large scale effluent treatment plants. This means that the results of laboratory experiments using high concentrations of alcohol as a frother must be viewed with some caution by the designer of an industrial effluent treatment plant.

Although not completely satisfactory, the use of a glass frit and a frother was considered to be the only suitable way of producing small bubbles with a reproducible size distribution.

4.6.4 Gas flow rate

Gas flow rate can also affect the bubble size distribution. A gas flow rate of 3.5 litres/hour at room temperature and pressure was chosen after studying the results and comments of Sheiham and Pinfold (1972) and Reay and Ratcliff (1974).

4.6.5 Bubble size determination

The bubble size distribution present in the flotation cell was determined photographically. A flash

unit was positioned behind the flotation cell and an Exacta 11A 35mm camera, fitted with its microscope attachment, was placed in front. A microscope fitted with a x7 objective provided sufficient magnification. With this arrangement a magnification of x6 was produced onto 35mm Panatomic-X film. The film was developed in Kodak D19 developer for 6 minutes at 20°C. The developed films were analysed on a P.C.D. Limited, Digital Data Recorder Model ZAE 3A. This instrument produces digital output from an analogue position sensing device. It has a built in scaling system and the great advantage of producing digitized position co-ordinates on punched paper tape. The total magnification from bubble to data recorder screen was x60 .

A computer programme was adapted from one written by P. Starkey, a fellow student, to determine the arithmetic mean diameter and the standard deviation of a sample of bubbles. The mean diameter from a number of negatives was 53 microns with a standard deviation of 9 microns. The distribution is shown in Figure 4.8 and Figure 4.9 is a photograph of the bubbles.

Under similar but not identical conditions Sheiham and Pinfold (1972) found a mean bubble diameter of 67 microns. Reay and Ratcliff (1974) quote Kaufmann (1974) producing a mean diameter of 40 microns on a fine frit of pore size 4 - 5.5 microns, and Kalman (1974) producing a mean diameter of 70 microns on a coarser frit

Figure 4.8 Bubble size distribution (sodium sulphate concentration 1.3×10^{-4} M)

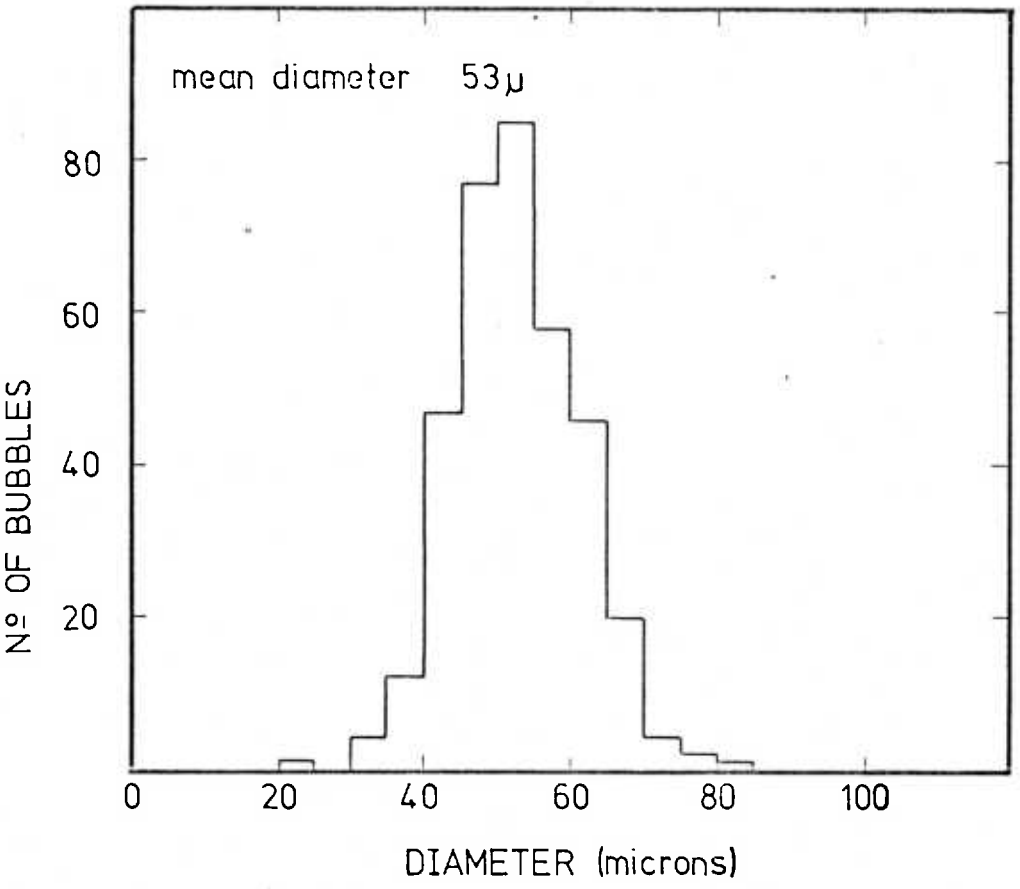

Figure 4.9 Photomicrograph of the bubbles

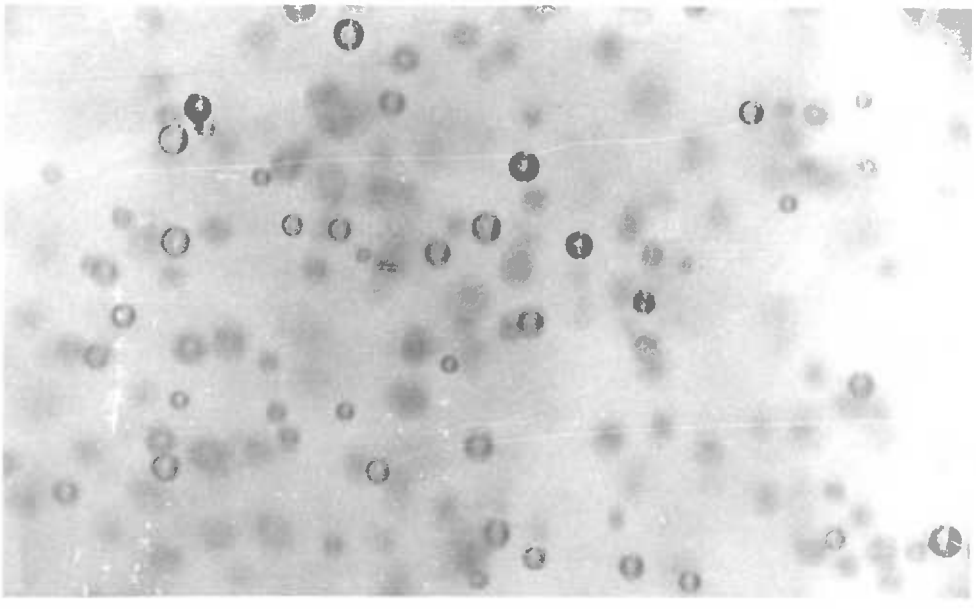

100 microns

of pore size 10 - 15 microns.

Bubble size determinations are notoriously difficult to make accurately. As much care as possible was taken to ensure an accurate value for the mean bubble diameter produced in the flotation cell, but only a small fraction of the bubbles could be measured, It would be foolish to say "the bubble diameter in the flotation cell was 53 microns", however we can confidently say that the bubbles in the flotation cell had diameters less than 100 microns.

4.6.6 Bubble sizes from glass frits and single orifices

As a final note on bubble size it is interesting to compare the sizes of bubbles produced on a fine frit with those produced at a single orifice.

The well known formula for the size of bubbles produced at a single orifice, balances buoyancy forces against surface tension forces. The formula can be written as:

$$a_0 = \frac{2 \rho_f \, g \, a_b^3}{3 \, \gamma}$$

Where a_0 is the radius of the orifice

ρ_f is the density of the fluid (for a gas bubble)

g is the acceleration due to gravity

a_b is the radius of the bubble

γ is the surface tension of the liquid

Taking ρ_f as 1 gm/cc, g as 980 cm/sec^2, a_b as 50 x 10^{-4}cms (50 microns) and γ as 30 dynes/cm then a_0 must be 2.5 x 10^{-6} cm, an impossibly small orifice, and two orders of magnitude less than the minimum pore size of the frit quoted by the manufacturer (5 x.10^{-4}cm).

Looking at it another way, given a pore size of 5 x 10^{-4}cm the surface tension would need to be 1.6 x 10^{-2} dynes/cm, again a difficult figure to accept.

It is interesting to speculate on the mechanism which produces such small bubbles on a glass frit.

4.7 Particle dispersion

A reproducible method for dispersing the particles in the flotation solution had to be found. Gentle mixing of the polystyrene powder was not successful, because the hydrophobic polystyrene particles simply remained on the surface of the solution. By trial and error it was found that the particles could be dispersed by stirring the mixture vigorously while it was in an ultrasonic bath. The particles appeared to be dispersed after about 20 minutes of this treatment. This judgement was tested as follows:

The usual quantity of polystyrene powder (0.5gms/litre) was added to the flotation solution. Samples were taken at intervals after the addition. The particle size distributions were determined with the Coulter Counter. The nonionic detergent was not added to the analysing

solution as it almost certainly would have dispersed any agglomerates. A paired students "t" test (Chatfield (1970)) was made between the counts in each size interval for the sample taken 20 minutes after the start of the experiment, and every other sample. The results of this comparison are shown in Table 4.2 .

Table 4.2 Comparison of samples to check dispersion of particles

Time (minutes)	"t" statistic
3	3.71
20	reference
40	1.57
60	1.23
80	0.56

The critical value of "t" for the experiment is 2.26 at the 95% confidence level. The analysis shows that there was statistically no difference between the size distributions of the sample taken after 20 minutes and every later sample. This result was taken to mean that the dispersion was complete after 20 minutes.

4.8 The experimental procedure

With the basic techniques required for the experiment

now described, it is possible to detail the procedure adopted for flotation experiments.

a) Two litres of flotation solution was prepared. As a reminder, the solution contained CTAB (5×10^{-5}M), ethanol (0.5% V/V) and varying amounts of sodium sulphate which was added to change the zeta potential of the particles and bubbles.

b) This solution was twice passed through a porosity 4 sintered glass filter to remove coarse particles.

c) 1500mls of the solution was adjusted to pH 8.0 ± 0.1 with N/10 NaOH.

d) The solution was placed in an ultrasonic bath and stirred vigorously.

e) After one minute a sample was taken. Samples were about 15mls taken with a 20ml pipette with the tip cut off which allowed for quick sampling. The sample was run into a test tube containing one drop of the nonionic surfactant solution described earlier. This particular sample was the blank background sample for the experiment.

f) The required amount of polystyrene powder, usually 0.75gms was added to the remainder of the 1500mls of the flotation solution stirring in an ultrasonic bath. This gave the solution a particle concentration of 0.5 gms/litre, well within the limit given for "free" flotation by Tomlinson and Fleming (1963)

g) After at least 40 minutes the pH was checked

and adjusted if necessary (as it usually was) to pH 8.0 ± 0.1 . A sample was taken to determine the electromobility of the particles. During the electromobility determination a visual check was made on coagulation. The remainder of the solution was placed back into the ultrasonic bath and stirred.

h) The flotation apparatus was prepared by rinsing the sintered glass disk with some particle free flotation solution. The nitrogen flow was then adjusted to 3.5 litres/hour, with a small quantity of the particle free flotation solution in the cell.

i) The pH of the solution was checked for the last time and adjusted to 8.0 ± 0.1 if necessary.

j) A sample was then taken which gave the initial concentration of particles. The remaining suspension was poured immediately into the flotation cell and the suction was started. Samples were taken at appropriate time intervals and transferred to test tubes containing one drop of nonionic surfactant. Six samples including the $t = 0$ sample were taken in early experiments, in later experiments seven samples were taken.

k) Each sample was analysed using the Coulter Counter. Coagulation of the polystyrene particles occurred in the test tubes if they were allowed to stand for more than a few minutes. This was reversed by placing the tubes in an ultrasonic bath immediately before analysis.

l) The general background count of the modified

Isoton was checked to make sure it was negligible (less than 0.1% of the expected particle count). 10mls of the sample from a test tube was then added to 150mls of the modified Isoton. The whole was then placed finally in the ultrasonic bath for about 5 minutes before analysis. At least duplicate counts were made at each instrument setting. The settings used in the experiments and the resulting particle sizes are given in Appendix A.2 . The temperature of the flotation solution was kept between $18^{o}C$ and $23^{o}C$.

4.9 Preliminary tests

With the general conditions of flotation fixed, a number of preliminary tests were conducted to determine the importance of subsidiary processes in the flotation cell.

4.9.1 Mixing in the cell

The particles in the cell were well mixed, this was checked by injecting a dye into the flotation cell. The dye was completely mixed in a few seconds.

4.9.2 Depletion of surfactant

A flotation solution containing 5×10^{-5}M CTAB and 0.5% V/V ethanol was poured into the flotation cell and 3.79 litres/hour of nitrogen (at room temperature and pressure), was passed through for 12 minutes. This gas flow rate was greater than the aim (3.50 litres/hour).

No polystyrene particles were added in case their presence affected the analytical technique.

Samples from the flotation cell were taken at intervals during the experiment, and analysed for CTAB colorimetrically. The method of analysis was essentially that of Sheiham and Pinfold (1969). A 20ml sample was diluted to 40mls with water, and 2mls of 0.1% W/W picric acid in 0.002M sodium hydroxide was added. The whole was shaken with 20mls of 1,2-dichloroethane for about 5 minutes; the optical density of the organic layer was measured at 3750Å in 1cm cells. The calibration graph did not adhere to Beer's Law as Sheiham and Pinfold had found, but it was quite reproducible.

The resultant graph of CTAB depletion is shown in Figure 4.10. In 10 minutes, longer than any flotation experiment, the CTAB concentration had fallen to 60% of its initial value. The result of an experiment to determine the effect of surfactant depletion on the flotation rate of the polystyrene particles is presented in a later section 5.3.2 .

4.9.3 Coagulation of particles in the flotation cell

It was important to be sure that the polystyrene particles did not coagulate in the flotation solution during flotation. If they did, any comparison between particle size and flotation rate would be meaningless.

Figure 4.10 Depletion of CTAB during flotation - % removal versus time

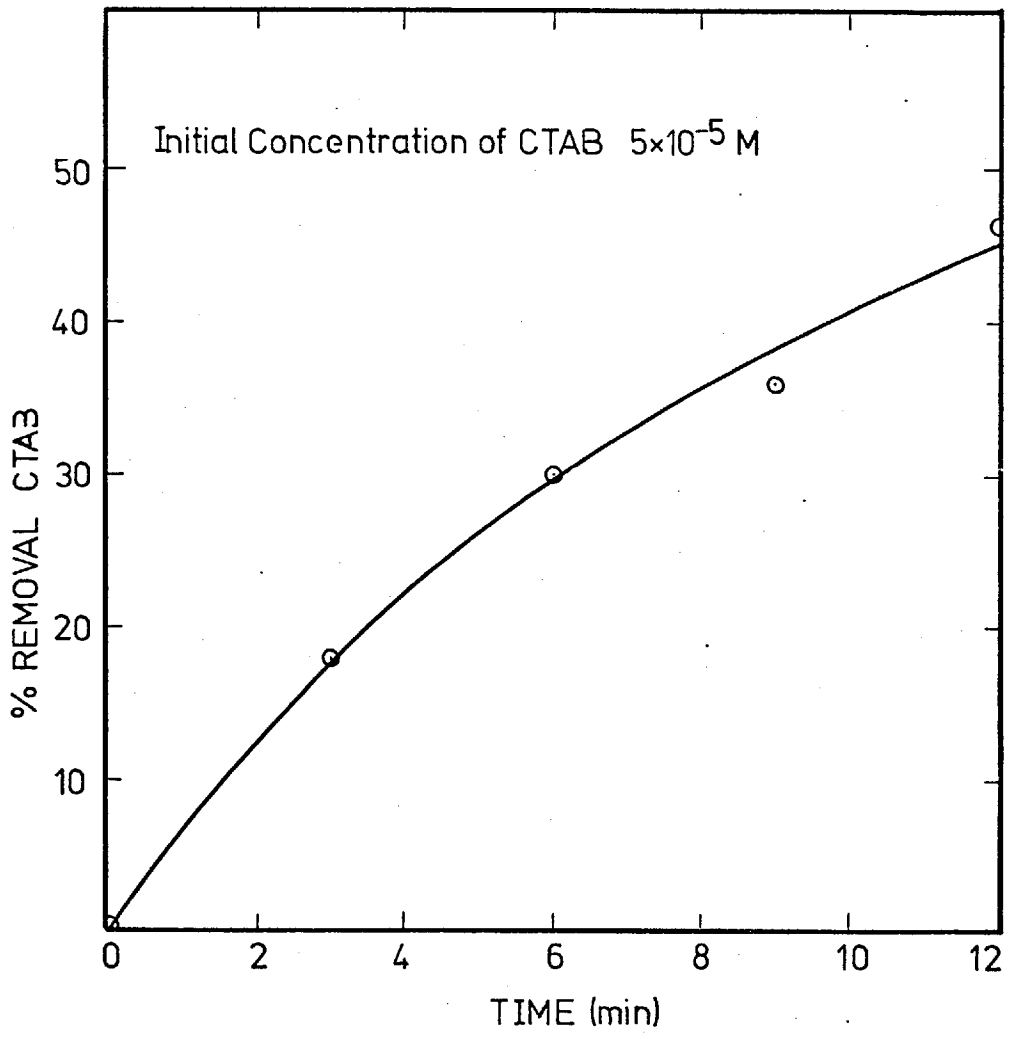

The critical zeta potential for suspensions is often quoted as 25 - 30mV (Kruyt (1952)). The minimum zeta potential reached in the present set of experiments was just over 30mV. So an experiment was run to see if coagulation in the flotation solution was important.

A solution was made up in the usual way, with a sodium sulphate concentration of 10^{-2}M. At this concentration (which was the highest used in the experiments) the zeta potential of the particles would be a minimum. The electromobility of the particles in the suspension was measured 40 and 210 minutes after mixing. The electromobilities were 3.1 and 2.9 microns/sec/Volt/cm respectively, quite consistent with the high salt concentration.

After two hours of mixing in the ultrasonic bath (the normal preparation time) the bath was switched off and the stirrer slowed to about 300 rpm. This was done to simulate the gentle stirring that the solution receives from the bubbles in the flotation cell. Samples of this suspension were taken at time intervals and transferred to a beaker containing 150mls of Isoton. The Isoton contained no nonionic dispersing agent as this would have biased the results. After exactly 15 seconds stirring, two counts were made as quickly as possible, to count the number of particles greater than 4.6 microns. This size was chosen to ensure maximum sensitivity to changes in particle concentration. The results of this experiment are given in Table 4.3 .

Table 4.3 Coagulation experiment results

Time t (minutes)	Mean count	N_o/N_t
0	12081	1.0000
6	12003	1.0065
12	12141	0.9951
19	12020	1.0051
40	11773	1.0265

Where N_o is the count at time = 0

N_t is the count at time t

Considering that the repeatability of the Counter is at best 1%, the counts are remarkably constant. So from the table it can be seen that coagulation did not occur until at least 40 minutes after mixing. The normal time taken for an experiment at this concentration of sodium sulphate was 4 minutes, and the maximum time taken for any experiment was 9 minutes. So we can confidently say that coagulation of polystyrene particles during flotation was not an important process.

4.9.4 Redispersion of the particles in the foam

The purpose of the suction box sitting above the flotation cell was to remove the foam produced, and so eliminate the transfer of particles from the foam back into the dispersed phase. To test its operation an experiment was required.

A particle suspension with a concentration of 10^{-2}M sodium sulphate was floated in the usual way. After 4 minutes the nitrogen line to the cell was disconnected and a sample taken. The suction box remained in operation and the solution was gently stirred with a spatula for another minute, another sample was then taken. Both samples were analysed and the results compared using the paired "t" test. There was no significant difference at the 95% confidence level between the two sets of data. This shows that redispersion was not an important process during flotation.

4.10 Summary

In this chapter the equipment, materials and techniques used in the investigation were described.

Tests were carried out and showed that:

a) The bubbles produced in the flotation cell had diameters less than 100 microns.

b) The polystyrene particles could be dispersed reproducibly in the flotation solution.

c) The particles were well mixed in the flotation cell.

d) Up to 40% of the surfactant was removed during a flotation experiment.

e) The particles did not coagulate during a flotation experiment, remaining discrete spheres.

f) Once removed from the dispersed phase the particles did not return, so froth processes could be ignored.

CHAPTER 5

EXPERIMENTAL RESULTS

The rate of flotation of the polystyrene particles was measured in the flotation system described in Chapter 4. The particle and bubble electromobilities were altered by the addition of various amounts of sodium sulphate to the flotation solution. In this chapter the methods used to treat the raw experimental data are explained. The results are then presented in graphical and tabular form and discussed in relation to the experimental and theoretical background. A discussion of errors completes the chapter.

5.1 The rate of flotation results

5.1.1 Calculation of the rate constant

The data from the Coulter Counter were worked up in the appropriate way. Details of the manipulations are given in Appendix A.2 . The corrected counts were subtracted successively from each other to provide the number of particles in a size interval. The diameter of all the particles in a size interval was assumed to be the arithmetic mean of the interval limits.

The assumption of first order kinetics with respect to particle concentration was made, and yielded the following equations:

$$-\frac{dN_t}{dt} = k_p N_t \qquad (5.1)$$

Where t is the time in minutes

N_t is the count at time t

k_p is the first order rate constant

It must be remembered that N_t is really the concentration of particles in the sample volume (10mls). Integrating equation 5.1 with the boundary condition:

$$N_t = N_o \text{ at } t = 0 \qquad (5.2)$$

We obtain:

$$\ln\left[\frac{N_o}{N_t}\right] = k_p t \qquad (5.3)$$

Equation 5.3 shows that a plot of $\ln [N_o/N_t]$ versus time should yield a straight line with a slope equal to k_p, the rate constant, which is a measure of the rate of flotation. The results were plotted and a least squares technique (a CERN routine) was used to estimate the slope, a subroutine was written to determine the standard error of the slope. The data manipulation described was carried out on a digital computer, a listing of the programme is given in Computer Programmes P1 .

5.1.2 The assumption of first order kinetics

The assumption of first order kinetics is attractive

if only for its simplicity, but the correctness of the assumption has been argued for many years. Klassen and Mokrousov (1963) say that first order kinetics should be observed in flotation, but they quote Bogdanov et al. (1954) as finding that the order varied in their experiments from first to sixth, and Arbiter (1954) found second order in his experiments. De Bruyn and Modi (1956) found that the rate was first order for particle sizes below 65 microns provided the solids content of the pulp was less than 5.2%. Tomlinson and Fleming (1963), Morris (1952), Bushell (1962) and Woodburn and Loveday (1963) agree that the assumption of first order kinetics is justified for equal sized, identical particles. Recently Sheiham (1970) and Reay and Ratcliff (1974) have used first order kinetics successfully in flotation experiments.

Flint (1973) says he is thankful that the time has passed when flotation researchers attached considerable importance to the order of the microkinetic equation 5.1 and there seems no point in upsetting him here. In this study first order kinetics was used because it provided a good measure for the rate of flotation.

5.1.3 The gas flow rate

The gas flow rate was determined from readings of the manometer and the soap film flow meter. The actual flow rate was never exactly 3.5 litres/hour which was the aim, so the values of the rate constants were corrected

to 3.5 litres/hour on the assumption:

$$k_p \propto \text{gas flow rate} \qquad (5.4)$$

All flow rates were calculated at room temperature and pressure. The relevant temperatures and pressures appear in Appendix A.3 .

5.2 Electromobility data

The electromobility data required no other treatment than the standard transformation of transit times in seconds to electromobility in microns/sec/Volt/cm.

5.3 The results

5.3.1 The plots of $\ln [N_o/N_t]$ versus time

The results of the experiments are given in Appendix A.3 . Figures 5.1 to 5.8 show the plot of $\ln [N_o/N_t]$ versus time for six particle diameters from eight representative experiments. It was more convenient to use particle diameter than particle radius in the experimental part of this work.

A number of comments can be made on these plots:

a) The assumption of first order kinetics was justified.

b) The slope decreases with particle diameter in each experiment.

c) Some of the lines of best fit do not intersect

Figure 5.1 Experimental results for 6 particle diameters - Experiment 2 Plot of $\ln(N_o/N_t)$ versus time

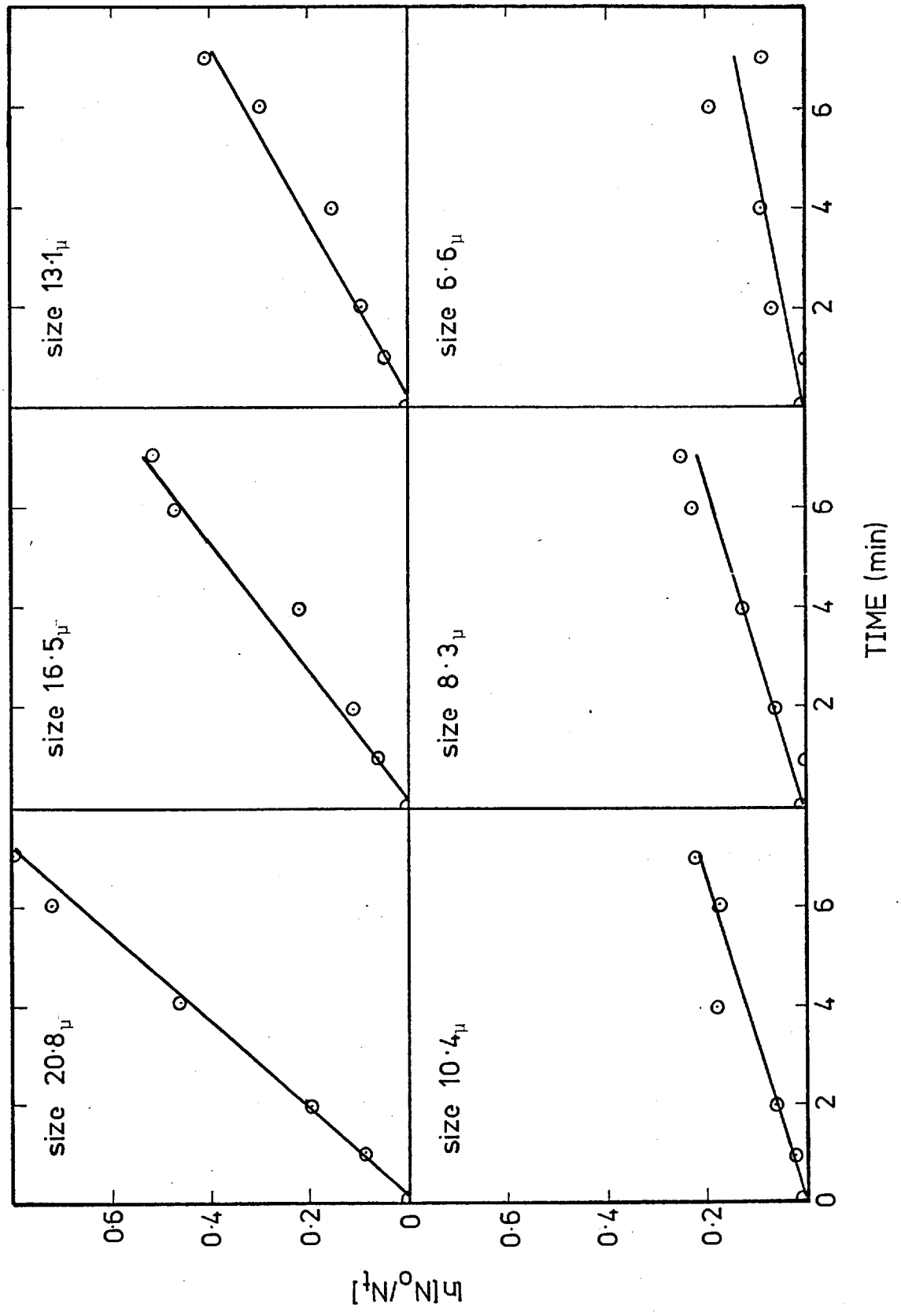

Figure 5.2 Experimental results for 6 particle diameters - Experiment 3 Plot of $\ln(N_o/N_t)$ versus time

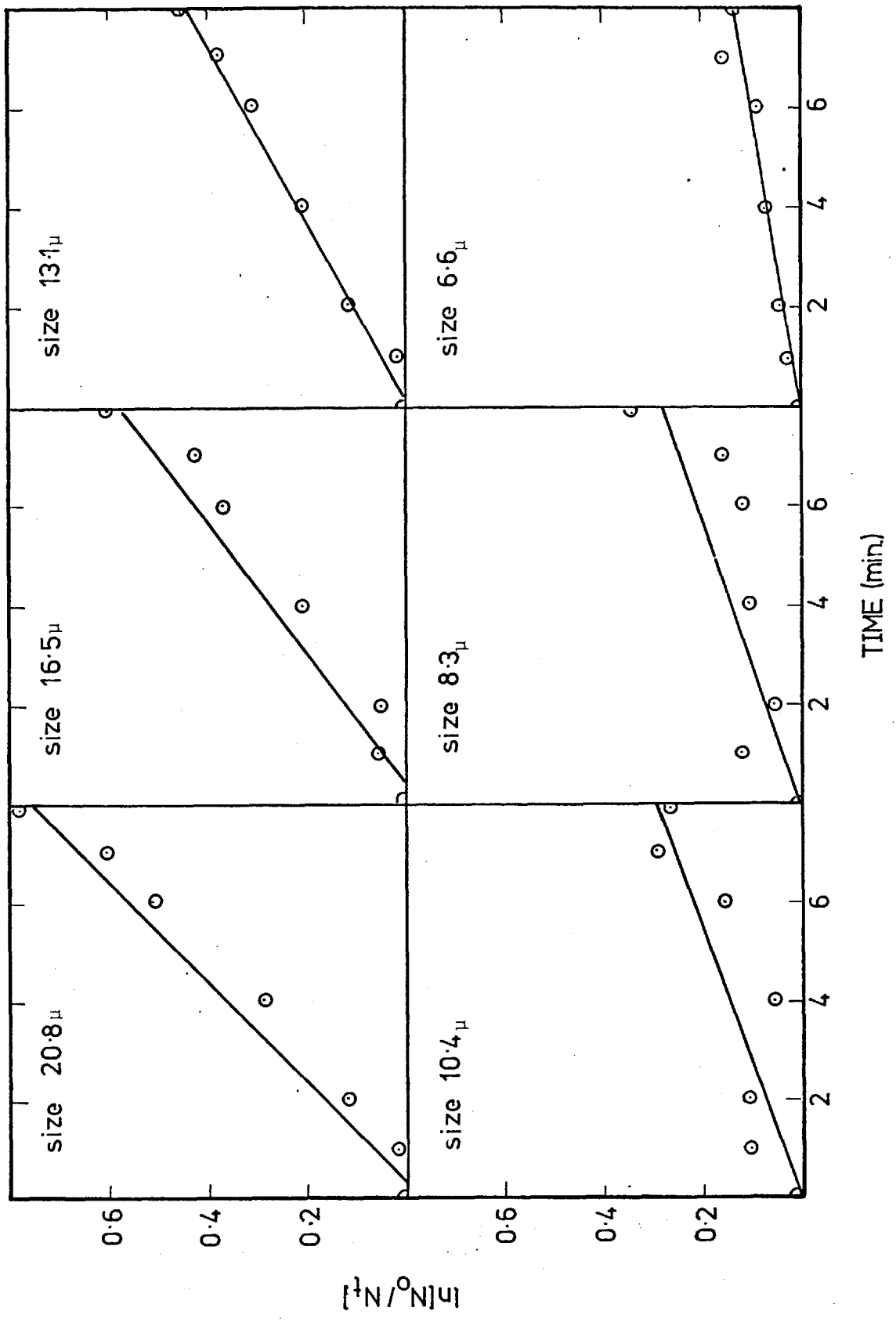

Figure 5.3 Experimental results for 6 particle diameters - Experiment 4 Plot of $\ln(N_o/N_t)$ versus time

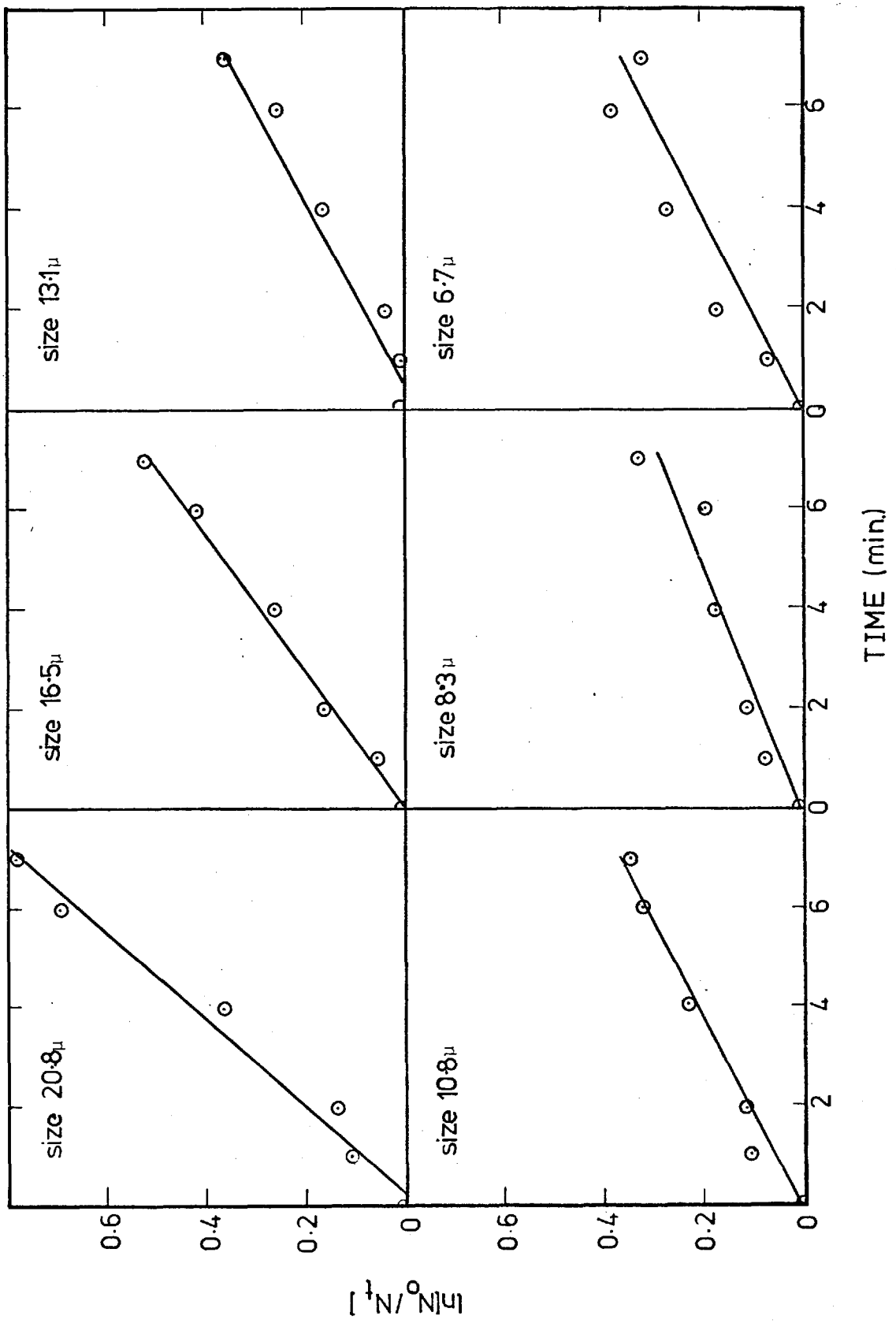

Figure 5.4 Experimental results for 6 particle diameters - Experiment 5 Plot of $\ln(N_o/N_t)$ versus time

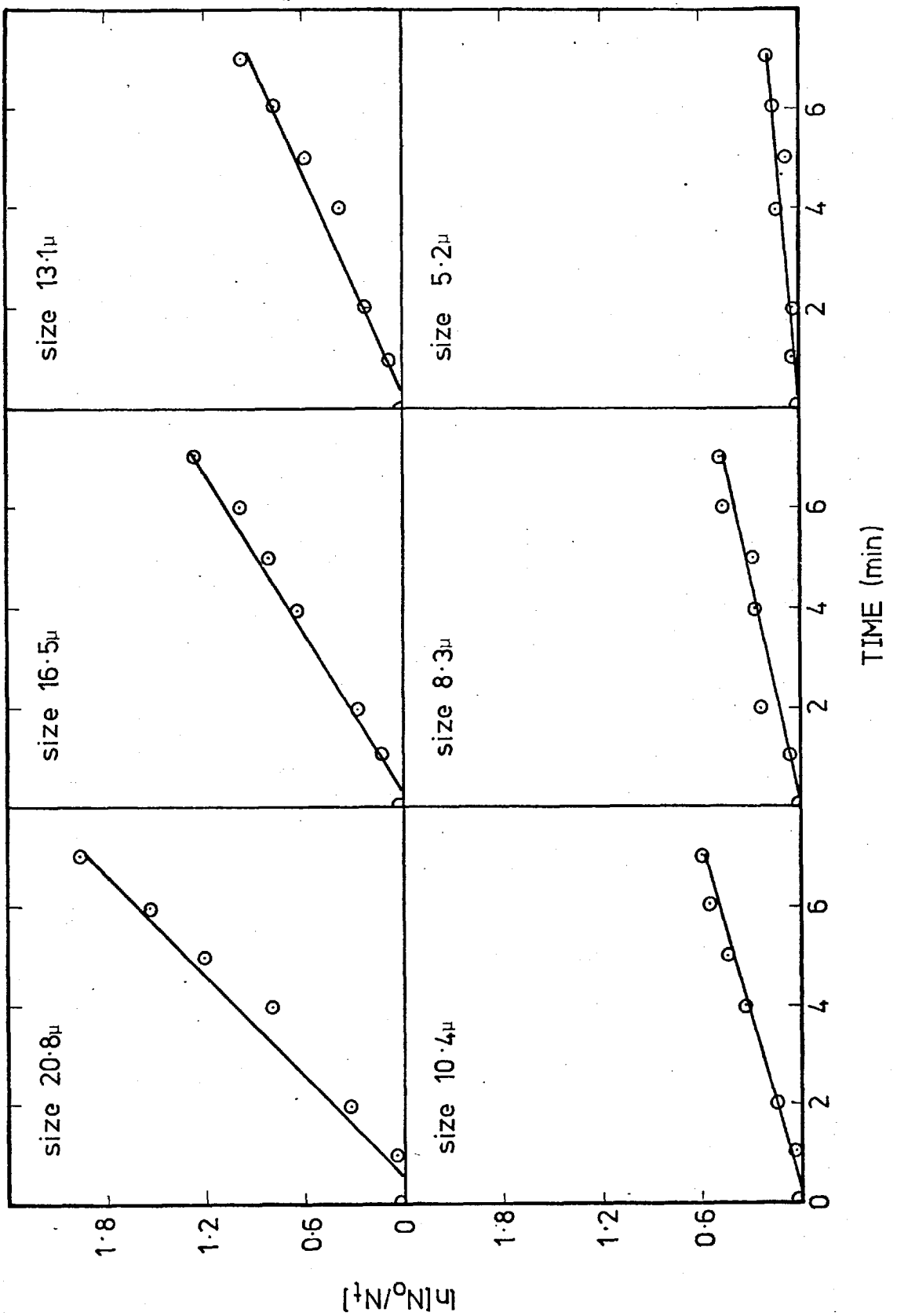

Figure 5.5 Experimental results for 6 particle diameters - Experiment 7 Plot of $\ln(N_o/N_t)$ versus time

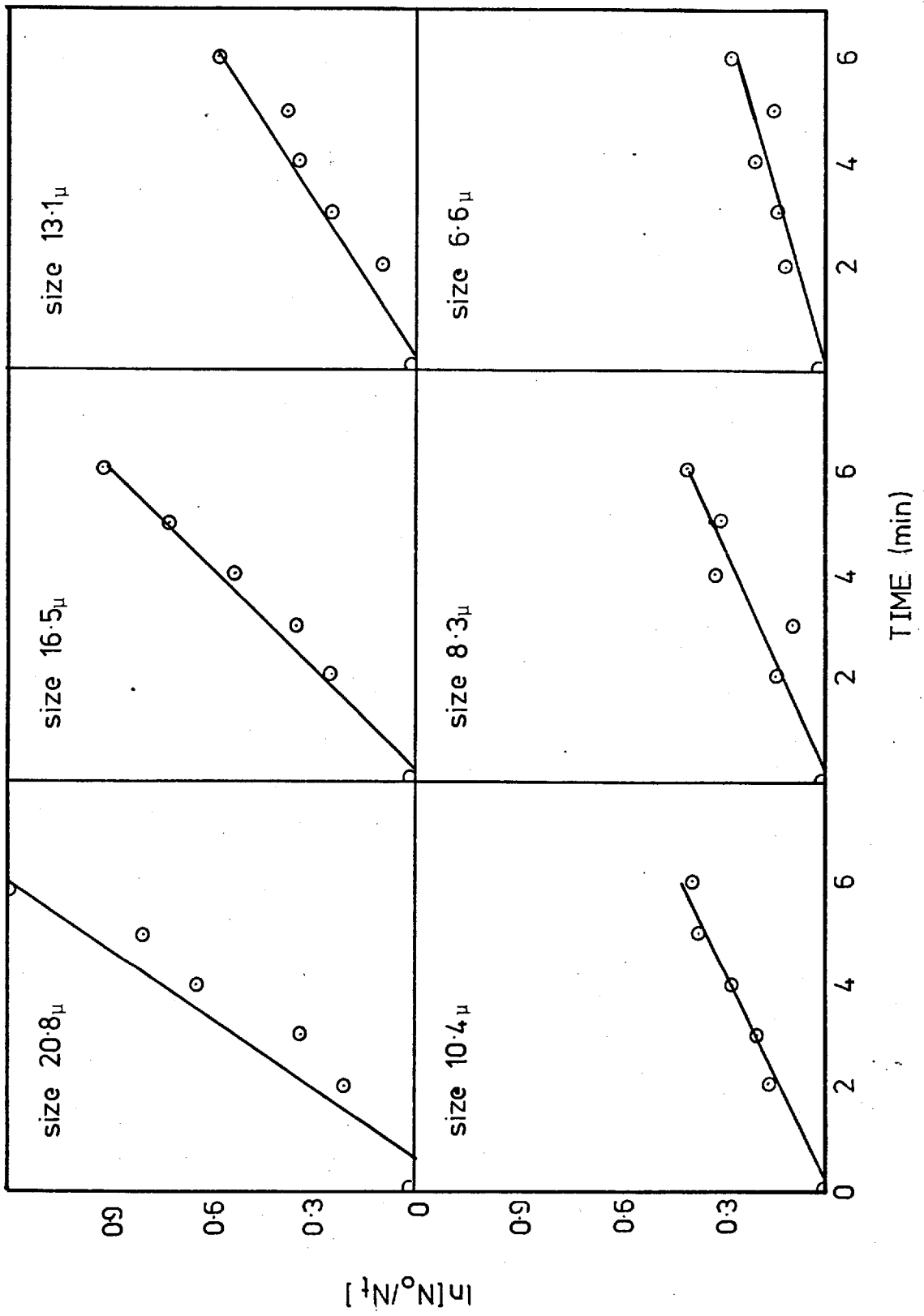

Figure 5.6 Experimental results for 6 particle diameters - Experiment 8 Plot of $\ln(N_o/N_t)$ versus time

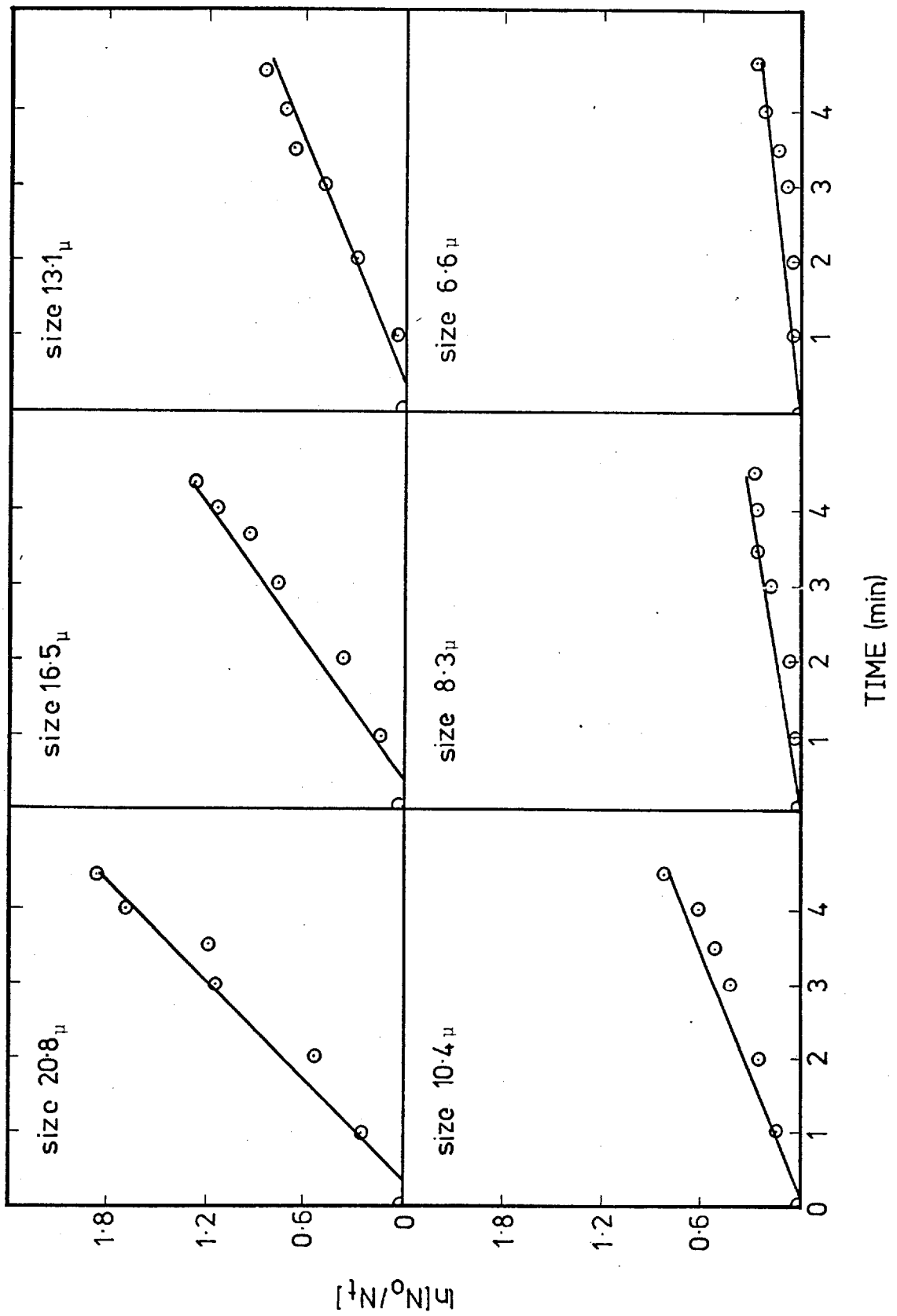

Figure 5.7 Experimental results for 6 particle diameters - Experiment 10 Plot of $\ln(N_o/N_t)$ versus time

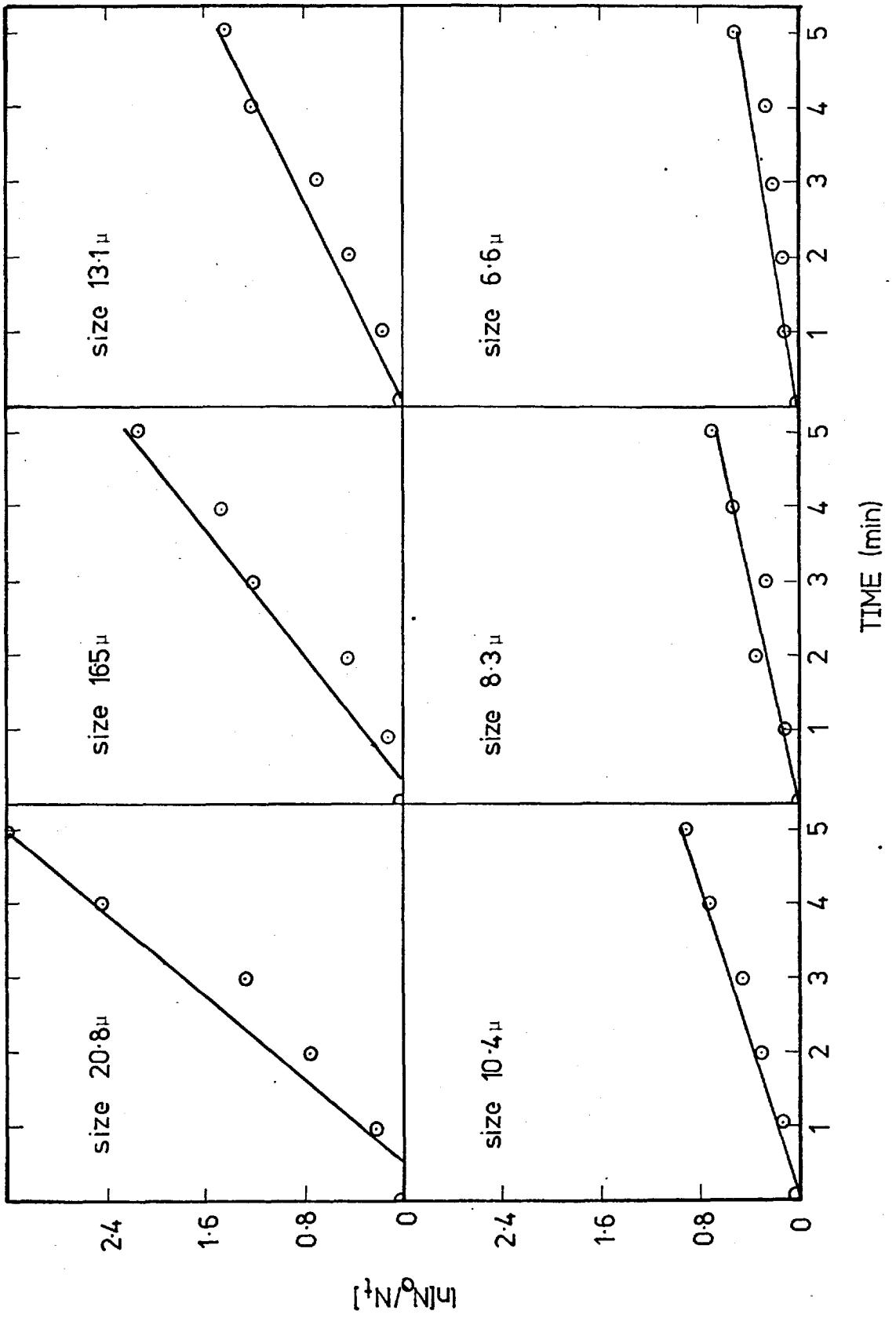

Figure 5.8 Experimental results for 6 particle diameters - Experiment 19 Plot of $\ln(N_o/N_t)$ versus time

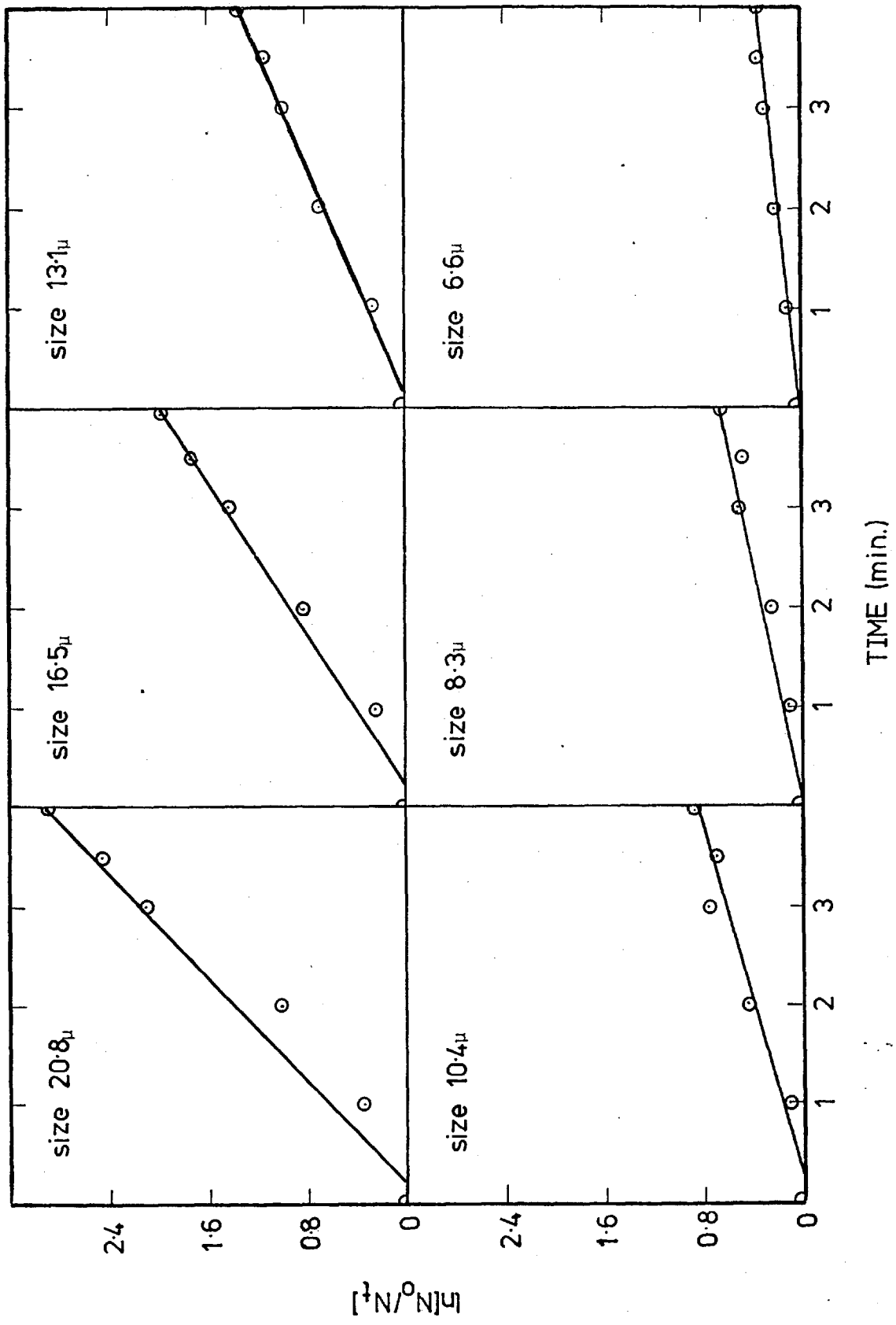

the time axis at zero as expected, but at 30 - 40 seconds. This has to be explained.

Sheiham (1970) was faced with the same problem. He attributed this to the uncertainty about the zero of time which was also uncertain in this work. Consider a 100 micron diameter bubble formed on the frit at the instant the flotation solution was placed in the cell. This time was assumed to be zero time. The 100 micron bubble would take about 20 seconds to rise to the top of the cell. During this time, although it may have captured particles it was still in the dispersed phase and its attached particles were capable of being sampled. Smaller bubbles obviously take longer to rise and complicate the matter further. The data of experiment 3 were calculated with 30 seconds taken from each time. The recalculated slopes were only 4% higher than the unadjusted slopes. Obviously the data from all the experiments could have been treated in this way, to produce lines of best fit which would pass through the origin. This was not done as there was some uncertainty about the correction to be applied, and the corrected slopes would not differ greatly from the uncorrected slopes.

5.3.2 The effect of surfactant concentration

In Chapter 4 it was shown experimentally that the surfactant concentration was reduced to about 60% if its original value by the end of a flotation experiment.

To see if this lowering of surfactant concentration greatly affected tha rate of flotation, an experiment was run with the initial concentration of surfactant 3.0×10^{-5}M, 60% of its normal value. The result of this experiment is presented graphically in Figure 5.9 which shows that the effect of the reduced concentration was small.

5.3.3 The relationship between the rate of flotation and particle diameter

The log of the rate of flotation (measured by the rate constant) was plotted against the log of the particle diameter; see Figures 5.10 to 5.14 . The results from replicate experiments (i.e. using the same concentration of sodium sulphate) were plotted on the same graph.

The data points were somewhat scattered but quite consistent. There was a definite linear relationship between the log of the rate constant and the log of the particle diameter. This suggests a relationship of the form:

$$k_p \propto (d_p)^N \qquad (5.5)$$

Where k_p is the rate constant
d_p is the particle diameter
N is the slope of the graph

The slope N was determined by a least squares method. The values of N are given in Table 5.1 .

Figure 5.9 The effect of reduced CTAB concentration on flotation rate

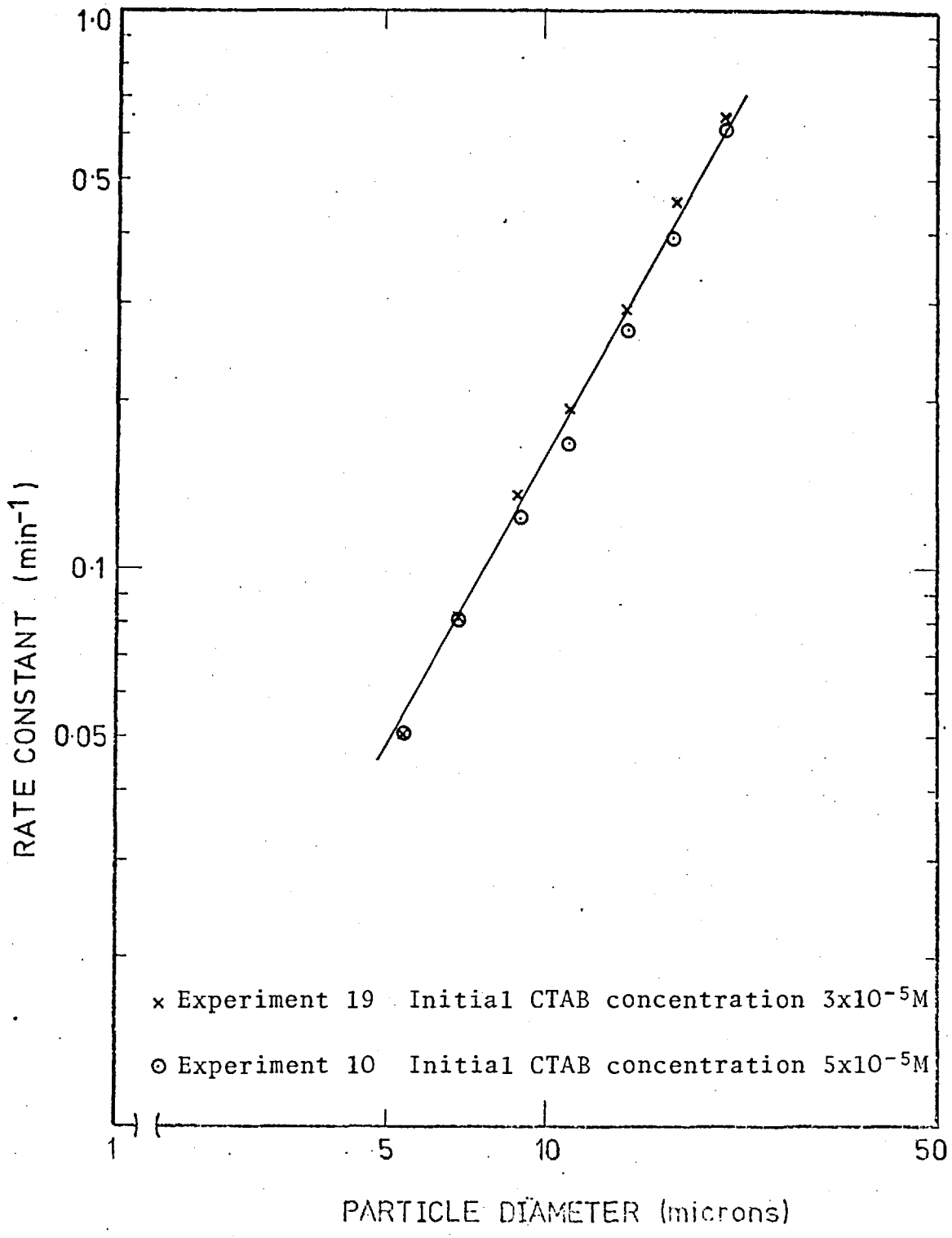

Figure 5.10 Experimental results - effect of particle diameter on flotation rate

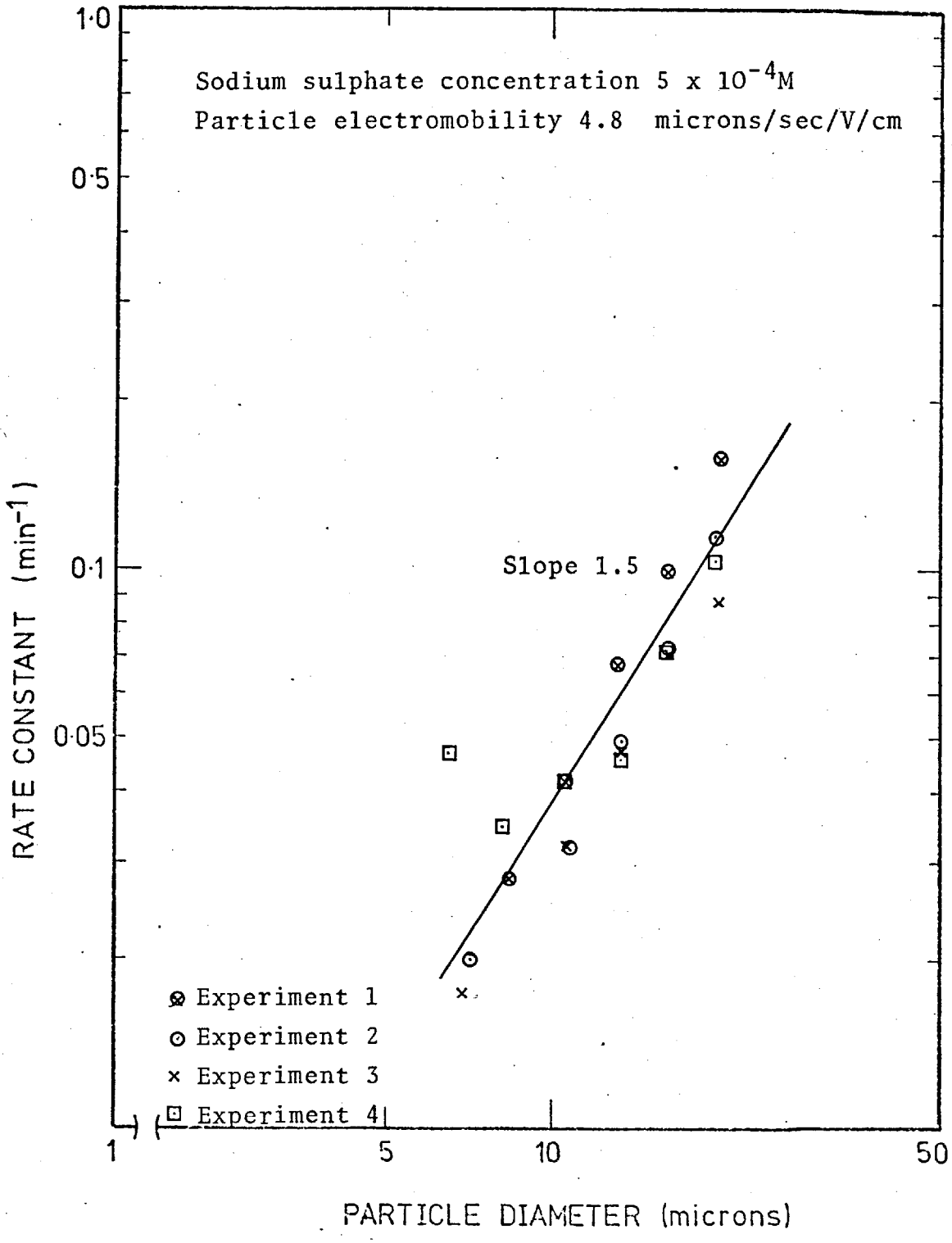

Figure 5.11 Experimental results - effect of particle diameter on flotation rate

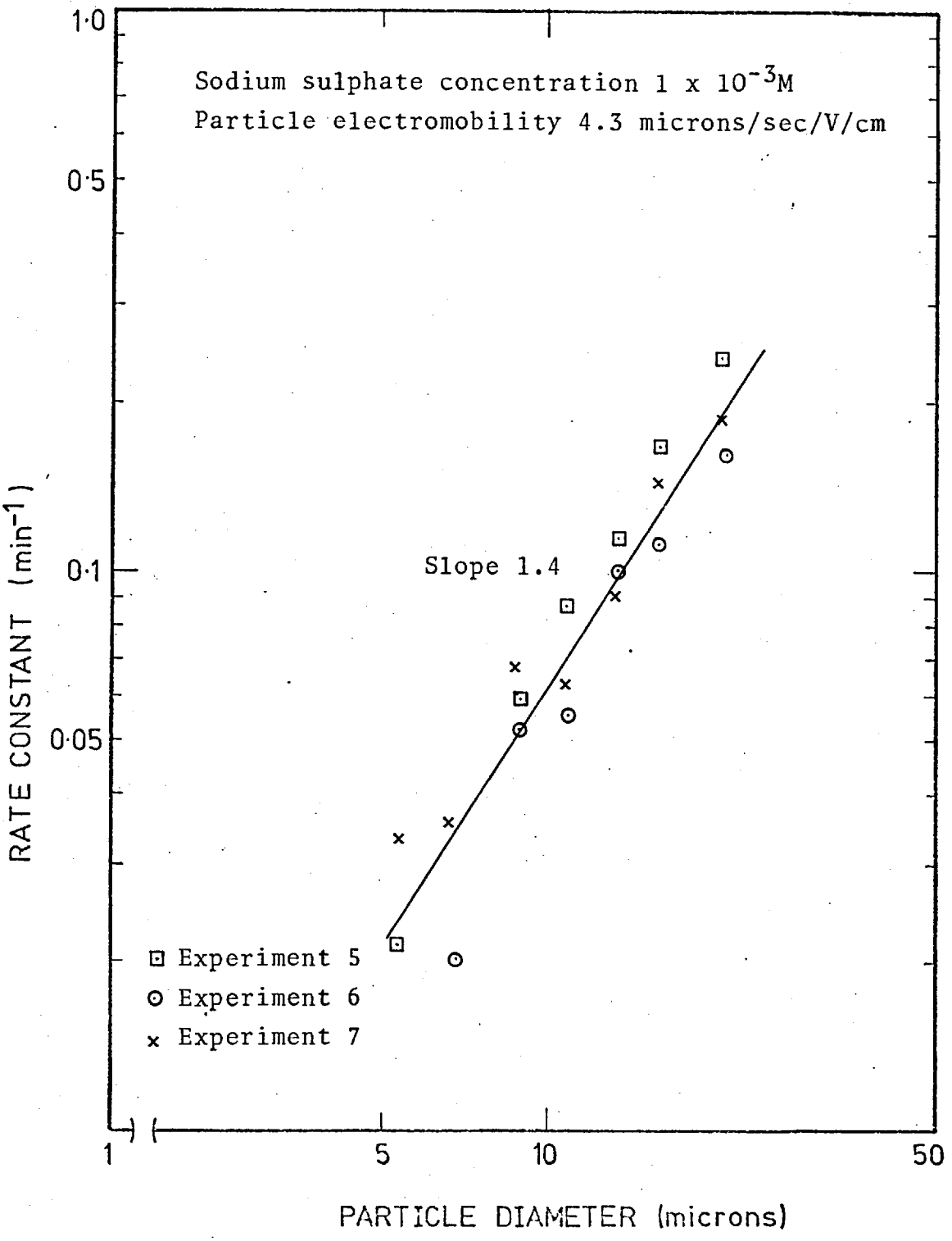

Figure 5.12 Experimental results - effect of particle diameter on flotation rate

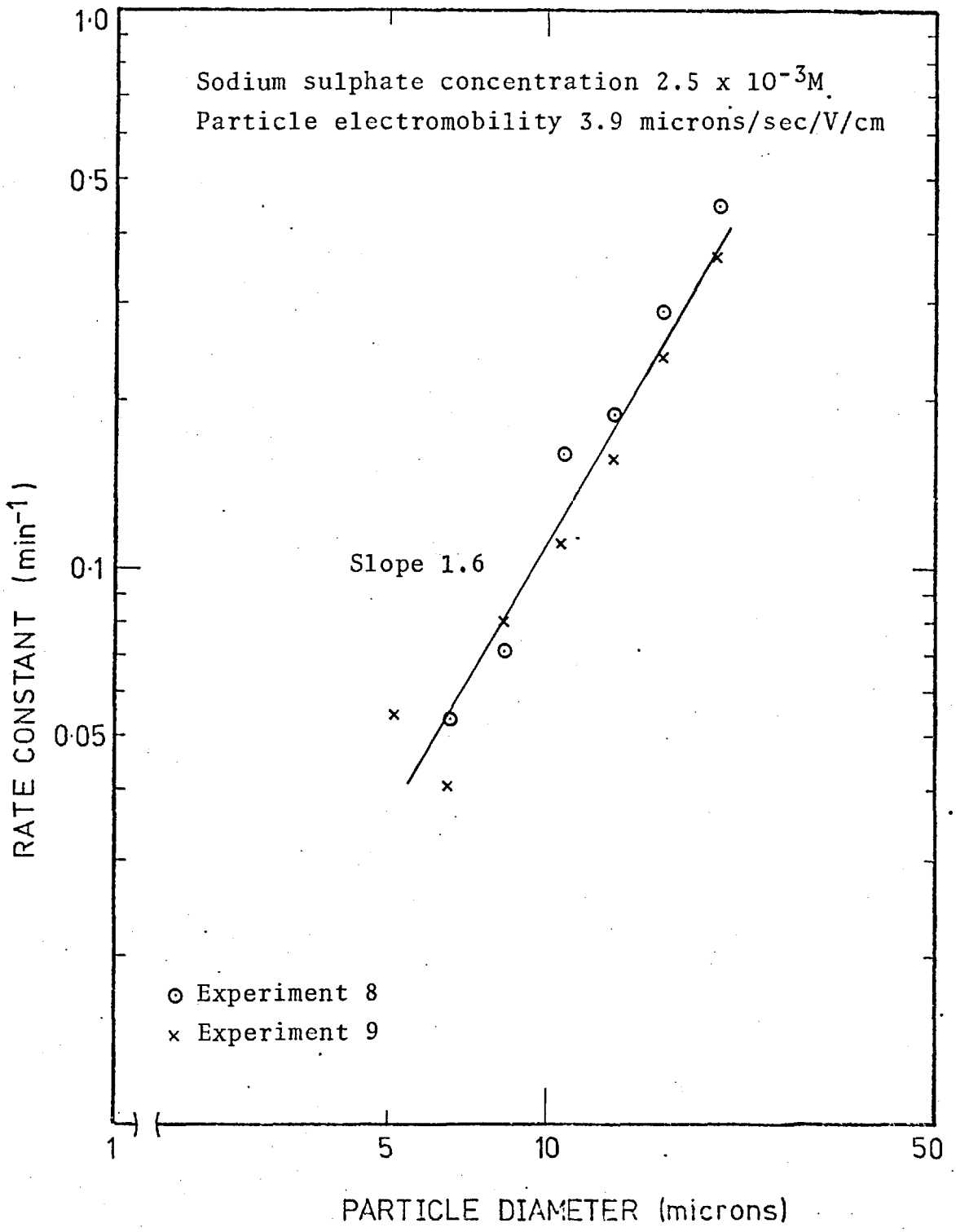

Figure 5.13 Experimental results - effect of particle diameter on flotation rate

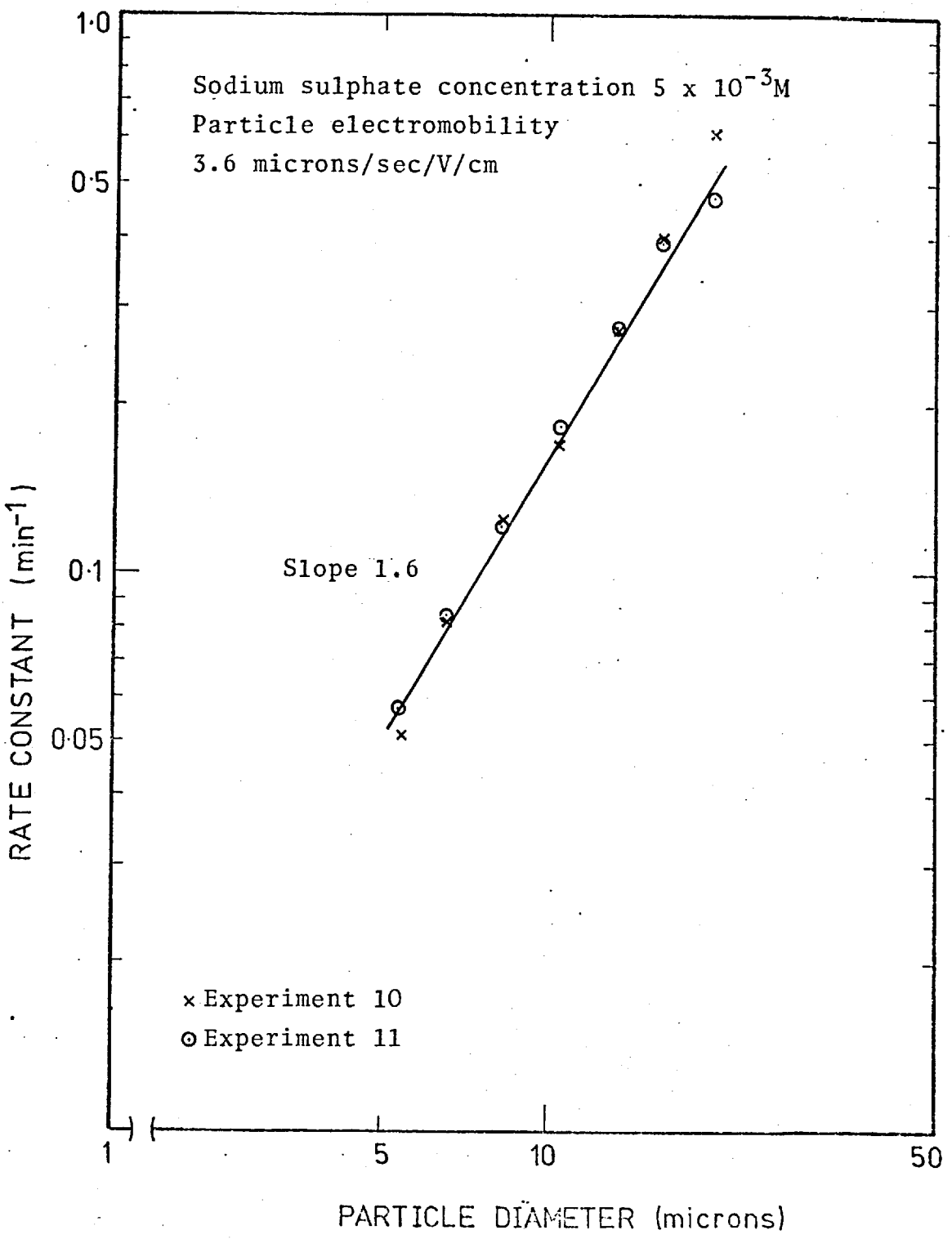

Figure 5.14 Experimental results - effect of particle diameter on flotation rate

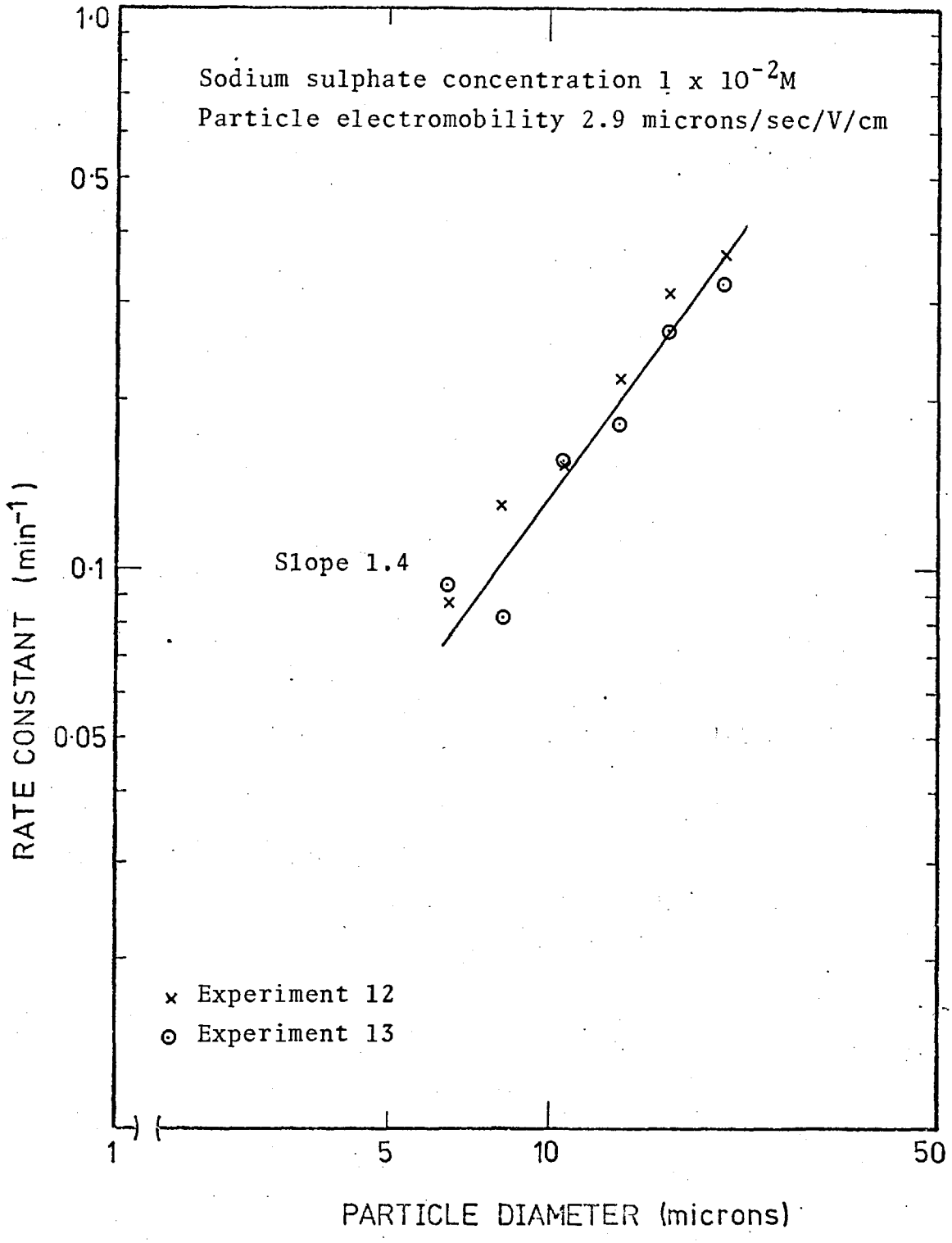

Table 5.1 The value of the exponent N in equation 5.5

Concentration of sodium sulphate	Mean mobility microns/sec/Volt/cm	Value of N
5.0×10^{-4}M	4.8	1.5
1.0×10^{-3}M	4.3	1.4
2.5×10^{-3}M	3.9	1.6
5.0×10^{-3}M	3.6	1.6
1.0×10^{-2}M	2.9	1.4

The value of the exponent for all experiments was about 1.5 . There was no systematic variation in the exponent for the different particle mobility conditions. The results for the sodium sulphate concentration of 1×10^{-4}M are not included because the flotation rate was very slow and the data were too scattered.

The value of the exponent (1.5) agrees very well with Reay and Ratcliff (1974) who obtained 1.5 for glass spheres. Their results for polystyrene particles could not be duplicated for any of the conditions tried in this work. The value of the exponent never approached the value of 0.49 that they had found. No explanation can be offered for their anomalous results for polystyrene particles.

Fitzpatrick and Spielman (1973) found that the filter coefficient in their experiments was proportional to the 1.0 - 1.5 power of the particle diameter in fair

agreement with the present work. The dependence strengthened to as much as the 3.0 power when the double layer repulsion between their particles and collectors was very high. This effect was not observed in these experiments.

5.3.4 The relationship between the rate of flotation and electromobility

It became obvious that there was a relationship between the rate constant and the electromobility of the particles (see tables in Appendix A.3). The data were replotted for each of the six particle sizes to determine the form of the relationship. Figures 5.15 to 5.20 show the replotted data. These graphs show the rapid increase in flotation rate that occurred as the electromobility of the particles was reduced. At an electromobility of about 3.5 microns/sec/Volt/cm there was a levelling off, or perhaps a maximum in the rate. These graphs bear a striking resemblance in shape to the graphs given by Fitzpatrick and Spielman (1973) for the plot of filter coefficient versus concentration of electrolyte in their filtration experiments. Now the electromobility of their test particles which were negatively charged, was related to this electrolyte concentration. The data from one of their experiments were taken and replotted in Figure 5.21 using a scale similar to the scale used in Figures 5.15 to 5.20 . Fitzpatrick and Spielman suggested that the sudden change in filter coefficient was due to the double layer

Figure 5.15 Effect of particle electromobility on flotation rate for particles with a mean diameter of 20.8μ

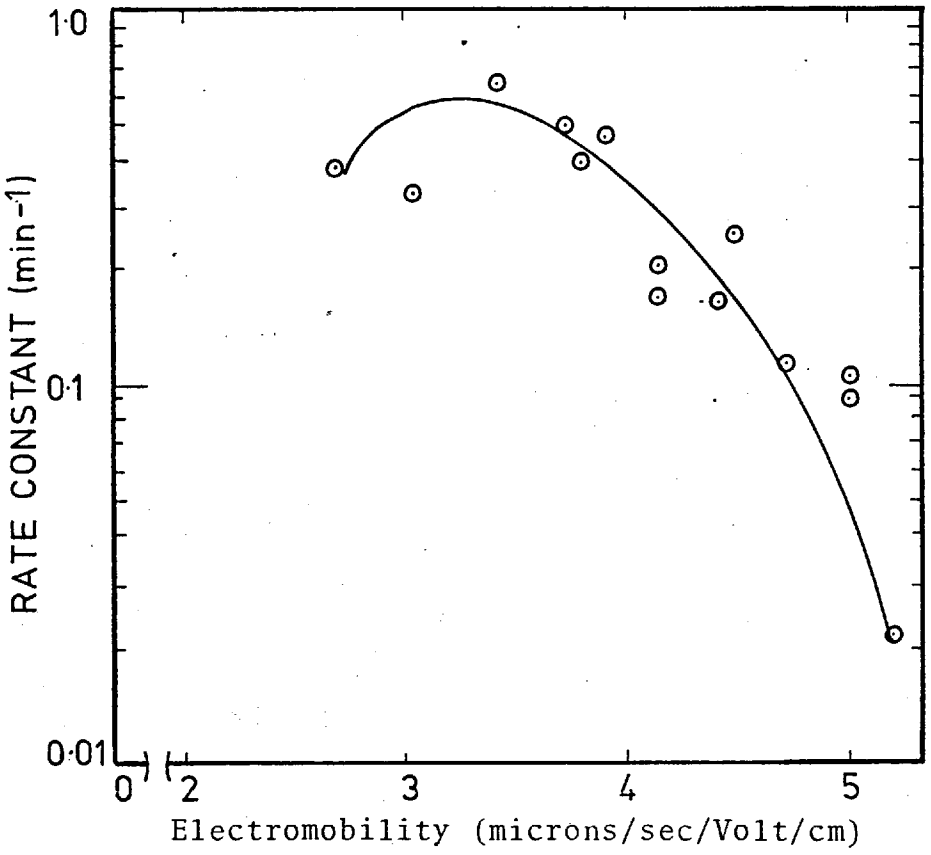

Figure 5.16 Effect of particle electromobility on flotation rate for particles with a mean diameter of 16.5μ

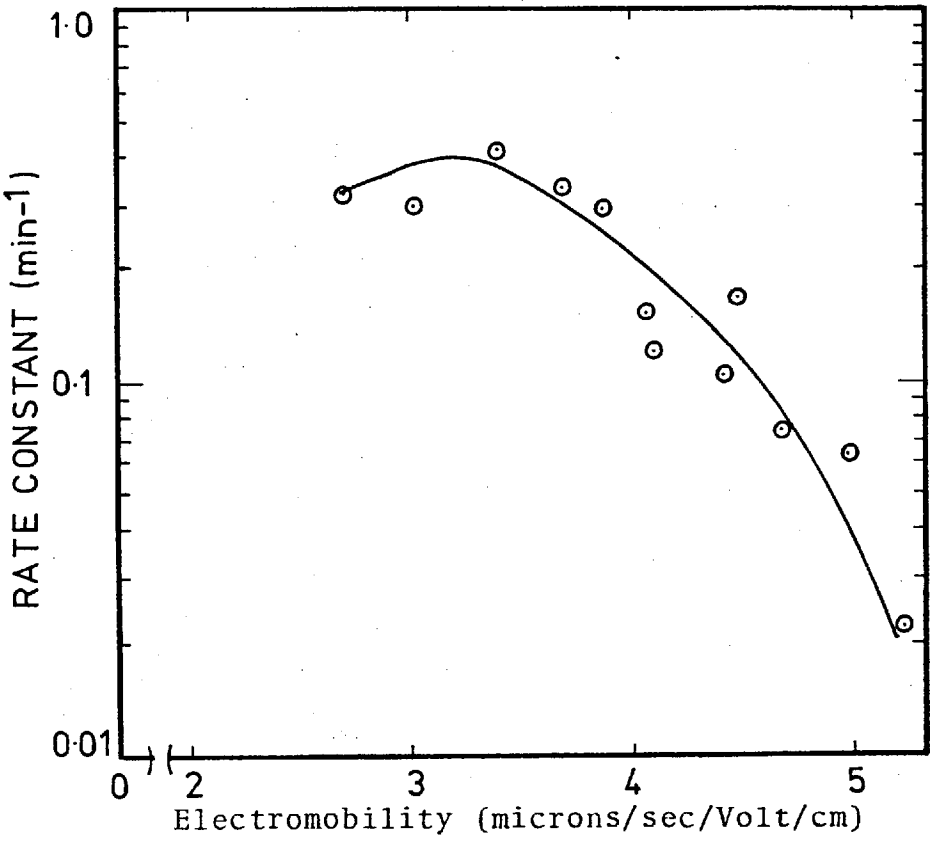

Figure 5.17 Effect of particle electromobility on flotation rate for particles with a mean diameter of 13.1μ

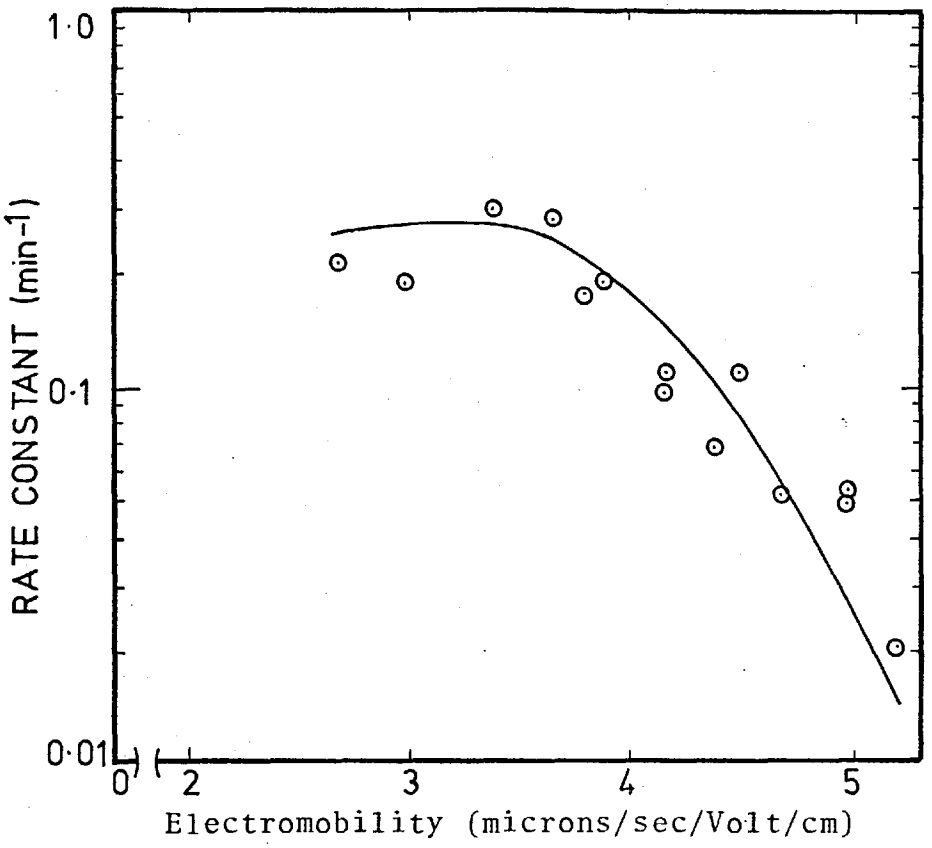

Figure 5.18 Effect of particle electromobility on flotation rate for particles with a mean diameter of 10.4μ

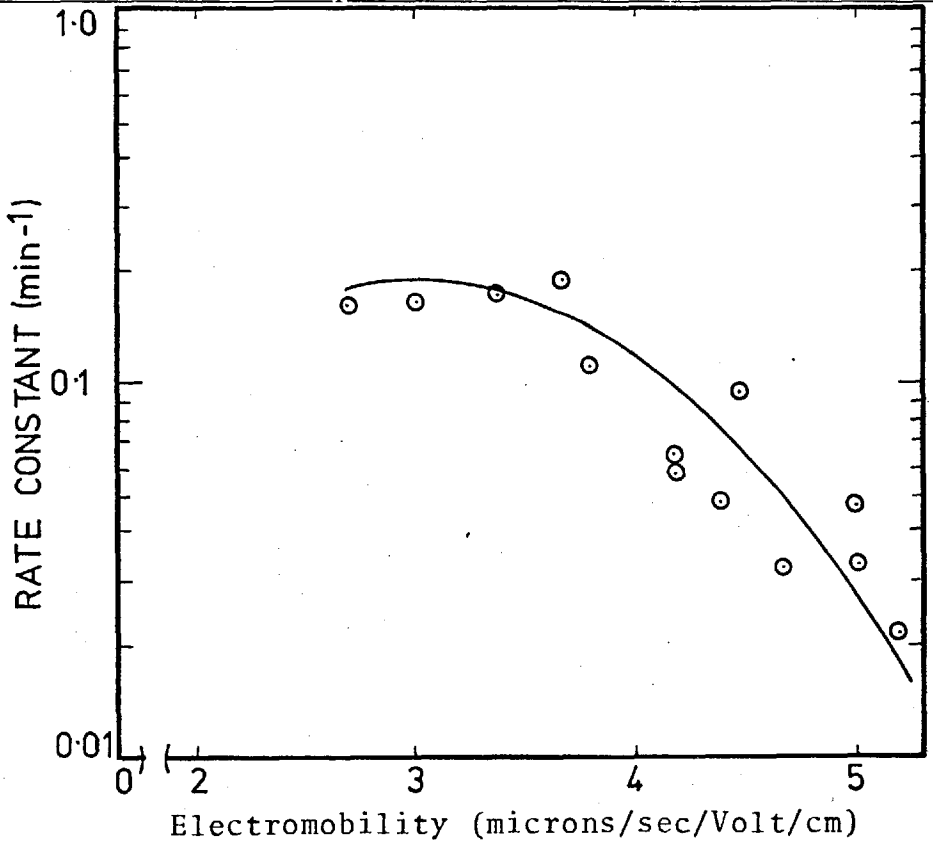

Figure 5.19 Effect of particle electromobility on flotation rate for particles with a mean diameter of 8.3μ

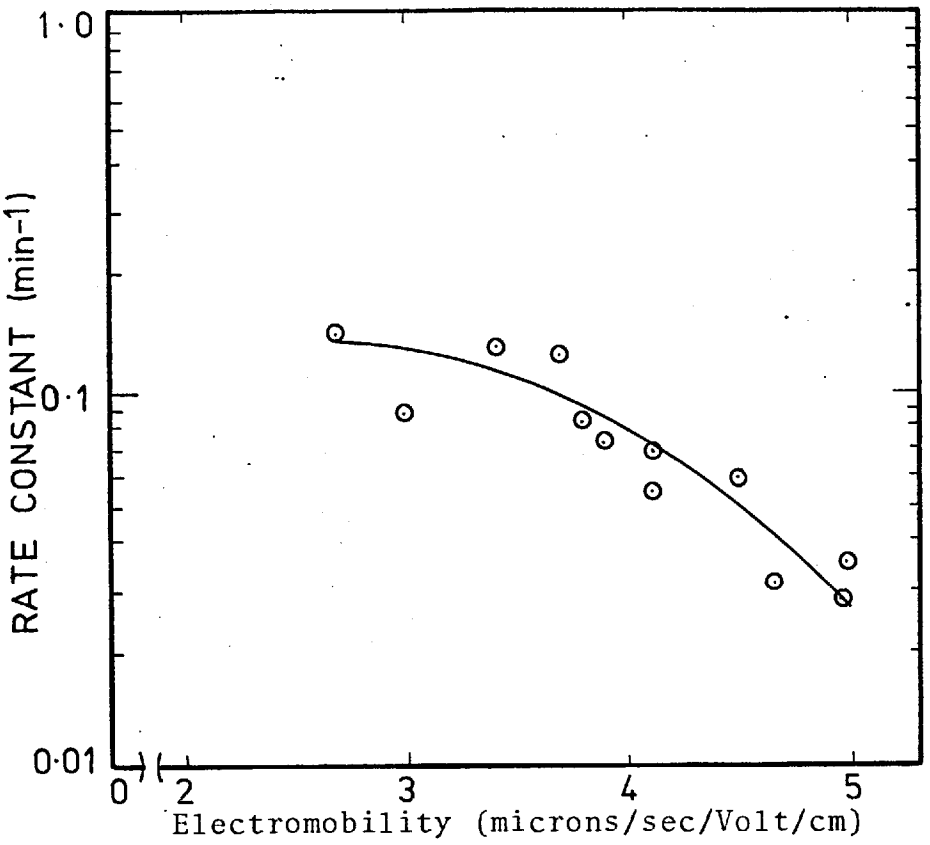

Figure 5.20 Effect of particle electromobility on flotation rate for particles with a mean diameter of 6.6μ

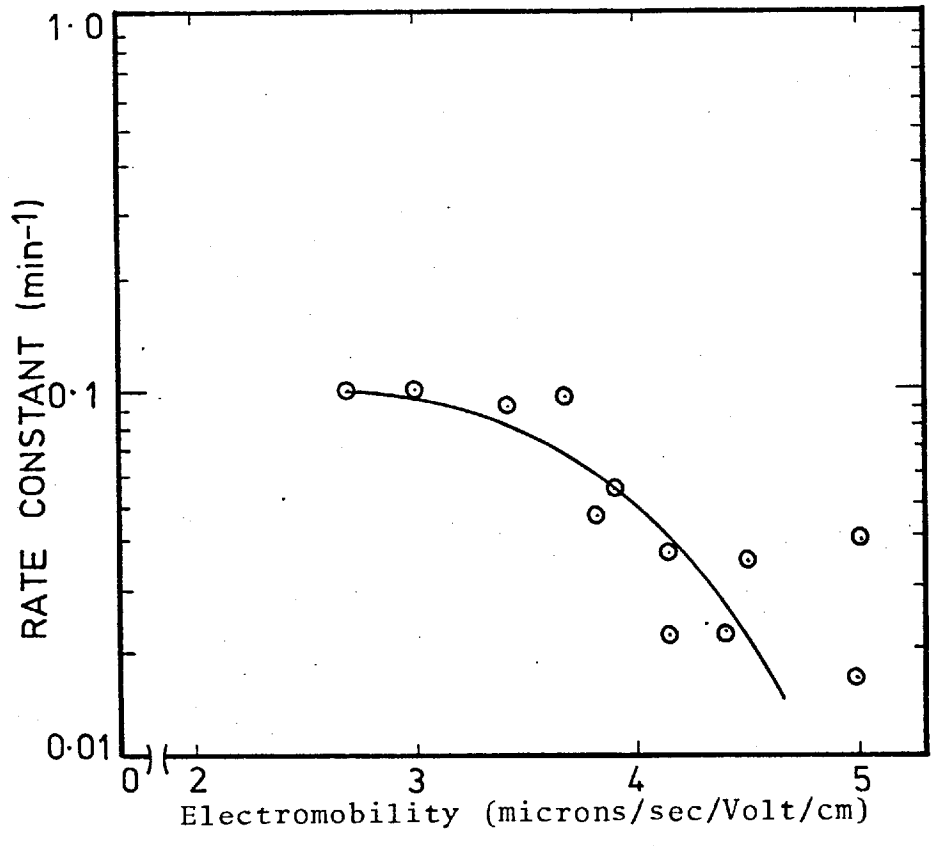

Figure 5.21 Fitzpatrick and Spielman's (1973) data for one filter experiment -- filter coefficient vs electromobility

superficial velocity 0.35 cm/sec
diameter of collector 0.25mm
diameter of particle 9.5μ

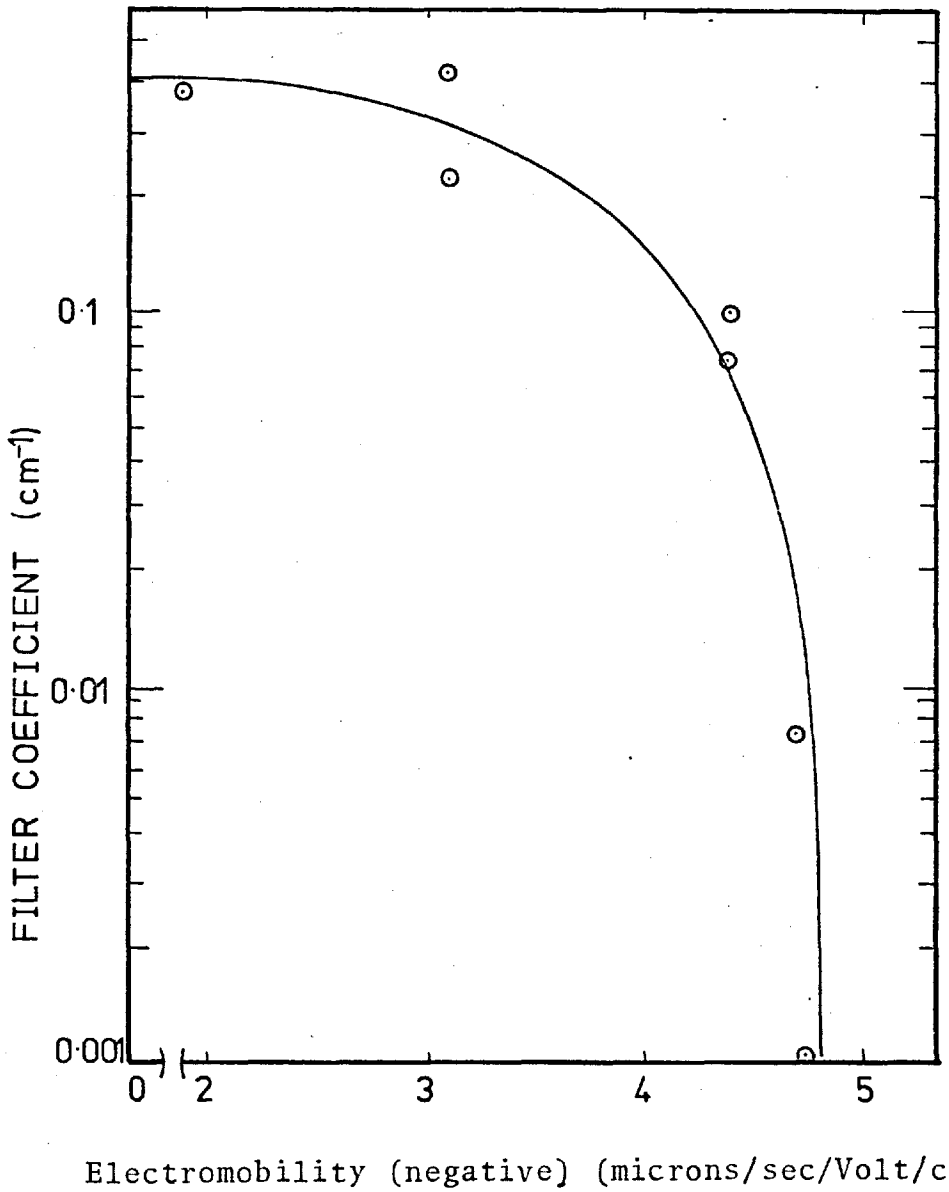

Professor J.T. Davies has suggested that a correlation of the form $\ln\left(\frac{k_p}{d_p^2 s}\right) = A + B \cdot U_E^2$ where U_E is the particle mobility and A and B are constants would be useful in linking the data. Such a correlation leads to the following values for A and B:

A= -4.5

B= -0.1

repulsion between particle and collector. The collector in their case was a negatively charged glass sphere, rather than an air bubble. Spielman and Cukor (1973) showed theoretically that the filter coefficient would behave in this way if double layer forces become important. Perhaps double layer repulsion was responsible for the dependence of flotation rate on electromobility of the polystyrene particles. See note on facing page.

In the next few sections, the experiments conducted to check this hypothesis are presented.

5.4 The charge on the bubble

To postulate that double layer repulsion was responsible for the behaviour of the flotation rate, the bubbles must be shown to carry a positive charge.

The electromobility of bubbles has been studied for over a century. McTaggart (1922) captured bubbles on the axis of a rapidly rotating tube. His results are complicated by the electro-osmotic flow of fluid superimposed on the electrophoretic velocity of the bubble. Bach and Gilman (1938) studied the horizontal electrophoretic velocity of bubbles as they rose in a fluid. According to Samygin et al. (1964) Bach and Gilman's results were the best available, but they were still not reliable. Recently Samygin et al. and Dibbs et al. (1972) have tried to determine the Dorn potential of a swarm of rising bubbles. Lyman (1974) considers that

the interpretation of their results is not possible because the bubbles they used were in the intermediate to high Reynolds number regime where theoretical analysis of the Dorn effect is very complicated, and as yet unsolved.

5.4.1 Theoretical considerations

The electric field associated with a rising bubble is complicated by the possibility of surface movement and non-uniform distribution of surfactant around the bubble. Lyman (1974) by extending the work of Harper (1972) has provided a criterion to judge if the surface of a rising bubble is immobile. It applies to bubbles with Reynolds numbers less than one, and Péclet numbers greater than one. The criterion depends basically on the activity of the surfactant measured by its adsorption depth. Lyman's criterion for an immobile surface is:

$$q = \frac{\alpha c_\infty RT}{U \eta_f} > 1.7618 \qquad (5.6)$$

Where α is the adsorption depth (cm)

c_∞ is the bulk concentration of surfactant

R is the universal gas constant

T is the absolute temperature (291^oK)

U is the bubble rise velocity (0.55 cm/sec for a 100 micron diameter bubble, 0.14 cm/sec for a 50 micron diameter bubble)

η_f is the fluid viscosity

The Reynolds number for a 100 micron diameter bubble is 0.55 and the Péclet number is 1100 (assuming a diffusivity of $5 \times 10^{-6} cm^2/sec$).

The adsorption depth can be determined from a surface tension versus concentration plot. If the surfactant solution is dilute the adsorption depth is given by:

$$\alpha = \frac{\Gamma}{c} = \frac{-1}{\beta RT} \frac{d\gamma}{dc} \qquad (5.7)$$

Where Γ is the surface excess or adsorption density

γ is the surface tension

β can vary between one and two. Pethica (1959) and Lemlich (1968) have discussed the value of β. For nonionic surfactants β equals two, for ionic surfactants in the presence of excess electrolytes with a common ion, β equals one. For salt free solutions of ionic surfactant β varies between one and two depending on concentration. The correct value of β in these experiments was assumed to be two.

By replotting the surface tension data from Figure 4.3 $d\gamma/dc$ was estimated to be -3.3×10^7 dynes cm^2/mole. From equation 5.7 the adsorption depth was then 7×10^{-4}cm, this is a reasonable value. According to Nilsson (1957) sodium dodecyl sulphate has an adsorption depth of 4×10^{-4}cm.

Substituting into equation 5.6:

$q \simeq 170 \gg 1.7618$ for a 100 micron diameter bubble

For bubbles with smaller diameters q is even higher. Based on the value of q Lyman (1974) has shown that the bubble surface will be immobile. Furthermore, the adsorption density (surface excess) variation around the bubble will be negligible. This means that the bubble can be treated as a solid sphere. The only electric field around the bubble, other than the double layer is the field associated with a sedimenting sphere. This field comes from the shearing of the double layer and is responsible for the sedimentation (Dorn) potential.

The process of bubble formation on a porous frit is necessarily a dynamic one and adsorption of surfactant onto a bubble takes a finite time. Perhaps the above arguments are not valid in a dynamic system. Fortunately Lyman also provides an estimate for the time taken for a bubble to take on an equilibrium load of surfactant. By solving the diffusion equation with the appropriate boundary conditions Lyman was able to show that the rate of change of the adsorption density on the bubble, in a stagnant liquid, depended on the value of the smaller of the two characteristic times T^2 and p^2.

$$T^2 = \frac{a_b \alpha}{D} \tag{5.8}$$

$$p^2 = \frac{\alpha^2}{D} \tag{5.9}$$

Where a_b is the bubble radius

D is the diffusivity of the surfactant

For the experimental bubbles $p^2 < T^2$ so taking the diffusivity of CTAB as $5 \times 10^{-6} cm^2/sec$ (typical for a large molecule (Perry (1963))):

$$p^2 = 9.8 \times 10^{-2} \text{ sec}$$

Lyman suggests that a bubble will pick up its full load of surfactant in about four characteristic times or about 0.4 seconds. In this time a free rising 100 micron diameter bubble will travel only about 0.2cm . The adsorption time will be further reduced by convection as the bubble rises. A bubble in a strong surfactant solution such as CTAB, carrying an equilibrium surface concentration of the $CTAB^+$ ion would be expected to be positively charged.

These arguments only apply to a solution containing one surface active substance. The flotation solution in this investigation contained large quantities of ethanol as well as the CTAB. Ethanol has an adsorption depth of $7 \times 10^{-6} cm$ according to Bakker (1966), two orders of magnitude less than the value for CTAB. The ethanol was present in such large amounts (0.09M) that the high activity of CTAB may have been swamped by the ethanol. Ethanol certainly had about ten times the effect of CTAB on reducing the bubble size produced on the frit, which indicated that it was "there first". Reay and Ratcliff (1974) speculated that the alcohol in their flotation system would have prevented adsorption of the cationic surfactant. They then explained their

results by assuming that the bubbles were negatively charged. Their assumption is the antithesis of the assumption necessary to explain the results here. For clues to the role of the ethanol we can look again at the surface tension data and the rate of removal of the CTAB.

5.4.2 Experimental considerations

The surface tension of a pure CTAB solution at 5×10^{-5}M was 68.9 dynes/cm at 20°C. The surface tension of a 0.5% V/V solution of ethanol was 71.0 dynes/cm. The surface tension of a solution of 5×10^{-5}M CTAB and 0.5% V/V ethanol was 67.0 dynes/cm. So at least at equilibrium the CTAB had the greatest effect on surface tension.

The CTAB concentration in the solution was reduced to 60% of its initial value (see section 4.9.2) after 10 minutes of flotation. The initial rate of removal of CTAB was estimated from Figure 4.10 to be 3×10^{-6} moles/min ($\sim 18 \times 10^{17}$ molecules/min). The number of bubbles with diameters of 50 microns passing through the cell at 63 mls/min was 9.4×10^{8}/min. So if we neglect any effects of foam drainage, each bubble carried on it 1.9×10^{9} molecules of CTAB. The surface area of a 50 micron diameter bubble is 7.9×10^{-5}cm^2. The surface area occupied by one molecule then was approximately 400Å^2. The area occupied at equilibrium by a molecule can be determined from the surface excess. If the value

of the adsorption depth of CTAB is 7×10^{-4}cm, the surface excess at a concentration of 5×10^{-5}M (5×10^{-8}moles/cm^3) is:

$$\Gamma = \alpha c$$
$$= 3.5 \times 10^{-11} \text{ moles/cm}^2 \qquad (5.10)$$

The area occupied by a molecule is given by:

$$\text{Area} = \frac{10^{16}}{6.02 \times 10^{23} \times \Gamma} \ (\text{Å}^2) \qquad (5.11)$$

According to Rubin and Jorne (1969).

Substituting the value of Γ from equation 5.10 the area was 480Å^2 which was almost identical to the value obtained from flotation data. This strongly suggests that at least by the time the bubbles had left the flotation solution they had collected their equilibrium load of CTAB, despite the presence of ethanol.

5.4.3 Direct determination of the bubble electromobility

A standard flat electrophoresis cell was modified slightly by sealing two thin platinum wires into the cell with Araldite, as shown in Figure 5.22 , Shaw (1969) sanctions the use of Araldite in an electrophoresis cell, as long as leaching of the adhesive does not occur. Cleaning was difficult, the Araldite had to be burned off before cleaning with chromic acid.

Flotation solutions containing various concentrations of sodium sulphate were first saturated with oxygen then

Figure 5.22 A schematic representation of the electrophoresis cell modified for bubble electromobility measurements

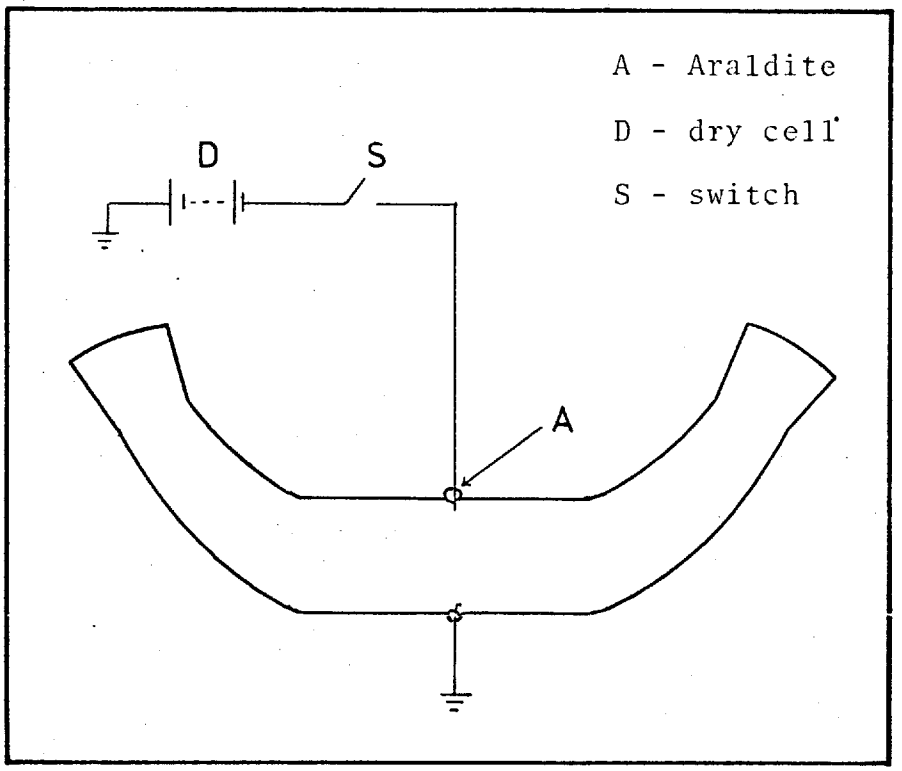

poured into the modified cell. A short burst of current at 12 Volts was passed through the solution via the wires. The bottom wire was connected to earth to ensure that the bubble was not charged by the circuit. Bubbles were produced which rose through the solution. The electric field of the instrument was switched on and the horizontal velocity of the bubbles was measured at a stationary level. Only the electromobility of bubbles with diameters of about 35 microns could be measured. If the bubbles were much smaller they dissolved, if they were much larger they rose too quickly to follow. The velocity of a 35 micron diameter bubble is about 0.05 cm/sec. At this velocity the bubbles could be followed by using the vertical micrometer adjustment on the microelectrophoresis apparatus.

The theory which predicts the position of the stationary levels in a flat cell assumes that the point of observation is at the centre of the cell (van Gils and Kruyt (1936)). The observations on the bubbles necessarily had to range vertically about 0.1cm on either side of the centre. The original equation of flow in a rectangular tube derived by Cornish (1928) was examined. This examination suggested that the velocity and hence the position of the stationary levels was roughly constant within about 0.15cm of the centre of an electrophoresis cell of 0.1 x 1 cm cross section.

To check this prediction the electrophoresis of human erythrocytes in M/15 phosphate buffer at pH 7.4 was

determined at various distances from the centre. The expected electromobility is -1.31 microns/sec/Volt/cm. The results are given in Table 5.2 .

Table 5.2 Electromobility of human erythrocytes

Position from cell centre (cm)	Mobility microns/sec/Volt/cm
+0.050	-1.27
-0.050	-1.35
-0.155	-1.21
-0.250	-1.16
-0.350	-1.12

The results presented in Table 5.2 showed that the electromobility could be determined up to 0.15cm away from the centre of the cell, if a possible systematic error of 8% could be accepted.

The electromobility of bubbles of oxygen was determined as described. Measurements could only be made at one stationary level because of the small area of the cell traversed by the bubbles. The results are given in Table 5.3

Table 5.3 The electromobility of oxygen bubbles

Conc of CTAB (M)	Conc of ethanol % V/V	Conc of sodium sulphate (M)	Mobility of bubbles microns/sec/V/cm
5×10^{-5}	0.5	5×10^{-4}	4.9
5×10^{-5}	0.5	1×10^{-3}	5.0
5×10^{-5}	0.5	5×10^{-3}	3.9
5×10^{-5}	0.5	1×10^{-2}	3.9

These results show that the bubbles in the electrophoresis cell were positively charged soon after being formed, despite the presence of ethanol. Interestingly the electromobility of the bubbles was of the same order as the electromobility of the polystyrene particles. These results and the discussion presented in the last two subsections make it reasonable to assume that the bubbles formed in the flotation cell were also positively charged.

5.5 Alternative explanations for the effect of sodium sulphate on flotation rate

5.5.1 The effect of inorganic salts on adsorption of surfactant

Connor and Ottewill (1971) showed that inorganic salts increase the adsorption of CTAB onto polystyrene surfaces, and it is well known that inorganic salts have

the same effect on the air/water interface. In the flotation experiments an inorganic salt, sodium sulphate, was added to reduce the zeta potential (electromobility) of the particles and the bubbles. Perhaps the effect of zeta potential on the rate of flotation postulated in Section 5.3 could be explained equally well by the increased adsorption of surfactant. In particular, if the surface tension of the surfactant solution was lowered perhaps the bubble size produced on the frit would be reduced. Reay and Ratcliff (1973) showed that the rate of flotation should vary as one over the cube of the bubble radius, could this explain the results? Increased adsorption of surfactant on the particle surface may have made the particles more hydrophobic and hence increased the rate of flotation. These alternative hypotheses had to be examined.

5.5.2 Surface tension and salt concentration

The surface tension of the flotation solution was determined with varying amounts of sodium sulphate added. The results are presented in Table 5.4 .

Table 5.4 The effect of sodium sulphate on the surface tension

Concentration sodium sulphate (M)	Surface tension dynes/cm at 20°C
0	67.0
1×10^{-4}	58.0
5×10^{-4}	54.8
1×10^{-3}	53.0
5×10^{-3}	50.7
1×10^{-2}	47.5

The surface tension was lowered by sodium sulphate as expected.

5.5.3 Bubble size and salt concentration

The lowering of surface tension may have reduced bubble size, although the size of the bubbles from a frit in the presence of alcohol does not seem to bear the same relationship to surface tension as a bubble produced at a single orifice. Photographs were taken of bubbles formed in the flotation solution in the presence of 1×10^{-2}M sodium sulphate, and their sizes determined as described in Section 4.6.5. The mean diameter of these bubbles was 56 microns with a standard deviation of 11 microns, this compares with a bubble size of 53 microns in the presence of 1.3×10^{-4}M sodium sulphate. The two

sets of photographs were taken under identical conditions, so although the more or less equilibrium surface tension of the solution was lowered by the addition of sodium sulphate, the bubble size remained constant.

5.5.4 Contact angle and salt concentration

An attempt was made to determine the contact angle of the polystyrene particles in flotation solutions containing various amounts of sodium sulphate. Bubbles were generated in the modified electrophoresis cell described earlier, and allowed to rise through polystyrene particles suspended in the flotation solution. When individual bubbles had risen to the top of the cell photographs were taken of the particles hanging below the bubbles, and the contact angle was measured from these photographs. Unfortunately, because of the small size of the particles the contact angle which was about 50^{o}-60^{o} was difficult to measure; so the results were not clear-cut. However there was no definite change in the contact angle as the sodium sulphate concentration was increased.

5.5.5 Simulating the "non-double layer" effect of sodium sulphate

Four experiments were carried out to try at least qualitatively, to simulate the effect of increased adsorption of CTAB or ethanol caused by the sodium sulphate. The conditions chosen for these experiments are given in Table 5.5 .

Table 5.5 Conditions for simulation experiments

Experiment number	Conc of CTAB (M)	Conc of ethanol % V/V	Conc of Na_2SO_4 (M)	Surface tension dynes/cm
15	5.00×10^{-5}	0.75	5×10^{-4}	54.0
18	5.00×10^{-5}	1.00	5×10^{-4}	53.0
17	6.25×10^{-5}	0.50	5×10^{-4}	55.0
16	7.50×10^{-5}	0.50	5×10^{-4}	51.8

As the increased adsorption of surfactant is only a second order effect (Kitchener (1975)), the results of these experiments should show the effect of the increased adsorption on the rate of flotation.

The results are given in Appendix A.3 and are presented graphically in Figure 5.23. The figure 5.23 has been drawn with the experimental points of all four experiments plotted together with the line of best fit calculated from experiments 1 , 2 , 3 , and 4 (normal surfactant/frother conditions). The surface tension of the solutions showed that increased adsorption had taken place at the air/water interface. Increased adsorption must also have taken place on the polystyrene particles. Despite this increased adsorption the flotation rate did not increase. In fact the rates of flotation in experiments 17 and 16, in which the CTAB concentration was increased, were considerably slower. This agrees

Figure 5.23 Simulation of the non-double layer effect of sodium sulphate (refer section 5.5.5)

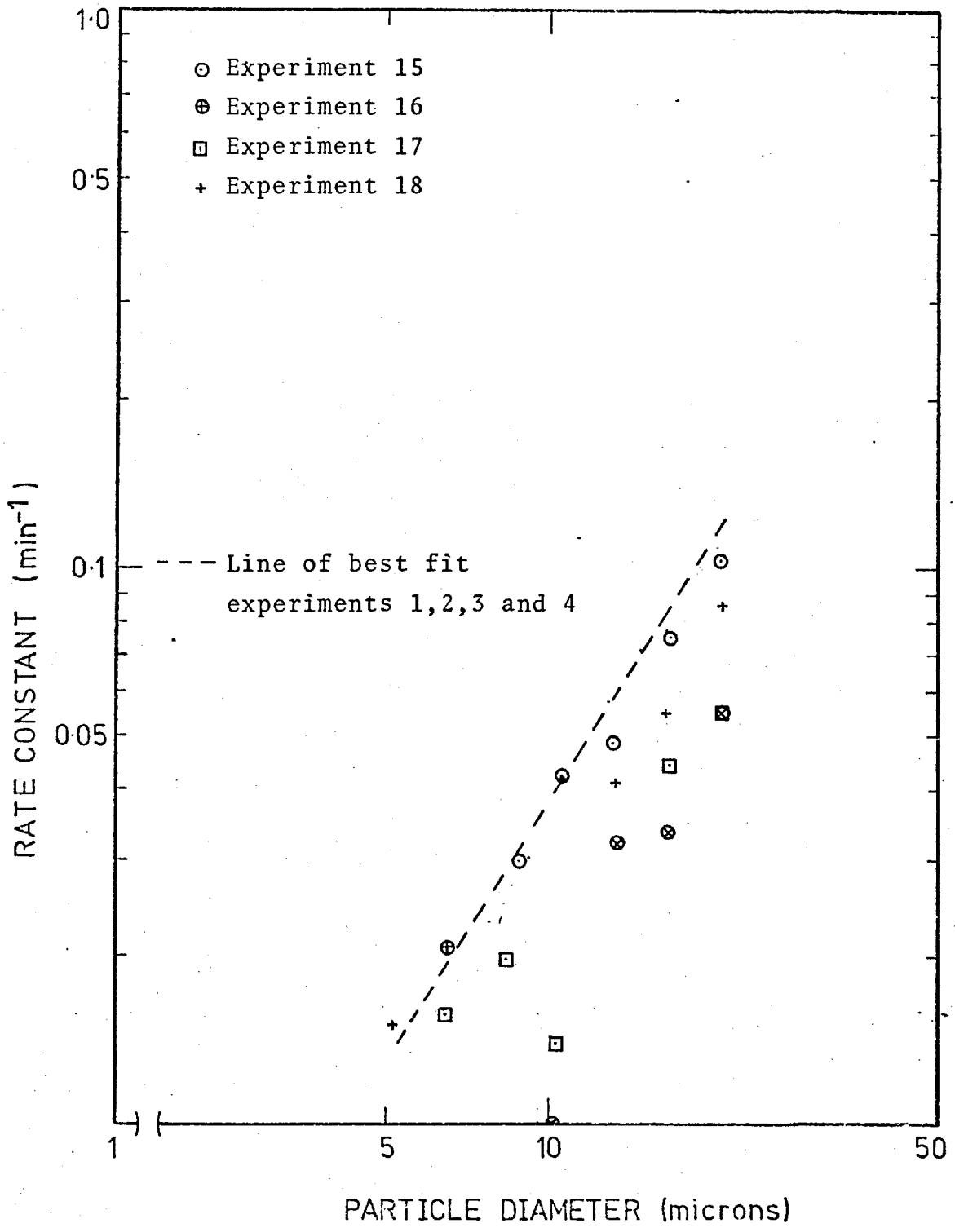

with the initial tests on flotation presented and discussed in section 4.5 .

5.6 The van der Waals dispersion and double layer interaction energies

The van der Waals dispersion and double layer forces have been discussed in general terms so far. Now let us examine the magnitude of these forces in terms of potential energy.

To calculate the van der Waals dispersion interaction energy, the Hamaker constant for the interaction of an air bubble with a polystyrene particle through a layer of water is required. A search of the literature showed that no calculation had been made for this particular system using the Lifshitz formula, equation 2.13 . The constant had to be estimated with the help of the combining law approximations: (see Section 2.2.5)

$$A_{130} \simeq \pm(A_{131} \cdot A_{030})^{\frac{1}{2}} \simeq \pm(A_{131} \cdot A_{303})^{\frac{1}{2}} \qquad (5.12)$$

Where medium 1 is polystyrene
medium 3 is water
medium 0 is air (vacuum)

Values for the quantities on the right hand side of equation 5.12 can be found in a number of reference papers; Visser (1972) for example. The values used

here were taken from a generally accepted paper by Krupp et al. (1972).

$$A_{131} = 0.34 \times 10^{-13} \text{ ergs}$$

$$A_{303} = A_{33} = 4.35 \times 10^{-13} \text{ergs}$$

So:

$$A_{130} \simeq \pm (0.34 \times 4.35)^{\frac{1}{2}} \times 10^{-13} \text{ ergs}$$

$$\simeq \pm 1.22 \times 10^{-13} \text{ ergs}$$

To decide the sign, we need to examine part of the equation 2.13 :

$$(\varepsilon_1(i\xi) - \varepsilon_3(i\xi)) \cdot (\varepsilon_0(i\xi) - \varepsilon_3(i\xi)) > 0 \qquad (5.13)$$

for $A_{130} > 0$. The frequency dependent dielectric constants are not known but can be approximated, according to Israelachvili and Tabor (1973), by the static dielectric constant $\varepsilon_i(0)$. The dielectric constants are to be estimated by the square of the refractive index of the particular material.

$$\varepsilon_1(0) = (1.56)^2 = 2.43$$

$$\varepsilon_3(0) = (1.33)^2 = 1.76$$

$$\varepsilon_0(0) = (1.00)^2 = 1.00$$

If we substitute these values into equation 5.13 we find that the sign of A_{130} is negative, so:

$$A_{130} \simeq -1.22 \times 10^{-13} \text{ ergs}$$

The value of A_{130} can be estimated in another way. Visser (1972) gives the following formula as a good estimate of A_{130}, it is a corrected version of equation 2.14 :

$$A_{130} \simeq K_m(A_{10} + A_{33} - A_{13} - A_{03}) \qquad (5.14)$$

Where K_m accounts for the transmission of the interaction through medium 3 . The value of K_m for water is 1.6 . Krupp et al (1972) found that the approximation:

$$A_{12} \simeq (A_{11} \cdot A_{22})^{\frac{1}{2}} \qquad (5.15)$$

was correct within 5% for all the substances tested. With the help of these two approximations and the value for polystyrene taken from Krupp et al:

$$A_{11} = 6.56 \times 10^{-13} \text{ ergs}$$

A_{130} can be calculated. The value of A_{130} estimated in this way is -1.55×10^{-13}ergs, in fair agreement with the first method. The important point is that both estimates give a negative Hamaker constant which means that the van der Waals dispersion contribution to the disjoining pressure is positive (repulsive). As a further check, Visser's condition for a negative Hamaker constant is satisfied:

$$A_{11} > A_{33} > A_{22} \quad ; \quad 6.56 > 4.35 > 0 \ (\text{all} \times 10^{-13} \text{ ergs})$$

The dispersion energy can be calculated by using equation 2.11 :

$$V_V = -\frac{A_{130}}{6h}\frac{(a_b\ a_p)}{(a_b+a_p)} \qquad (2.11)$$

Where V_V is the van der Waals dispersion energy

a_b is the bubble radius

a_p is the particle radius

h is the distance of separation

A_{130} is the Hamaker constant (- 1.22 x 10^{-13} ergs)

The energy of interaction for double layer forces can be calculated using equation 2.6 for approach at constant potential. Hogg et al. (1966) have shown that it is a good approximation for Ψ_p and Ψ_b up to about 60mV:

$$V_{DL} = \frac{\varepsilon\, a_p\, a_b}{4(a_p + a_b)} \left\{ 2\,\Psi_p\,\Psi_b \ln \frac{1 + \exp(-\kappa h)}{1 - \exp(-\kappa h)} \right\}$$

$$+ \ (\Psi_p^2 + \Psi_b^2) \ln\ 1 - \exp(-2\kappa h$$

Where V_{DL} is the potential energy of the double layer

Ψ_p, Ψ_b are the surface potentials of the particle and bubble respectively

Figure 5.24 shows the interaction energies for two particle/bubble flotation conditions. The usual assumption that Ψ_p and Ψ_b can be approximated by the zeta potentials ζ_p and ζ_b was made. Zeta potentials can be calculated from the electromobility by means of the relation: $\zeta = 12.85 U_E$ at 25^oC $\cdot (\kappa a \gtrsim 300)$
The particle and bubble radii were taken as 5 and 50 microns respectively. The particle/bubble conditions

are given in Table 5.6 .

Table 5.6 Conditions chosen for the interaction calculations

Condition	κ cm^{-1}	ζ_p mV	ζ_b mV
1	6.6×10^5	60	60
2	4.6×10^6	40	50

Condition 1 was typical for the slowest flotation, condition 2 was typical for the fastest flotation found. As can be seen in Figure 5.24, for condition 1 double layer repulsion predominated for all distances. The range and the size of the double layer interaction was reduced drastically for condition 2 . Double layer repulsion predominated at small distances of separation for condition 2 but at larger distances the van der Waals dispersion interaction was larger. The van der Waals potential was calculated for unretarded forces and the retardation effect would reduce the size of the potential for $h \gtrsim 200$ Å . The behaviour shown in Figure 5.24 is consistent with the hypothesis that double layer forces controlled the rate of flotation. The dominance of double layer forces at condition 1 and the reduction of the forces for condition 2 is necessary for the hypothesis.

Figure 5.24 Potential energy curves for conditions 1 and 2 and the van der Waals dispersion energy

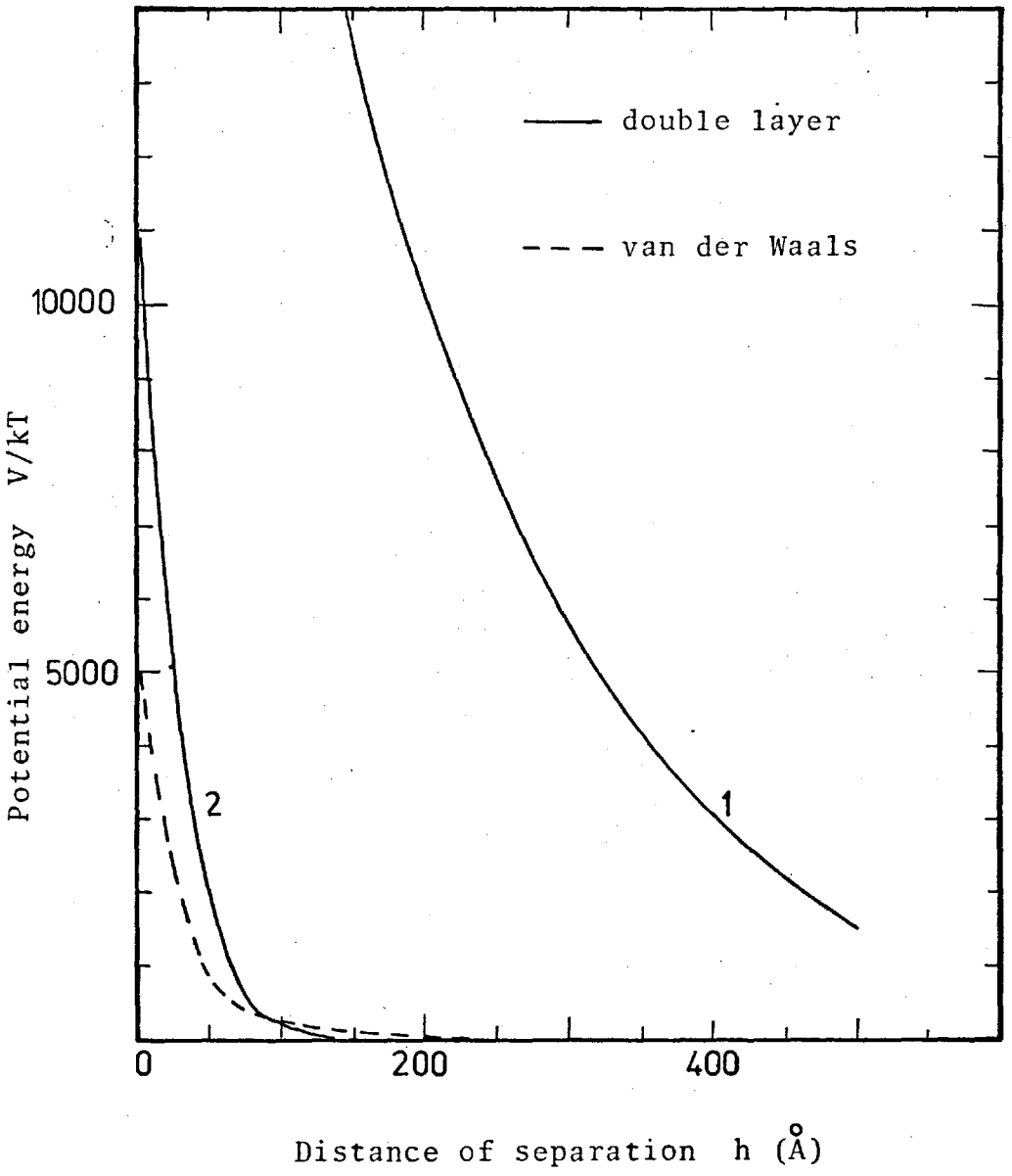

5.7 Discussion of the effect of double layer forces

The results and arguments presented in sections 5.4 to 5.6 all support the hypothesis that double layer forces controlled the rate of flotation of the polystyrene particles. Indeed there seems to be no other explanation. The hypothesis is strongly supported by Blake and Kitchener's (1972) results on film thinning. Their work had demonstrated that double layer repulsion could be expected to influence flotation kinetics and this is just what was observed. The only doubt lies with the specific surface term. Perhaps the magnitude and/or range of these forces was altered by the addition of electrolyte. In assuming that this effect can be ignored, we are in the good company of Read and Kitchener (1967) and Blake and Kitchener (1972).

The behaviour of the rate constant in these experiments and the behaviour of the filter coefficient found by Fitzpatrick and Spielman (1973) is so similar that it cannot be accidental. On a microscopic scale the two processes differ in the sign of the van der Waals dispersion energy. In the filtration experiments there was an attractive van der Waals dispersion force, while in the flotation experiments the van der Waals dispersion force was apparently repulsive. We know however that an attractive force must exist at some distance of separation or flotation would not occur, so the two processes are still qualitatively similar

in having a net attraction between particle and collector.

The flotation results were for rather restricted (but important) conditions. The bubbles were small and the surfactant active, which meant the bubbles would behave like solid spheres, both hydrodynamically and electrically. As a consequence of the bubble size, Stokes flow was a good approximation for flow around the bubble. Spielman and Fitzpatrick's collectors were solid and the flow around them was slow enough for Stokes flow to hold. Under different flotation conditions there may be no similarity. This can only be checked by careful experimentation. For the particular flotation conditions used in this study there is a strong case for making use of experimental and theoretical filtration work.

5.8 Discussion of errors

5.8.1 The rate of flotation experiments

Volumetric errors were kept to a minimum by using the same volumetric glassware throughout the experimental programme. Errors in the gas flow rate were quite small, less than 2%. The accuracy of the clock used in the flotation experiments was checked against the electro-mechanical clock of the microelectrophoresis instrument. It was found to be accurate to one second in ten minutes. The zero of the time was uncertain as discussed earlier,

but this was not due to timing errors.

Counting errors were thought to be responsible for most of the scatter of the data points. These counting errors arose because of the accumulation of the normal Coulter Counter errors in the final rate constants. In Appendix A.4 two examples are presented which illustrate how relatively small errors in cumulative counts can produce larger errors in the value of the ratio $\ln [N_o/N_t]$. The total error in the rate constants was expressed as the standard error. These errors are included in tables of Appendix A.3.

5.8.2 Electromobility experiments

All care was taken to ensure that systematic errors were eliminated from the determination of the particle electromobility results. Random errors due to timing of transit times. temperature variations, accuracy in determining the positions of stationary levels, etc. were present as they will be in any electromobility determination. Shaw (1969) discussed electromobility errors. From his comments and conclusions the typical standard deviation (10% of the mean of individual particle mobilities) found in this work seems satisfactory.

The bubble electromobility results were subject to a possible systematic error of about 8% because the determination was made away from the centre of the cell.

Experimental errors are part of any investigation but despite the errors encountered in this work, the dependence of the flotation rate on particle size and double layer repulsion was conclusively demonstrated.

CHAPTER 6

A THEORETICAL INVESTIGATION OF COLLISION EFFICIENCY

In this chapter an assumption is made about the attractive force that must exist between a bubble and a particle. A mass transport equation is derived, then the equation is put into a suitable form and solved. The results of the numerical solution are presented graphically and then discussed.

6.1 Introduction

We have seen in Chapter 5 that the rate constant for flotation behaved in a very similar manner to the filtration coefficient in Fitzpatrick and Spielman's (1973) experiments. As discussed in Chapter 5 there are many similarities in the two processes. It was decided to investigate collision efficiency in flotation by using the method of Prieve and Ruckenstein (1974) who had calculated filtration collector efficiency.

In Chapter 5 we found that the Hamaker constant for the particle/bubble interaction was negative, which implies a repulsive van der Waals dispersion contribution to the disjoining pressure. The double layer and van der Waals contribution to the disjoining pressure should ensure that the particles are hydrophilic, but the particles are hydrophobic. They form a non-zero contact

angle and are floatable. The specific surface forces term has been ignored so far and it obviously must be the most important term making up the disjoining pressure. The fact that a non-zero contact angle is formed implies an attractive force (negative disjoining pressure) acts at some distance of separation. In principle we could define an effective Hamaker constant that would account for the attractive force. The value of this effective Hamaker constant is unknown, indeed the form of the attractive force is unknown, but for the purpose of the theoretical analysis let us assume that the effective Hamaker constant is 4×10^{-13} ergs, about 10kT at $290^{o}K$. Let us further assume that the form of the attractive force is the same as the nonretarded van der Waals dispersion force.

6.2 The model

Consider an isolated spherical bubble held stationary in a creeping (Stokes) flow field (i.e. with $Re < 1$). The Reynolds number is defined as $\frac{2a_b U \rho_f}{\eta_f}$ and $Re < 1$ means that inertial forces are negligible compared with viscous forces. Small spherical particles are suspended in the surrounding fluid.

The following assumptions are made:

a) Both particle and bubble are rigid, smooth spheres. The velocity of the fluid a long way from the bubble is equal to the bubble's terminal velocity U .

The assumption of a rigid surface is obviously correct for the particle, and from Lyman's (1974) work it is also correct for the bubble. The assumption of Stokes flow is good for bubbles less than about 100 microns in diameter.

b) The total interaction between particle and bubble is attractive as discussed above.

c) Any particles collected are immediately swept to the rear of the bubble leaving the front always clear. Tomlinson and Fleming (1963) obtained photographic proof of this movement of particles.

d) The terminal velocity of the bubble is not affected by any collected particles. At a particle concentration of 0.5 grams/litre one 50 micron diameter bubble only captures one or two particles of nearly neutral buoyancy, so the assumption is a reasonable one.

6.3 Derivation of governing equations

To obtain the collision efficiency we are going to determine the concentration of particles near to the bubble and hence the flux onto the bubble. Integration of the flux over the bubble, after some manipulation, will yield the collision efficiency.

The equation of continuity for mass diffusion in spherical coordinates is given by Bird et al. (1960) as:

$$\frac{1}{r^2}\frac{\partial}{\partial r}(r^2 N_r) + \frac{1}{r \sin\theta}\cdot\frac{\partial}{\partial\theta}(N_\theta \sin\theta) = 0 \qquad (6.1)$$

for azimuthal symmetry and assuming that the time dependent term $\frac{\partial c}{\partial t}$ can be neglected (i.e. steady state conditions)

Where r is the radial coordinate

θ is the angular coordinate

N_r is the radial component of the particle flux

N_θ is the angular flux

Figure 6.1 is a diagram showing the sphere, the particle and the coordinate system.

The radial and angular fluxes are made up from convection and diffusion terms:

$$N_r = v_r c - D\frac{\partial c}{\partial r} \qquad (6.2)$$

$$N_\theta = v_\theta c - D\frac{\partial c}{\partial \theta} \qquad (6.3)$$

Where v_r and v_θ are the radial and angular velocities of the particle respectively

c is the particle concentration

D is the position dependent diffusion coefficient of the particle

For simplicity $D\frac{\partial c}{\partial \theta}$ is assumed to be negligible. This assumption is made mainly for numerical convenience, as we shall see later. The assumption is justified according to Levich (1962) because the derivatives along the surface of the sphere are small compared with the

Figure 6.1 Coordinate system for particle and bubble

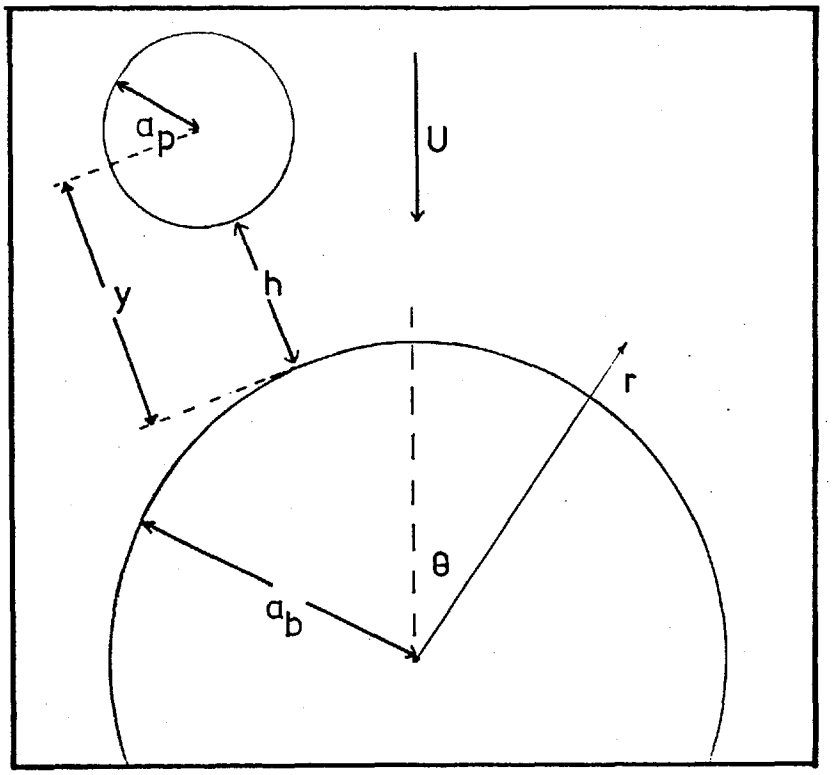

Figure 6.2 The effect of the transformation $\eta=1-e^{-bH}$

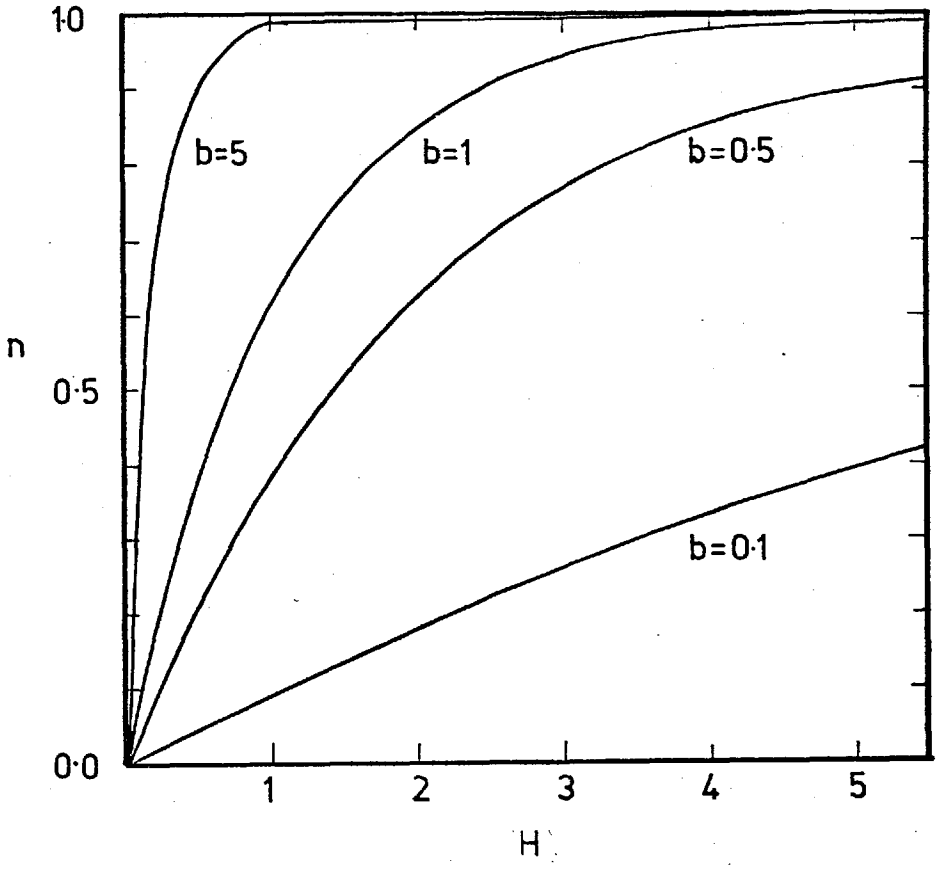

derivatives along the radius vector. Equation 6.3 becomes:

$$N_\theta = v_\theta c \tag{6.4}$$

By performing a radial force balance Spielman and Fitzpatrick (1973) determined the radial velocity of a particle attracted to a spherical collector by van der Waals dispersion forces.

$$\underbrace{\frac{v_r(h,\theta)}{m(h/a_p)}}_{\text{viscous drag}} = \underbrace{\frac{s_r(h,\theta)\ f_2\ (h/a_p)}{m_\infty}}_{\text{fluid motion force}} - \underbrace{\frac{2}{3}\frac{Aa_p^3}{(h+2a_p)^2\,h^2}}_{\substack{\text{attractive} \\ \text{dispersion force}}} \tag{6.5}$$

Where $m(h/a_p)$ is the position dependent particle mobility (velocity/unit force)

m_∞ is the particle mobility far from the bubble

A is the effective "Hamaker constant"

Hamaker's (1937) expression for the nonretarded force was used. The expression for the force exerted by the fluid was taken from Goren and O'Neill (1971). The factor $f_2\ (h/a_p)$ corrects the radial force exerted on a stationary spherical particle by an axisymmetric stagnation flow over a plane, a distance h from the surface of the sphere.

The tangential diffusion has been assumed to be zero, so only fluid motion contributes to the tangential particle velocity. Near the collector the fluid is in uniform shear flow. Goldman et al. (1967) studied the viscous motion of a sphere in Couette flow and found that the particle velocity was less than the undisturbed fluid velocity at the particle centre, hence:

$$v_\theta(h,\theta) = s_\theta(h,\theta)\ f_3(h/a_p) \qquad (6.6)$$

Where s_θ is the angular fluid velocity

The factor $f_3(h/a_p)$ is the appropriate correction factor.

Brenner (1961) calculated the motion of a sphere very near a solid object and derived a modified Stokes equation:

$$\frac{v_r}{F} = m(h/a_p) = \frac{f_1(h/a_p)}{6\,\pi\,\eta_f\,a_p} \qquad (6.7)$$

Where F is an applied force

$f_1(h/a_p)$ is a correction factor

We introduce a position dependent diffusion coefficient D. According to the Nernst - Einstein equation:

$$D = m(h/a_p)\cdot k \cdot T \qquad (6.8)$$

Where k is Boltzmann's constant

T is the absolute temperature

Then from equation 6.7 the position dependent diffusion coefficient of the particles can be expressed as:

$$D = D_\infty \, f_1 (h/a_p) \qquad (6.9)$$

Where D_∞ is $k T / 6 \pi \eta_f a_p$

The three factors f_1, f_2 and f_3 are strictly only correct for a sphere and a flat plate. We will assume they are correct for a small particle and a much larger spherical bubble.

The fluid velocities s_r and s_θ can be easily obtained because we are dealing with a system in Stokes flow. Bird et al. (1960) give the equations as follows (with the appropriate signs):

$$\frac{s_r}{U} = -\left[1 - \frac{3}{2}\left(\frac{a_b}{r}\right) + \frac{1}{2}\left(\frac{a_b}{r}\right)^3\right]\cos\theta \qquad (6.10)$$

$$\frac{s_\theta}{U} = \left[1 - \frac{3}{4}\left(\frac{a_b}{r}\right) - \frac{1}{4}\left(\frac{a_b}{r}\right)^3\right]\sin\theta \qquad (6.11)$$

It is convenient to make equations 6.1 , 6.5 , and 6.6 dimensionless. This reduces the number of variables and puts the equations into a more manageable form without loss of generality. The following substitutions were made:

$C^* = \frac{c}{c_\infty}$:- the dimensionless concentration relative to the concentration c_∞ a long way from the bubble

$H = h/a_p$:- the dimensionless distance between bubble and particle surfaces relative to the particle radius

$Y = y/a_p = H + 1$:- the dimensionless distance between particle centre and the bubble surface

$R = a_b/a_p$:- the ratio of bubble to particle radius

$Pe = \frac{2a_b U}{D_\infty}$:- the Péclet number for the particles; the ratio of convectional to diffusional transport

$u^* = v_\theta/U$:- the dimensionless angular velocity relative to the bubble's terminal velocity U

$v^* = v_r/U$:- the dimensionless radial velocity relative to the bubble's terminal velocity U

$A_{kT} = A/kT$:- the dimensionless "Hamaker constant" relative to kT

When these substitutions are made and it is recognised that $s_\theta \cot\theta = \frac{\partial s_\theta}{\partial \theta}$ the following dimensionless equation is produced:

$$\frac{2R}{Pe} f_1(H) \frac{\partial^2 C^*}{\partial H^2} + \left[\frac{2R}{Pe}\left(\frac{df_1}{dH} + \frac{2f_1(H)}{R+Y}\right) - v^*\right]\frac{\partial C^*}{\partial H}$$

$$- \left[\frac{2}{R+Y}\left(v^* + \frac{\partial u^*}{\partial \theta}\right) + \frac{\partial v^*}{\partial H}\right] C^* = \frac{u^*}{R+Y}\frac{\partial C^*}{\partial \theta} \qquad (6.12)$$

with:

$$u^* = \left[\frac{3}{2} R^2 + Y\left(\frac{9}{4} R + Y\right)\right] \frac{Y f_3(H) \sin\theta}{(R + Y)^3} \qquad (6.13)$$

and:

$$v^* = -Y^2\left(\frac{3}{2} R + Y\right) \frac{f_1(H) f_2(H) \cos\theta}{(R + Y)^3}$$

$$- \frac{4}{3} A_{kT} \left(\frac{R}{Pe}\right) \frac{f_1(H)}{(Y^2 - 1)^2} \qquad (6.14)$$

The boundary conditions are:

$$C^* = 1 \qquad \text{as } H \to \infty \quad \text{for all } \theta \qquad (6.15a)$$

$$C^* = 0 \qquad \text{at } H = 0 \quad \text{for all } \theta \qquad (6.15b)$$

$$\frac{\partial C^*}{\partial \theta} = 0 \qquad \text{at } \theta = 0 \quad \text{for all } H \qquad (6.15c)$$

Condition 6.15a expresses the fact that far from the bubble the concentration approaches c_∞. Condition 6.15b results because once the particles have contacted the bubble they are no longer part of the dispersed phase so the local concentration is zero. Condition 6.15c is the result of symmetry about $\theta = 0$.

6.4 Solving the equation

6.4.1 The factors making up the coefficients of the equation

The equation 6.12 has variable coefficients which have to be evaluated before solving the equation.

The factor $f_1(H)$ was taken from Brenner (1961). The expression needed to evaluate the factor is given in Appendix A.6 . The derivative of $f_1(H)$ with respect to H is also required. This is a complicated expression also given in Appendix A.6 .

The factor $f_2(H)$ was taken from Goren and O'Neill (1971). The tabulated values for $f_2(H)$ given in their paper are correct, but the formula they quote near their equation 3.14 contains two typographical errors. The corrected equation was obtained with the help of Dr. M.E.O'Neill (1975). It is odd that the error had not been noticed before, as a number of workers had used the factor without mentioning the error. The corrected expression and the expression for the derivative of $f_2(H)$ with respect to H are given in Appendix A.6 .

The factor $f_3(H)$ was taken from Goldman et al. (1966). The analytic form of $f_3(H)$ is difficult to obtain, and interpolation between the tabulated values given by Goldman et al. was at first not possible. After a suitable transformation however, the form of the equation was changed and accurate interpolation was possible. The method of generating $f_3(H)$ is given in Appendix A.6 .

The other quantities were calculated fairly easily although some of the expressions look a bit horrific. The expressions for all the quantities are given in Appendix A.6 .

6.4.2 Transformation of the boundary conditions

The boundary conditions are unsuitable in their present form because of the infinite outer boundary. The infinite radial domain ($0 \leq H < \infty$) can be compressed into a finite domain ($0 \leq \eta \leq 1$) by using the transformation:

$$\eta = 1 - e^{-bH} \tag{6.16}$$

Where b is an expansion parameter

The effect of this transformation in the radial domain is shown in Figure 6.2*. Note the transformation variable η is not to be confused with the symbol for viscosity η. Their use is sufficiently different for this not to occur.

Equation 6.12 with its attendant boundary conditions 6.15, can now be written in a suitable form for solution.

The transformed equation is:

$$\frac{2R}{Pe} f_1 \frac{\partial^2 C^*}{\partial \eta^2} \left[b(1-\eta)\right]^2 + \left[\frac{2R}{Pe}\left(\frac{df_1}{dH} + f_1\left(\frac{2}{R+Y} - b\right)\right) - v^*\right] \cdot$$

$$\frac{\partial C^*}{\partial \eta}\left[b(1-\eta)\right] - \left[\frac{2}{R+Y}\left(v^* + \frac{\partial u^*}{\partial \theta}\right) + \frac{\partial v^*}{\partial H}\right] C^* = \frac{u^*}{R+Y} \cdot \frac{\partial C^*}{\partial \theta} \tag{6.17}$$

With u^* and v^* given by equations 6.13 and 6.14

* Figure 6.2 is on page 146

The boundary conditions are now:

$$C^* = 1 \quad \text{at} \quad \eta = 1 \quad \text{for all} \quad \theta \tag{6.18a}$$

$$C^* = 0 \quad \text{at} \quad \eta = 0 \quad \text{for all} \quad \theta \tag{6.18b}$$

$$\frac{\partial C^*}{\partial \theta} = 0 \quad \text{at} \quad \theta = 0 \quad \text{for all} \quad \eta \tag{6.18c}$$

Equation 6.17 is a second order partial differential equation in a form suitable for solution by a standard method. The complicated nature of the coefficients should not hide its basic form.

$$\frac{\partial C^*}{\partial \theta} = A(\eta,\theta) \frac{\partial^2 C^*}{\partial \eta^2} + B(\eta,\theta) \frac{\partial C^*}{\partial \eta} + D(\eta,\theta) \tag{6.19}$$

If we had retained the diffusional contribution to the angular flux the equation would have been elliptic instead of parabolic. An elliptic equation would require a more time consuming numerical technique and an additional boundary condition would be needed.

6.4.3 Method of solution

We have a relatively standard second order partial differential equation but no "starting" condition, i.e. the values of C^* at $\theta = 0$. We have the boundary condition:

$$\frac{\partial C^*}{\partial \theta} = 0 \quad \text{at} \quad \theta = 0 \quad \text{for all} \quad \eta \tag{6.18c}$$

Substituting this boundary condition into equation 6.17 , it is reduced to a second order ordinary differential equation with two boundary conditions, 6.18a and 6.18b . This equation can now be solved and the resulting concentration profile can be used as a starting condition for the equation 6.17 .

6.4.4 Computer programmes

Considerable time and programming effort was saved by the use of suitable existing programmes from the library facilities at Imperial College. The Harwell subroutine library (United Kingdom Atomic Energy Authority (1973)) includes two subroutines called DD01A and DP01A .

DD01A solves a two point boundary value problem for a second order ordinary differential equation of the form:

$$\frac{d^2y}{dx^2} + F(x)\frac{dy}{dx} + G(x)y = Q(x) \qquad (6.20)$$

using the method of Fox (1947).

DP01A advances the solution of a two point boundary problem for a parabolic linear partial differential equation of the form:

$$\frac{\partial y}{\partial t} = A(x,t)\frac{\partial^2 y}{\partial x^2} + B(x,t)\frac{\partial y}{\partial x} + D(x,t)y + E(x,t) \qquad (6.21)$$

That is, given the solution at $t = t_o$ the routine finds the solution at $t = t_o + \delta t$. The term $\frac{\partial y}{\partial t}$ is replaced by a finite difference formula and the resulting equation is solved by calling DDO1A . DPO1A requires a subroutine FUNCTS to be written by the user to calculate the coefficients $A(x,t)$, $B(x,t)$, $D(x,t)$ and $E(x,t)$ in equation 6.21 . To test that DDO1A and DPO1A were working correctly they were used to solve equations with known solutions, (see Appendix A.5).

The subroutine DPO1A is designed to solve an open ended problem. The problem here is not strictly open ended, being the concentration profile around a sphere. An examination was made of all the coefficients in equations 6.12 , 6.13 and 6.14. It was found they were symmetric about the vertical axis of the bubble and hence the solution of equation 6.17 would be cyclic. The solution of the equation 6.17 is possible using DPO1A if the solution is taken from $\theta = 0$ to $\theta = \pi$. The angle θ here being equivalent to t in equation 6.21 .

6.4.5 Additional routines

A number of subroutines had to be written mainly to satisfy the requirements of FUNCTS . These subroutines and a brief description of their function are given below.

Subroutine F1(A,ATOT) This routine calculates the factor $f_1(H)$ (i.e.ATOT) from the equation given in Appendix A.6 . A is the quantity $\ln(Y + (Y^2 - 1)^{\frac{1}{2}})$ where Y is the quantity H + 1 , the distance from the bubble surface to the centre of the particle.

Subroutine F2(A,YA,FE2) This routine calculates the factor $f_2(H)$ (i.e.FE2). YA, is Y .

Subroutine DF1(A,YA,DFDH) This routine calculates the derivative of the factor $f_1(H)$ (i.e.DFDH) .

Subroutine DF2H(A,YA,DF2DH) This routine calculates the derivative of the factor $f_2(H)$.

Subroutine VCALC(YA) This routine calculates the dimensionless radial particle velocity, which is passed into COMMON.

Subroutine UCALC(YA) This routine calculates the dimensionless angular particle velocity and its derivative in the angular direction. Both quantities are passed into COMMON . The routine contains the means of generating the factor $f_3(H)$. It uses two IBM SSP routines ALI and ATSM to interpolate between data points.

Subroutine DVDH(A,YA,DV) This routine calculates the derivative of the dimensionless radial velocity with respect to H .

FACTS This routine is simply a time saving routine

It calculates the values of a number of quantities and stores them in arrays to be used by other subroutines.

These routines, like all the routines used in this work were thoroughly tested to ensure that they were functioning correctly.

6.4.6 Calculation of collision efficiency

We are now in a position to calculate the concentration profile, but it is the collision efficiency that is required. This is obtained as follows; the radial flux can be calculated from equation 6.2:

$$N_r = v_r c - D\frac{\partial c}{\partial r} \qquad (6.2)$$

and integrated over the surface of the bubble. When the particles contact the surface of the bubble their diffusion coefficient vanishes and the product $v_r c$ is indeterminate at the surface. This indeterminancy can be avoided by integrating over some surface other than $r = a_b$. The Gauss Divergence Theorem and the continuity equation show that the radial particle flux over any spherical surface concentric with the bubble will have the same value. Thus the following expression for the overall rate, I, will be independent of r:

$$I = 2\pi r^2 \int_0^{\pi} -N_r(r,\theta) \sin\theta \, d\theta \qquad (6.22)$$

In addition to avoiding the indeterminancy at $r = a_b$ the observation that equation 6.22 is independent of r

provides a test of the accuracy of the numerical technique used to evaluate the concentration profile.

The efficiency can now be calculated as follows:

$$E_c = \frac{I}{\pi a_b^2 Uc_\infty} \qquad (6.23)$$

The denominator in equation 6.23 is equal to the rate at which particles pass through the volume swept out by the bubble. In terms of the variable η, equation 6.23 becomes:

$$E_c = 2\left(1 + \frac{Y}{R}\right)^2 \int_0^{\pi} \left(\frac{2R}{Pe} \cdot f_1 \cdot \frac{\partial C^*}{\partial \eta} \cdot b(1-\eta) - v^*C^*\right) \sin\theta \, d\theta \qquad (6.24)$$

Subroutine HOPE(CONC,EFFIC,NA,IER) was written to handle the calculations required in equation 6.24. CONC was a 2 x 101 array containing the concentration profile. EFFIC was the final efficiency, NA was the number of points in the angular domain and IER was an error flag.

The efficiency was calculated at the first nine grid points away from the bubble surface. An IBM SSP subroutine, DET3, calculated the partial derivative in equation 6.24 . An integration routine SIMS based on Simpson's rule and Newton's $\frac{3}{8}$ rule, kindly supplied by Dr. A.L. Halmos was used to evaluate the integral in equation 6.24 .

The main programme was called CONT and controlled

the progress of the calculation. A flow diagram showing the way the programme worked is presented in Figure 6.3 . A listing of all the subroutines is given in the Computer Programmes P 2 .

6.4.7 Using the programme

The main difficulty in obtaining results once the programme had been written was the choice of the parameter b in equation 6.16 . This parameter controls the distribution of points in the radial direction, at which the solution is to be found. Increasing the value of b moves all the grid points closer to the surface. If they are too close the outer boundary condition will be ignored, if they are too far from the surface they will be outside the diffusional boundary layer and of no use.

Initially a trial and error method had to be used to determine b . The concentration profile was determined directly ahead of the bubble ($\theta = 0$) for particular values of Pe and R . A value of b was guessed and the concentration profile and the error indicator produced by DD01A was examined. The value of b was changed and the new profile was examined. This procedure was repeated until a reasonable concentration profile resulted, with the error indicator set at 1 . Experience showed that when the correct value of b had been found, the value of the dimensionless concentration at the first grid point was about 0.02 and the error indicator was 1 . The full calculation of collision

Figure 6.3 Flow diagram for collision efficiency calculation

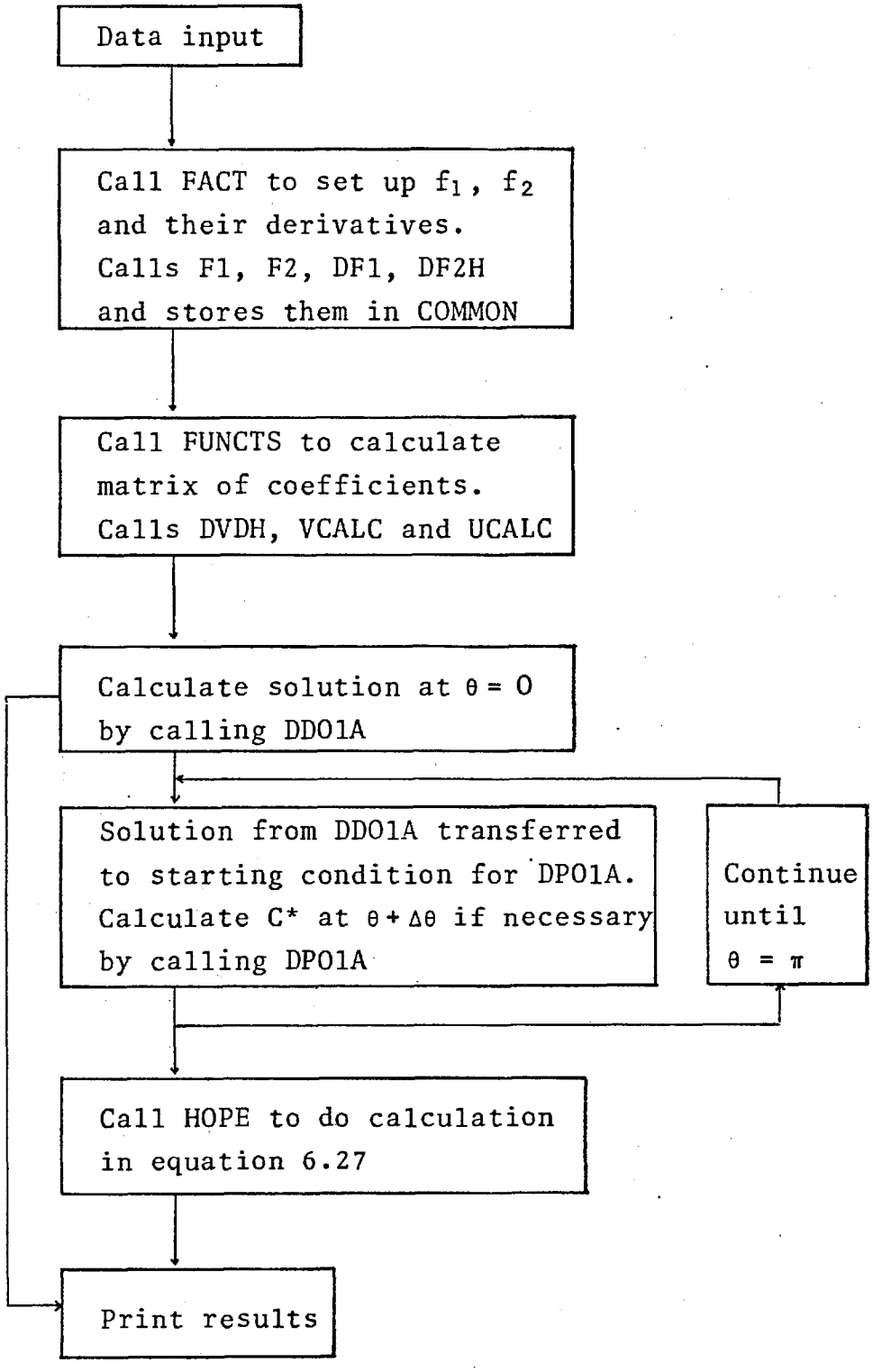

efficiency was then made using this value of b and values slightly larger and slightly smaller. If all efficiencies were within 0.5% of each other and if the efficiency was independent of r, the radial coordinate, the efficiency was assumed correct. The process was rather tedious, and it was soon learnt that the correct value of the parameter b followed in a logical way from the correct value obtained with slightly different values of Pe and R. The criterion of constant efficiency for different r was found so sensitive that it was eventually used to check the correctness of the efficiency.

For all but the highest value of the Péclet number Pe, 100 grid points were taken ($\Delta\eta = 0.01$). For all values of Pe $\Delta\theta = \pi/20$. Halving the grid spacing in the radial domain did not alter the efficiency. This is a good indication that the mesh size is fine enough.

If $Pe \geq 10R^3$ the concentration profile displayed a maximum greater than one (i.e. $c > c_\infty$). Physically this means that material is being brought close to the bubble faster than it can be deposited. It also means that the concentration profile cannot be calculated successfully using the transformation 6.16, and another more flexible transformation is needed. Such a transformation is:

$$H = -\frac{1}{b_1}\ln(1-\eta) - \frac{1}{b_2}\ln(1-\eta^m) \qquad (6.25)$$

Where b_1 , b_2 , and m are expansion parameters

The new transformed equation then becomes:

$$\frac{2R}{Pe} \cdot f_1 \cdot \frac{\partial^2 C^*}{\partial \eta^2} \cdot \left(\frac{d\eta}{dH}\right)^2 + \left\{ \left[\frac{2R}{Pe} \left(\frac{df_1}{dH} + f_1 \left(\frac{2}{R+Y} \right) \right) - v^* \right] \cdot \frac{d\eta}{dH} - \frac{2R}{Pe} f_1 \left(\frac{\partial}{\partial \eta} \left(\frac{d\eta}{dH} \right) \cdot \frac{d\eta}{dH} \right) \right\} \frac{\partial C^*}{\partial \eta} - \left[\frac{2}{R+Y} \left(v^* + \frac{\partial u^*}{\partial \theta} \right) + \frac{\partial v^*}{\partial H} \right] C^*$$

$$= \frac{u^*}{R + Y} \cdot \frac{\partial C^*}{\partial \theta} \qquad (6.26)$$

$$\frac{d\eta}{dH} = \frac{A_1}{B_1}$$

$$\text{and } \frac{\partial}{\partial \eta} \left(\frac{d\eta}{dH} \right) = B_1 \frac{dA_1}{d\eta} - A_1 \frac{dB_1}{d\eta}$$

Where $A_1 = b_1 \cdot b_2 (1 - \eta)(1 - \eta^m)$

and $B_1 = b_2 (1 - \eta^m) + b_1 \cdot m \cdot \eta^{m-1} (1 - \eta)$

The efficiency becomes:

$$E_c = 2 \left[1 + \frac{Y}{R} \right]^2 \int_0^{\pi} \left(\frac{2R}{Pe} \cdot f_1 \frac{\partial C^*}{\partial \eta} \cdot \frac{d\eta}{dH} - v^* C^* \right) \cdot \sin\theta \, d\theta \qquad (6.27)$$

The two transformation equations 6.16 and 6.25 are identical if $m = 1$ and $b_1 = b_2 = 2 \times b$. The new

transformation was tested by recalculating a "known" efficiency, with appropriate values for b_1 , b_2 and m. The results were identical to four decimal places. The values of b_1 , b_2 and m were determined subject to three conditions $m \geq 1$; $b_1, b_2 > 0$. The condition used to fix the three parameters was $H'/H_1 = 100$ where H' is the value of H corresponding to $\eta = 0.5$ (the location of the maximum) and H_1 corresponds to $\eta = \Delta\eta$ (the point closest to the bubble).

6.5 The results

6.5.1 Correlation of the results

Prieve and Ruckenstein showed that the quantity E_c should depend on Pe , R and A_{kT} . In this work the term A_{kT} is rather artificial because it is a measure of the guessed attractive force. Variations in A_{kT} will be ignored and only variations in Pe and R will be considered. We can expect for fixed A_{kT} that:

$$E_c R^2 = f(Pe/R^3) \qquad (6.28)$$

This correlation will break down as Pe/R^3 becomes small, because R then affects $E_c R^2$, nevertheless it is still useful.

6.5.2 The calculated efficiency

The efficiency of collision was calculated for a wide range of values of Pe/R^3 and some different

values of R . The value of A_{kT} was fixed at 10. The results are shown graphically in Figure 6.4 . A large number of curves could be generated by varying A_{kT} , but this was unnecessary. Values of the transformation parameters for selected values of Pe/R^3 are given in Table 6.1 . Two typical concentration profiles generated during the calculation are given in Figures 6.5 and 6.6 .

The solutions for the concentration profile immediately behind the bubble ($\theta=\pi$) were found to be unstable. This is a consequence of the method of solution. The mass transfer at $\theta \simeq \pi$ is probably small, according to Levich (1962), so this anomalous behaviour was ignored.

6.6 Discussion of results

Inspection of Figure 6.4 shows that R affects the correlation at small Pe/R^3 . For small Pe/R^3 and R = 1000 the solution approaches the Levich - Lighthill result (Levich 1962):

$$E_c R^2 = 4 \, x \left(\frac{Pe}{R^3}\right)^{-2/3} \qquad (6.29)$$

which proves that the solution of the equation was correct. For large Pe/R^3 the solution is almost a straight line.

If we consider these straight or almost straight lines the relation:

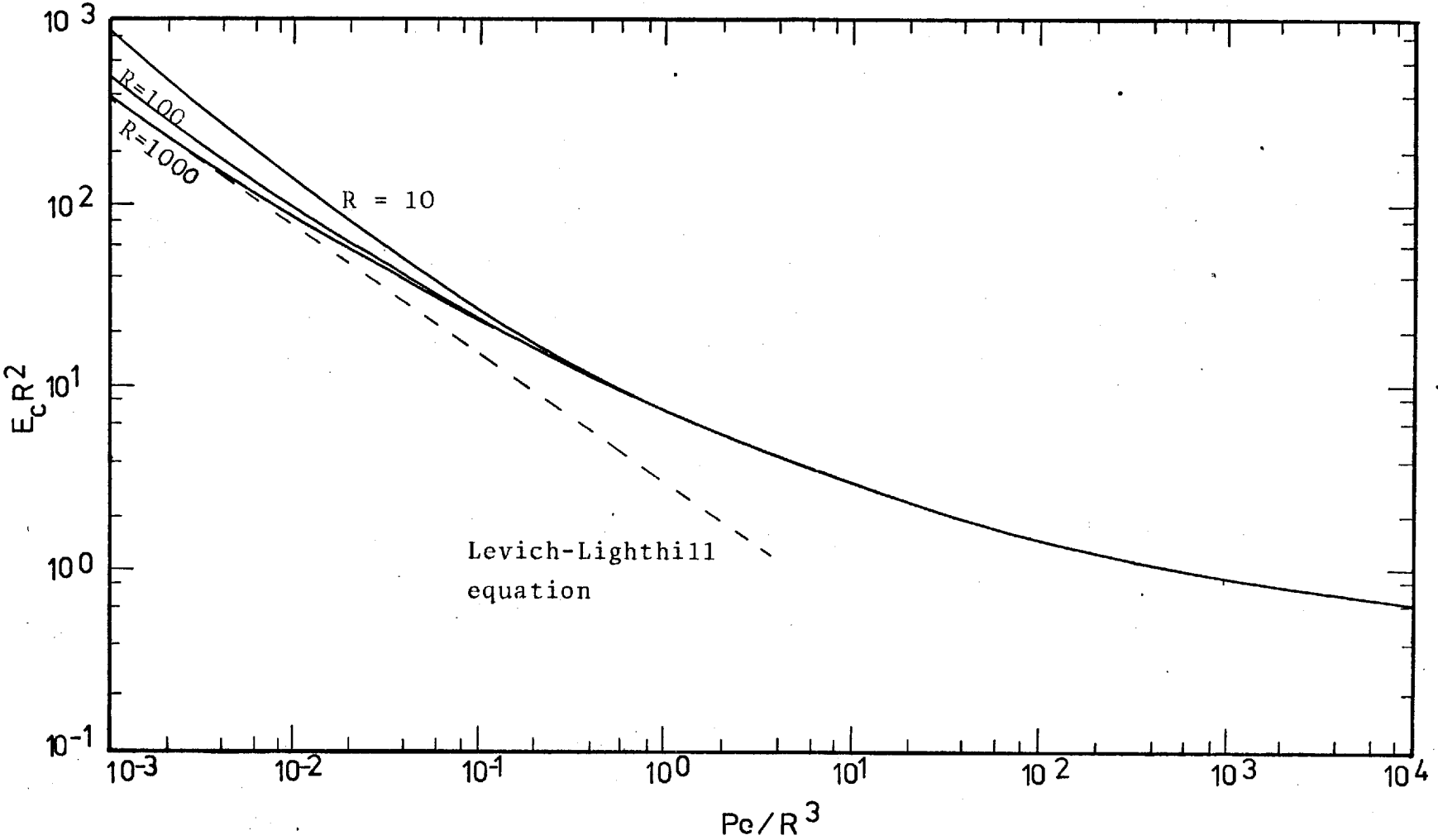

Figure 6.4 Plot of $E_c R^2$ versus Pe/R^3

Table 6.1 Values of the transformation parameters b_1 , b_2 and m for selected values of Pe/R^3 for R = 1000

Pe/R^3	b_1	b_2	m
10^{-3}	0.04	0.04	1
10^{-2}	0.12	0.12	1
10^{-1}	0.20	0.20	1
10^{0}	0.68	0.68	1
10^{1}	2.20	2.20	1
10^{2}	7.18	0.30	6.24
10^{3}	25.13	1.22	6.06
10^{4}	91.14	2.34	6.98

Figure 6.5 C* vs H for $Pe/R^3 = 0.1$, R = 1000

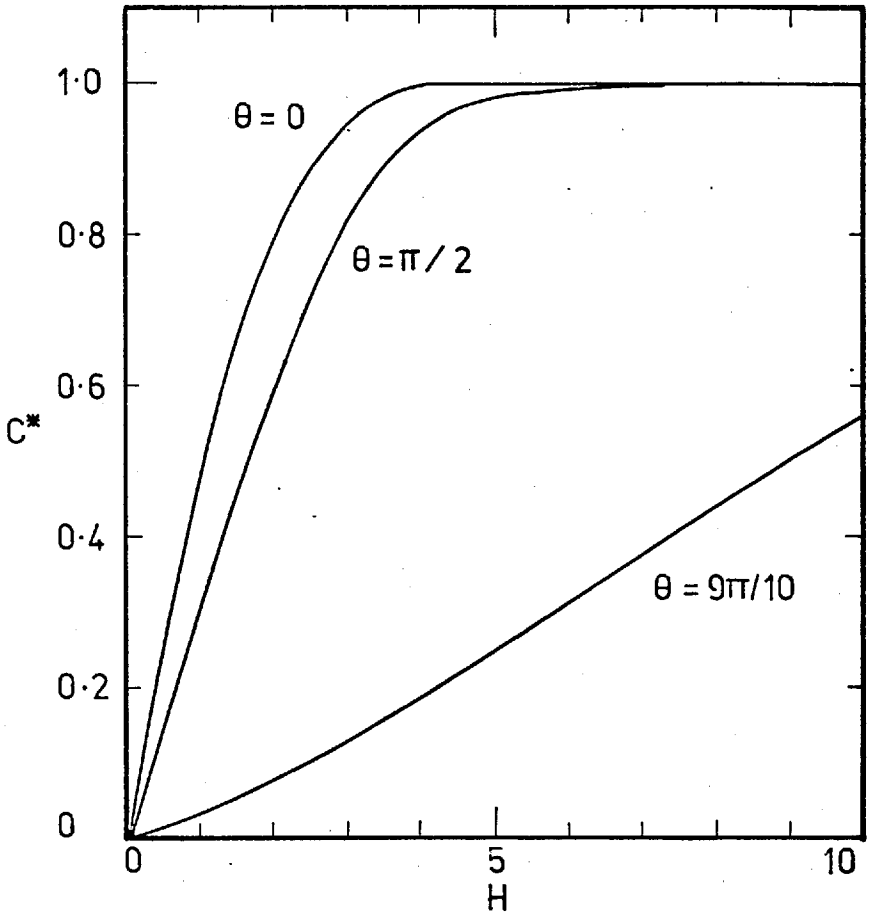

Figure 6.6 C* vs H for $Pe/R^3 = 5$, R = 10

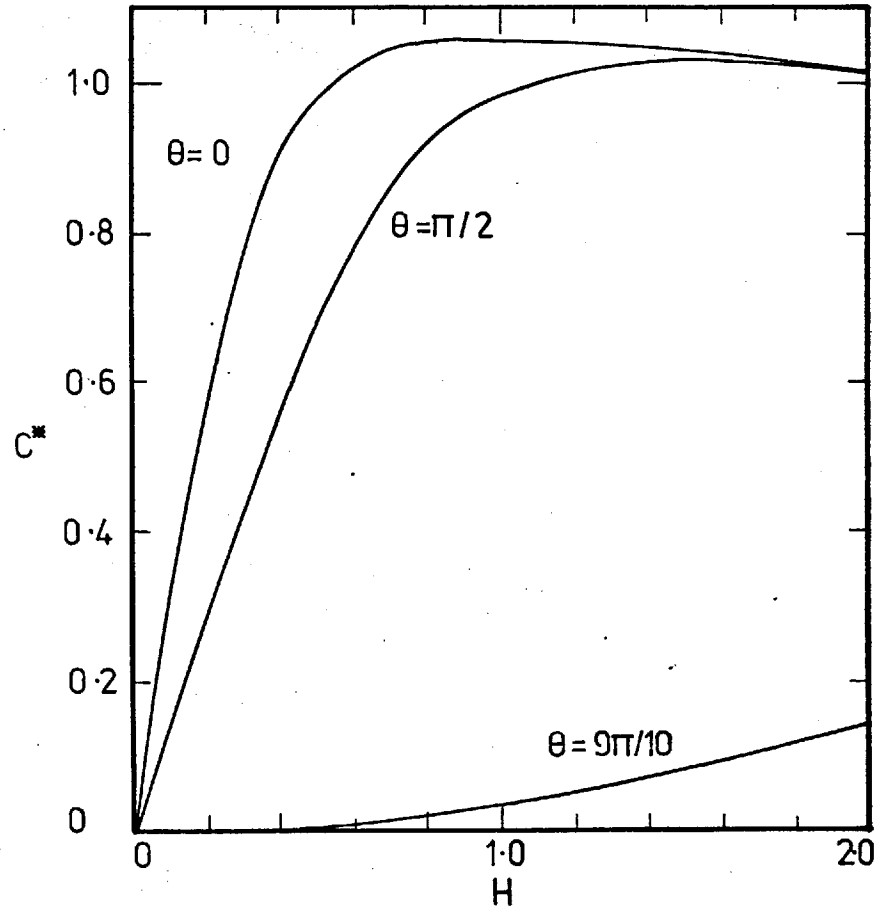

$$E_c R^2 \propto \left[\frac{Pe}{R^3}\right]^N \qquad (6.30)$$

is suggested. If Pe/R^3 is fully expanded we find that:

$$\frac{Pe}{R^3} = \frac{8\pi \rho_f g a_p^4}{3kT} \qquad (6.31)$$

and hence:

$$E_c R^2 \propto (a_p^4)^N \qquad (6.32)$$

Where N can be evaluated from the slope of the lines. The dependence of efficiency on a_b and a_p can be calculated from:

$$E_c \propto (a_p^4)^N \cdot \frac{a_p^2}{a_b^2} \qquad (6.33)$$

Taking typical values from the flotation system investigated in Chapters 4 and 5:

$a_p = 5 \times 10^{-4}$cm

$a_b = 5 \times 10^{-3}$cm

$\rho_f = 1$ gm/cc

$g = 980$ cm/sec^2

the value of Pe/R^3 can be calculated from the equation 6.31 and is approximately 1×10^4 . The slope of the graph at $Pe/R^3 = 1 \times 10^4$ is -0.18, so equation 6.33 becomes:

$$E_c \propto \frac{a_p^{1.3}}{a_b^2} \qquad (6.34)$$

This result is very similar to Reay and Ratcliff's

(1973) result:

$$E_c \propto \frac{a_p^{1.9}}{a_b^2} \qquad (6.35)$$

but the dependence on particle radius is considerably weaker due to the attractive force, and the influence of the hydrodynamic correction factors f_1, f_2 and f_3 included in this work.

For the case of very small particles $a_p = 1 \times 10^{-5}$ cm, $a_b = 5 \times 10^{-3}$ cm, the value of Pe/R^3 is approximately 2×10^{-3} and $R = 500$. The slope at $Pe/R^3 = 2 \times 10^{-3}$ and $R = 1000$ is -0.67 as it approaches the Levich - Lighthill solution, and so equation 6.33 becomes:

$$E_c \propto \frac{1}{a_p^{0.67}\, a_b^2} \qquad (6.36)$$

This is the same result Reay and Ratcliff (1973) obtained for submicron particles in equation 3.10 .

The results can be expressed in a more illustrative way by plotting efficiency against particle size, Figure 6.7 shows the plot for two bubble sizes; 50 microns and 25 microns in radius. The effect of particle size and bubble size on efficiency is clearly demonstrated, the absolute value of the efficiency is not really significant because of the assumptions made about the attractive force.

As a final note, the fact that $E_c R^2 \neq f(a_b)$ shows

Figure 6.7 Efficiency vs particle radius for two bubble sizes

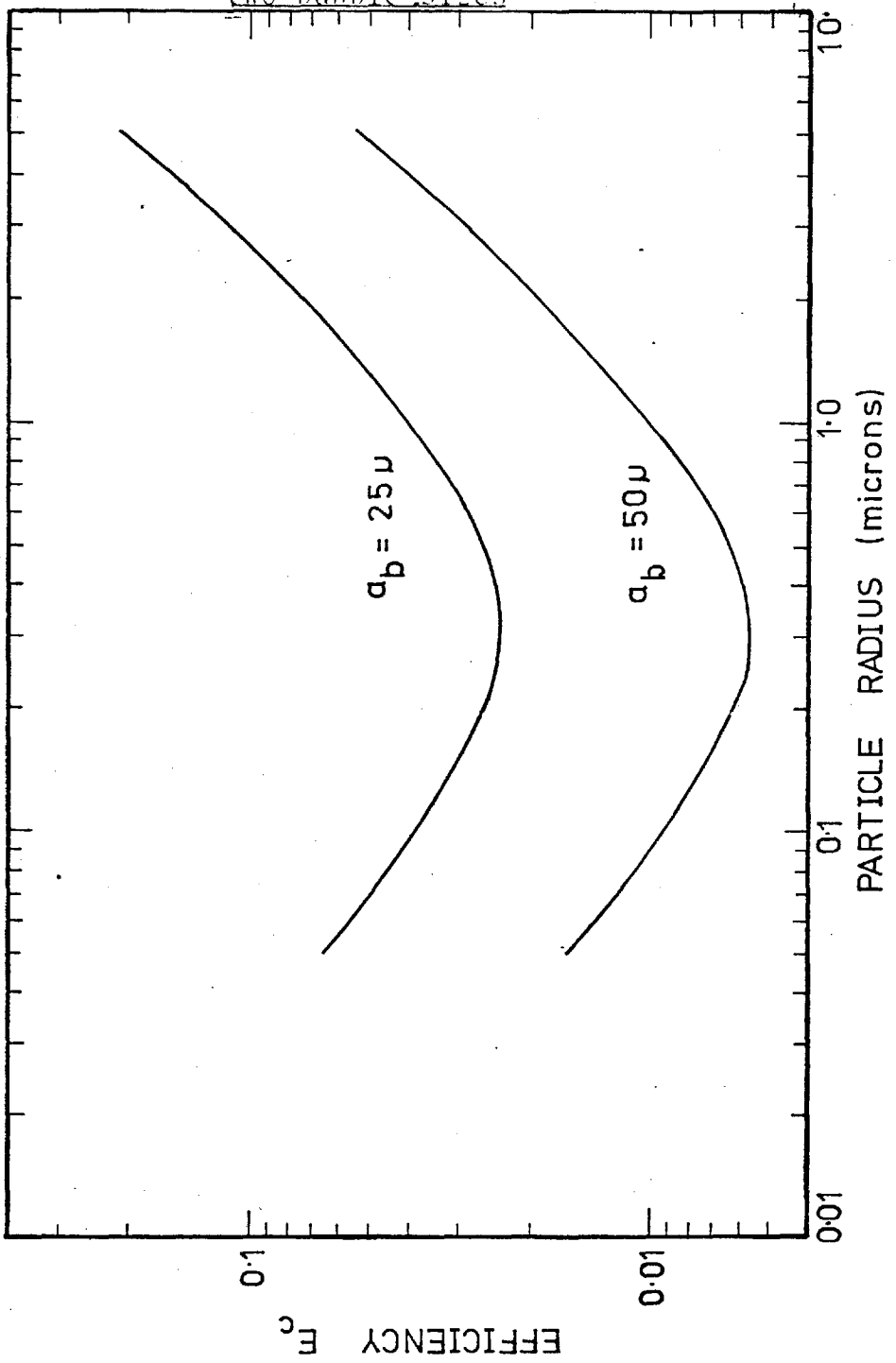

that the collision efficiency will be proportional to $1/a_b^2$ for all particle sizes and hence the rate of flotation should be proportional to $1/a_b^3$.

6.7 Comparison with experimental results

Equation 6.34 predicts that E_c will be proportional to a_p to about the 1.3 power. If we can assume that the adhesion efficiency is independent of particle size then the rate of flotation could be expected to be proportional to the 1.3 power also. This prediction depends on the attractive force and so must be viewed with some caution. As we have seen in Chapter 5 the rate of flotation depended on the 1.5 power of the particle radius. This agreement between theory and experiment is good considering that a rather crude assumption was made about the attractive force for the bubble/particle interaction.

We must be careful not to draw too many conclusions from the good agreement of the theory with experiment. The agreement certainly does not imply that the assumptions made about the attractive force are correct. The results of the theoretical investigation really tell us nothing about the attractive force. Its magnitude and form will hopefully be determined at a later date.

In the later stages of this work a term was added to the radial particle velocity to take account of double layer repulsion. Although the term was correct

the solution of the mass transport equation became unstable. It would seem that the method of solution is unsuitable in this case, and the trajectory method of Spielman and Cukor (1973) may be a better method for dealing with the double layer repulsion.

CHAPTER 7

GENERAL CONCLUSIONS AND IDEAS FOR FUTURE WORK

In this chapter the results and arguments presented in the thesis are brought together and discussed. Ideas for future work are then listed.

The aim of this investigation was to gain some understanding of the physical variables which control the kinetics of effluent flotation. Effluent flotation involves the removal of fine particles from relatively dilute suspensions. The bubbles employed by an effluent treatment plant are usually less than 100 microns in diameter, much smaller than the bubbles in a mineral flotation cell.

The results of a series of careful batch experiments with polystyrene particles showed that the rate of flotation was proportional to about the 1.5 power of the particle radius (diameter). This was in excellent agreement with the result for glass spheres obtained by Reay and Ratcliff (1974). The purely hydrodynamic theories of Flint and Howarth (1971) and Reay and Ratcliff (1973) predicted that the rate should be dependent on the square of the particle size, so they slightly overestimated the dependence, but considering the simplicity of the models the agreement is reasonable.

The experiments also showed that the rate of flotation depended strongly on the double layer repulsion between particle and bubble; the flotation rate falling rapidly as the double layer repulsion increased. Some earlier investigations had shown that the zeta potential of the particles in a flotation cell affected the rate of flotation, but all these investigators had either been concerned with mineral flotation and/or had used large bubbles. These large bubbles have electrical properties which are impossible to quantify at present, and after all, when analysing double layer repulsion we must include in the analysis, the double layer of both the bubble and the particle. In many of these earlier investigations flocculation of the particles, or changes in bubble size etc. could well have accounted for the results. In this study the alternative explanations for the behaviour of the flotation rate were eliminated.

The dependence of flotation rate on particle size and double layer repulsion was very similar to the behaviour of the filter coefficient found by several investigators studying deep-bed filtration. There is hydrodynamic similarity in the two processes and the special surface properties of the small bubbles used in this study add to the similarity.

The theoretical part of this investigation grew from the desire to see if a model developed specifically for filtration work could be adapted to suit the analysis of flotation. The result of this investigation showed

that:

a) The efficiency of collection for very small particles for which the main transport mechanism is diffusion, was:

$$E_c \propto \frac{1}{a_b^{\,2}\, a_p^{\,2/3}}$$

b) For larger particles unaffected by diffusion:

$$E_c \propto \frac{a_p^{1.3}}{a_b^{\,2}}$$

The dependence of flotation rate on particle size for larger particles agreed well with the experimental study.

How does the information gathered in this investigation help the designer who wants to remove fine particles from suspension in an effluent flotation cell? Firstly he must know the particle size of the material to be separated. The particles should be made as large as possible, but the theory suggests that coagulation of sub-micron particles will only be beneficial if the agglomerate size is brought well into the non-diffusion region. The designer must also know the zeta potential of the particles and be able to estimate the bubble zeta potential. The results of this investigation showed that the zeta potential of the particle and the bubble need not be reduced to zero for maximum flotation, this may

be economically useful in certain circumstances. The theoretical results on bubble size, namely that the rate should be proportional to $1/a_b^3$ should make the designer use the smallest bubbles that are economically feasible. The designer should look closely at the experimental and theoretical information gathered by filtration workers.

Recommendations for future work

There are several problem areas which require further research:

a) The effect of bubble size on flotation rate has not been proven satisfactorily. A prerequisite to this study would be a need to produce small uniform bubbles of a controllable and predetermined size.

b) The magnitude and form of the specific surface force term must be found. The specific surface force is the component of the disjoining pressure not accounted for by double layer or van der Waals dispersion forces.

c) The effects of gravity and other forces on the collision efficiency should be determined theoretically as soon as a reasonable estimate of the specific surface forces can be made.

APPENDICES

APPENDIX A.1

Theory of the Coulter Counter

(Taken essentially from the Coulter Counter ZB Manual)

The Coulter Counter determines the number and size of particles suspended in an electrically conductive liquid. This is done by forcing the suspension to flow through a small aperture having an immersed electrode on either side.

As a particle passes through the aperture, it changes the resistance between the electrodes. This produces a voltage pulse of short duration having a magnitude proportional to particle size. The series of pulses is then electronically scaled and counted.

When the stopcock is opened, a controlled external vacuum initiates flow from the beaker through the aperture and unbalances the mercury siphon. Closing the stopcock then isolates the system from the external vacuum, and the siphoning action of the mercury continues the sample flow (see Figure A.1.1).

The advancing mercury column contacts start and stop probes to activate the electronic counter. The probes are placed precisely $\frac{1}{2}$cc apart, providing a constant sample volume for all counts.

The voltage pulses are amplified and fed to a threshold circuit having an adjustable threshold level. If this

level is reached or exceeded by a pulse, the pulse is counted. The threshold level is indicated on an oscilloscope screen by a brightening of the pulse segments above the threshold, facilitating the selection of appropriate counting levels.

By taking a series of counts at selected threshold levels, data are directly obtained for plotting cumulative frequency (larger than stated size) versus particle size. Integration of all or part of the resultant curve provides a measure of the particle content of the suspension.

The counts have first to be corrected for coincident particle passages (doublets, triplets, etc.). These corrections are quite precise, and if kept to a moderate level (say 15%), an overall accuracy of measurement of better than 1% is readily achieved. This is due in part to the large numbers of particles counted (tens of thousands), which provide low statistical deviations.

The pulse height and instrument response are essentially proportional to particle volume, and to fluid resistivity. The particle resistivity has very little effect on the response, unless it is quite close to the resistivity of the fluid. If particle conductivity changes from one millionth to one hundredth that of the electrolyte, there is less than 1% change in the response. Either the fluid or the particle may be the better conductor, as only a simple signal polarity reversal is needed to switch from one case to the other. Charges on the particles are too minute to have detectable effect on the count.

Figure A.1.1

THEORY OF THE COULTER COUNTER

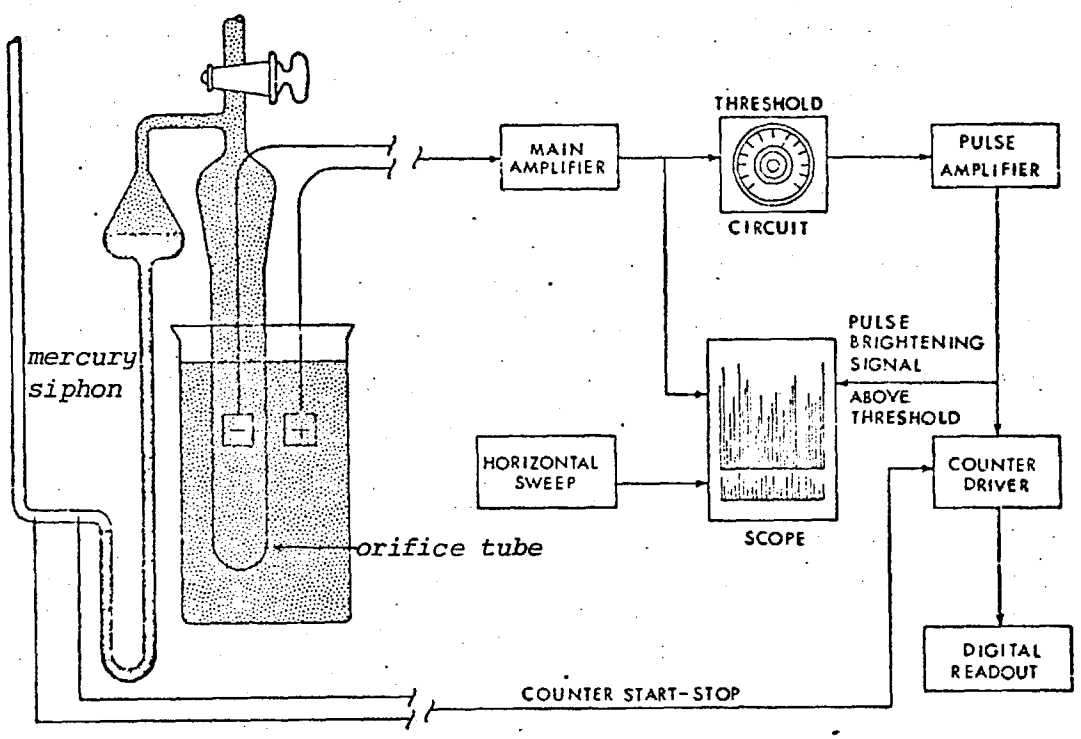

SCHEMATIC DIAGRAM OF COULTER PRINCIPLE

APPENDIX A.2

A.2.1 Settings of the Coulter Counter ZB

Table A.2.1 gives the settings for the Coulter Counter and the resulting particle diameter for a calibration factor of 2.14 .

Table A.2.1 Coulter Counter settings

Attenuation setting (A)	Threshold setting (t_L)	Aperture current setting (I)	Diameter (microns)	Mean diameter (microns)
8	20	8	23.23	20.8
4	20	8	18.44	16.5
2	20	8	14.63	13.1
1	20	8	11.62	10.4
1	20	4	9.22	8.3
1	20	2	7.32	6.6
1	20	1	5.81	5.2
$\frac{1}{2}$	20	1	4.61	

The rate of flotation for the first six particle diameters was usually determined. For some experiments in which the rate of flotation was slow the counting errors for the smallest particle sizes were too high and the rate of flotation could not be determined for these.

For some experiments it was possible to include the rate of flotation for the seventh particle size.

A.2.2 Working up the raw Coulter Counter data

The following is a brief description of the treatment given to raw Coulter Counter data. The raw counts at each instrument setting were averaged and the coincidence correction was added:

$$\text{correction} = P\left(\frac{\bar{N}'}{1000}\right)^2 \qquad \text{(A.2.1)}$$

Where $\bar{N}'$ is the mean raw count

P is the coincidence correction factor

The averaged blank count was subtracted from the corrected count producing the final corrected particle count (N_t)

The particle diameter d_p was calculated from the instrument settings and the calibration factor.

$$d_p = M \cdot \sqrt[3]{t_L \cdot I \cdot A} \qquad \text{(A.2.2)}$$

Where M is the calibration factor (2.14)

t_L is the threshold setting

I is the aperture current setting

A is the attenuation setting

APPENDIX A.3

Experimental conditions and results

A.3.1 Experimental conditions

Table A.3.1 Ambient conditions for the rate of flotation experiments

Expt. No.	Atmospheric pressure (mmHg)	Air temperature (^{o}C)	Solution temperature (^{o}C)	Gas flow rate litres/hr at room temp and pressure
1	740	18.0	21.0	3.72
2	752	22.0	22.5	3.76
3	750	22.0	21.0	3.72
4	750	22.5	22.1	3.77
5	748	22.1	22.5	3.66
6	761	22.1	22.8	3.62
7	760	21.0	22.0	3.53
8	751	19.5	22.0	3.53
9	752	20.0	21.5	3.56
10	753	19.0	23.5	3.62
11	769	21.5	22.0	3.68
12	773	22.0	22.0	3.55
13	770	22.1	22.0	3.64
14	754	21.8	22.0	3.69
15	762	22.0	23.5	3.61
16	756	22.0	21.5	3.71

Expt. No.	Atmospheric pressure (mmHg)	Air temperature (^{o}C)	Solution temperature (^{o}C)	Gas flow rate litres/hr at room temp and pressure
17	755	21.0	20.0	3.77
18	767	20.0	20.5	3.66
19	760	20.5	23.0	3.85

A.3.2 Experimental results

Table A.3.2 presents the nineteen rate of flotation experiments. The table includes the mean particle diameter (d_p) in microns, the first order rate constant (k_p) corrected to 3.50 litres/hour at room temperature and pressure, and its standard error (S.E) .

The first fourteen experiments were conducted under standard surfactant/alcohol conditions (5 x 10^{-5}CTAB, 0.5% V/V ethanol). The last five were conducted under different conditions as detailed in the tables.

Table A.3.2 Rate of flotation results

	Diameter μ d_p	Rate (min^{-1}) k_p	S.E.
Experiment 1	20.9	0.164	0.009
Sodium sulphate $5x10^{-4}$	16.6	0.109	0.010
Mobility 4.4 ± 0.2	13.2	0.071	0.009
	10.6	0.044	0.009
	6.9	0.020	0.006
Experiment 2	20.9	0.112	0.012
Sodium sulphate $5x10^{-4}$	16.6	0.071	0.008
Mobility 4.7 ± 0.4	13.2	0.052	0.002
	10.5	0.030	0.001
	8.3	0.027	0.002
Experiment 3	20.8	0.092	0.006
Sodium sulphate $5x10^{-4}$	16.5	0.068	0.008
Mobility 5.0 ± 0.4	13.1	0.053	0.002
	10.4	0.032	0.007
	8.3	0.027	0.010
	6.6	0.016	0.003
Experiment 4	20.8	0.107	0.008
Sodium sulphate $5x10^{-4}$	16.5	0.068	0.004
Mobility 5.0 ± 0.4	13.1	0.049	0.005
	10.4	0.045	0.004
	8.3	0.048	0.007
	6.6	0.048	0.007

	Diameter μ d_p	Rate (min^{-1}) k_p	S.E.
Experiment 5	20.8	0.255	0.022
Sodium sulphate $1x10^{-3}$	16.5	0.170	0.008
Mobility 4.5 ±0.4	13.1	0.120	0.010
	10.4	0.090	0.007
	8.3	0.060	0.012
	6.6	0.038	0.017
	5.2	0.022	0.006
Experiment 6	20.8	0.161	0.019
Sodium sulphate $1x10^{-3}$	16.5	0.118	0.005
Mobility 4.1 ±0.4	13.1	0.101	0.010
	10.4	0.056	0.007
	8.3	0.051	0.018
	6.6	0.020	0.009
Experiment 7	20.8	0.198	0.027
Sodium sulphate $1x10^{-3}$	16.5	0.150	0.011
Mobility 4.1 ± 0.3	13.1	0.095	0.011
	10.4	0.064	0.005
	8.3	0.069	0.012
	6.6	0.038	0.009
	5.2	0.035	0.007
Experiment 8	20.8	0.472	0.043
Sodium sulphate $2.5x10^{-3}$	16.5	0.299	0.023
Mobility 3.9 ± 0.2	13.1	0.194	0.013

	Diameter μ d_p	Rate (min^{-1}) k_p	S.E.
Experiment 8(cont.)	10.4	0.169	0.015
	8.3	0.070	0.018
	6.6	0.054	0.001
Experiment 9	20.8	0.375	0.052
Sodium sulphate 2.5×10^{-3}	16.5	0.242	0.024
Mobility 3.8 ± 0.2	13.1	0.165	0.021
	10.4	0.113	0.017
	8.3	0.080	0.008
	6.6	0.040	0.007
	5.2	0.056	0.002
Experiment 10	20.8	0.646	0.061
Sodium sulphate 5×10^{-3}	16.5	0.418	0.035
Mobility 3.42 ± 0.2	13.1	0.280	0.018
	10.4	0.174	0.007
	8.3	0.130	0.018
	6.6	0.085	0.014
	5.2	0.052	0.014
Experiment 11	20.8	0.476	0.070
Sodium sulphate 5×10^{-3}	16.5	0.373	0.045
Mobility 3.76 ± 0.3	13.1	0.283	0.037
	10.4	0.190	0.019
	8.3	0.127	0.016
	6.6	0.090	0.004
	5.2	0.058	0.014

	Diameter μ d_p	Rate (min^{-1}) k_p	S.E.
Experiment 12	20.8	0.371	0.075
Sodium sulphate $1x10^{-2}$	16.5	0.324	0.055
Mobility 2.7 ± 0.3	13.1	0.222	0.026
	10.4	0.165	0.032
	8.3	0.137	0.014
	6.6	0.091	0.027
Experiment 13	20.8	0.337	0.069
Sodium sulphate $1x10^{-2}$	16.5	0.275	0.037
Mobility 3.01 ± 0.3	13.1	0.189	0.021
	10.4	0.166	0.023
	8.3	0.081	0.017
	6.6	0.100	0.021
Experiment 14	20.8	0.022	0.004
Sodium sulphate $1x10^{-4}$	16.5	0.030	0.003
Mobility 5.2 ± 0.5	13.1	0.016	0.005
	10.4	0.022	0.003

Experiments with non-standard conditions

Experiment 15	20.8	0.112	0.010
CTAB 5×10^{-5}	16.5	0.078	0.007
EtOH 0.75%V/V	13.1	0.049	0.004
Sodium sulphate $5x10^{-4}$	10.4	0.042	0.007
Mobility 4.3 ± 0.3	8.3	0.031	0.006
	6.6	0.021	0.001

	Diameter μ d_p	Rate (min^{-1}) k_p	S.E.
Experiment 16	20.8	0.057	0.011
CTAB 7.5×10^{-5}	16.5	0.034	0.003
EtOH 0.5%V/V	13.1	0.033	0.005
Sodium sulphate 5×10^{-4}	10.4	0.010	0.004
Mobility 4.4 ± 0.4			
Experiment 17	20.8	0.056	0.005
CTAB 6.25×10^{-5}	16.5	0.046	0.008
EtOH 0.5%V/V	13.1	0.038	0.006
Sodium sulphate 5×10^{-4}	10.4	0.014	0.006
Mobility 4.9 ± 0.5	8.3	0.020	0.007
	6.6	0.016	0.006
Experiment 18	20.8	0.090	0.007
CTAB 5×10^{-5}	16.5	0.058	0.007
EtOH 1%V/V	13.1	0.043	0.004
Sodium sulphate 5×10^{-4}	10.4	0.045	0.004
Mobility 4.4 ± 0.4	6.6	0.021	0.007
	5.2	0.015	0.007
Experiment 19	20.8	0.682	0.025
CTAB 3×10^{-5}	16.5	0.470	0.029
EtOH 0.5% V/V	13.1	0.309	0.012
Sodium sulphate 5×10^{-3}	10.4	0.206	0.027
Mobility 3.0 ± 0.2	8.3	0.146	0.014
	6.6	0.087	0.008
	5.2	0.051	0.014

APPENDIX A.4

Errors in the estimation of the rate of flotation

Experimental errors in the determination of the rate of flotation arose mainly from the counting of particles.

The Coulter Counter relies for its accuracy, in part, on the large numbers of particles counted. This provides low statistical deviations. To check the accuracy, ten counts were taken on a single sample of polystyrene particles at different size levels. The standard deviation (σ) was taken as a measure of error. The results are shown in Table A.4.1

Table A.4.1 Errors in the Coulter Counter results

Size (diameter microns)	Cumulative mean count	Standard deviation (σ)	
		actual	% of mean
23.2	144	12	8.5
18.4	721	24	3.4
14.6	2090	36	1.7
11.6	3501	49	1.4
9.2	4684	87	2.0
7.3	5650	51	0.9
5.8	6702	120	1.8
4.6	7827	73	0.9
2.9	9751	98	1.0

The results show a fairly typical pattern of errors, with the percentage error being largest when the counts are smallest. The small errors between 1% and 2% are fairly typical for cumulative counts greater than about 5000.

In flotation experiments it was the differences between the cumulative results that were important, not the cumulative results themselves. Quite obviously the percent error in the differences was much greater than the error in the cumulative totals. These counting errors manifested themselves as errors in the position of the points in the plot of $\ln(N_o/N_t)$ versus time, which was used to calculate the rate of flotation. Two examples taken from the flotation experiments will serve to illustrate the effect of these errors on the value of $\ln(N_o/N_t)$ which we will call "x" .

Data

Mean diameter = 13.1 μ

$N_o = 2000 \pm 50$

$N_2 = 1199 \pm 50$

The errors δN_o and $\delta N_2 = \pm 50$ are typical for cumulative counts of 3000 - 4000 .

Now:

$$x = \ln(N_o/N_t)$$

$$(dx)^2 \simeq \left(\frac{\partial x}{\partial N_o} \cdot \delta N_o\right)^2 + \left(\frac{\partial x}{\partial N_2} \cdot \delta N_2\right)^2$$

Substituting numerical values we obtain:

$$x = 0.52 = \ln(N_o/N_t)$$

$$dx = 0.05 = \text{standard deviation of } \ln(N_o/N_t)$$

So a standard deviation of 1% - 2% in the cumulative counts of the Coulter Counter has produced a standard deviation of 10% in the value of $\ln(N_o/N_t)$.

A second example is more disturbing. A particular initial count N_o for particles having a mean size of 6.6 microns was 1893 . The count after two minutes N_2 was 1913 . Obviously this makes the value of $\ln(N_o/N_t)$ negative and therefore meaningless. Apart from gross volumetric errors etc. this situation can arise as follows:

The count for particles with a mean size of 6.6 microns arose from cumulative counts of about 10,000. An error of 1% or 100 counts, which is reasonable, could quite easily account for the meaningless result; especially if the rate of flotation is slow. Small particles floated slower than larger particles.

When this situation arose in an experiment the value of $\ln(N_o/N_t)$ was set to zero.

APPENDIX A.5

A.5.1 Testing the computer programme DP01A

DP01A is a Fortran subroutine used for solving a linear parabolic partial differential equation. The way this routine was used has already been described in the text (see Chapter 6).

The routine was however first tested by using it to solve an equation with a known analytical solution. A suitable "known" equation is presented by Smith (1965). He presents both an analytical and numerical solution.

The equation is a simple one:

$$\frac{\partial U}{\partial t} = \frac{\partial^2 U}{\partial x^2} \qquad \text{(A.5.1)}$$

This is a dimensionless equation which represents the distribution of U (say temperature) at a distance x from the end of a thin uniform rod after time t.
If the initial distribution of U is:

$$\begin{aligned} U &= 2x && 0 \leqslant x \leqslant \tfrac{1}{2} : t = 0 \\ U &= 2(1-x) && \tfrac{1}{2} \leqslant x \leqslant 1 : t = 0 \end{aligned} \qquad \text{(A.5.2)}$$

and the boundary conditions are:

$$\begin{aligned} U &= 0 && x = 0 : \text{all } t > 0 \\ U &= 0 && x = 1 : \text{all } t > 0 \end{aligned} \qquad \text{(A.5.3)}$$

then the analytical solution is known to be:

$$U = \frac{8}{\pi^2}\sum_{n=1}^{\infty}\frac{1}{n^2}\,(\sin\tfrac{1}{2}n\,\pi)(\sin\, n\,\pi x)\exp(-n^2\pi^2\, t) \qquad (A.5.4)$$

Such an equation and set of initial conditions and boundary conditions provide a reasonable test because there is a discontinuity in the initial value of $\partial U/\partial x$, from $+2$ to -2 at $x = 0.5$.

Equations A.5.1, 2, 3 were prepared in the form required for routine DP01A and the equations solved with ten x-intervals in the range $0 \leqslant x \leqslant 1.0$.

The results of the investigation are tabulated in Table A.5.1. Inspection of the table shows that the routine DP01A is indeed as accurate as the Crank-Nicolson implicit method of solution for similar time steps; both methods are computationally more rapid and more accurate than the explicit methods. The routine DP01A was thus confidently applied to the solution of the diffusion equation.

A.5.2 Testing the computer programme DD01A

The Harwell routine DD01A was tested in a similar way. The "known" equation was taken from Levy and Baggott (1950). The equation was:

$$\frac{d^2y}{dx^2} - 2(1 + 2x^2)y = 0 \qquad (A.5.5)$$

to be solved with the boundary conditions:

$$y = 1 \quad \text{at} \quad x = 0$$
$$y = 1 \quad \text{at} \quad x = 1 \qquad \text{(A.5.6)}$$

A small routine was written to supply DDO1A with the value of the coefficients. The results for various values of x are presented in Table A.5.2. The results show that DDO1A can be used with confidence to solve the ordinary differential equation part of the diffusion equation.

Table A.5.1 Values of U at x = 0.5 for the solution of equations A.5.1, 2, 3 by various methods

Time t	Analytical	Crank-Nicolson $\Delta t = 0.01$	DP01A $\Delta t=0.01$	DP01A $\Delta t=0.005$
0.00	1.0000	1.0000	1.0000	1.0000
0.01	0.7743	0.7691	0.7700	0.7842
0.02	0.6809	0.6921	0.6904	0.6874
0.10	0.3021	0.3069	0.3050	0.3049

Table A.5.2 Values of y for various values of x from equations A.5.5, 6

x	DD01A	Levy and Baggott (1950)
0.0	1.0000	1.0000
0.2	0.8266	0.8266
0.4	0.7257	0.7256
0.6	0.7026	0.7026
0.8	0.7783	0.7782
1.0	1.0000	1.0000

APPENDIX A.6

Quantities required for the numerical work of Chapter 6

This appendix presents the quantities $f_1(H)$, $f_2(H)$ etc. which are required for the numerical work of Chapter 6 .

A.6.1 The factor $f_1(H)$ and its derivative

This factor corrects the radial velocity of a particle induced by a unit radial force for the presence of a plane, H particle radii from the surface of the sphere.

$$f_1(H) = \frac{1}{\lambda} \qquad \text{(A.6.1)}$$

λ was derived by Brenner (1961)

$$\lambda = \frac{4}{3}\sinh\alpha \sum_{n=1}^{\infty} \frac{n(n+1)}{(2n-1)(2n+3)} \left[\frac{BINUM}{BIDEN} - 1\right] \qquad \text{(A.6.2)}$$

Where $BINUM = 2\sinh\cdot(2n+1)\alpha + (2n+1)\sinh 2\alpha$

$$BIDEN = 4\sinh^2(n+\tfrac{1}{2})\alpha - (2n+1)^2\sinh^2\alpha$$

$$\alpha = \ln\left[Y + (Y^2 - 1)^{\frac{1}{2}}\right] : Y = H + 1$$

BINUM and BIDEN refer to the names given to these expressions in subroutine F1 .

The derivative of $f_1(H)$ was determined analytically and is given by:

$$\frac{df_1}{dH} = \frac{df_1}{d\lambda} \times \frac{d\lambda}{d\alpha} \times \frac{d\alpha}{dH} \qquad \text{(A.6.3)}$$

Where $\frac{df_1}{d\lambda} = \frac{-1}{\lambda^2}$: $\frac{d\alpha}{dH} = \frac{1}{(Y^2-1)^{\frac{1}{2}}}$

and

$$\frac{d\lambda}{d\alpha} = \frac{4}{3}\cosh\alpha \sum_{n=1}^{\infty} \frac{n(n+1)}{(2n-1)2n+3)} \left[\frac{BINUM}{BIDEN} - 1\right]$$

$$+ \frac{4}{3}\sinh\alpha \sum_{n=1}^{\infty} \frac{n(n+1)}{(2n-1)(2n+3)} \left\{\frac{BIDEN \times DNUM - BINUM \times DDEN}{(BIDEN)^2}\right\}$$

(A.6.4)

Where DNUM = $(4n+2)\cosh(2n+1)\alpha + (4n+2)\cosh 2\alpha$

DDEN = $(4n+2)\sinh(2n+1)\alpha - (2n+1)^2 \sinh 2\alpha$

Subroutine DF1 calculates this quantity.

A.6.2 The factor $f_2(H)$ and its derivative

This factor corrects the radial force exerted on a stationary particle by an axisymmetric stagnation flow over a plane, H particle radii from the surface of the particle.

$$f_1(H) = \frac{f_o}{Y^2} \qquad \text{(A.6.5)}$$

f_o was derived by Goren and O'Neill (1971)

$$f_o = \frac{-2\sqrt{2}}{3}\sinh^3\alpha \sum_{n=1}^{\infty} \frac{(2n+1)\ b_n}{2n+3} \qquad \text{(A.6.6)}$$

This is the equation that contains two typographical errors in the original paper.

The term b_n is generated from the solution of four simultaneous equations. Only the final result will be given:

$$b_n = \frac{U_1 S - U_2 Q}{S R - T Q} \qquad (A.6.7)$$

Where $Q = \cosh(j_n \alpha) - \cosh(k_n \alpha)$

$R = \sinh(j_n \alpha) - P \sinh(k_n \alpha)$

$S = j_n \sinh(j_n \alpha) - k_n \sinh(k_n \alpha)$

$T = j_n \cosh(j_n \alpha) - P k_n \cosh(k_n \alpha)$

$$U_1 = \frac{-2\sqrt{2}}{3} \frac{n(n+1)}{2n+1} \left\{ \left[j_n e^{-j_n \alpha} - k_n e^{-k_n \alpha} \right] + \coth\alpha \left[e^{-j_n \alpha} - e^{-k_n \alpha} \right] \right\}$$

$$U_2 = \frac{-2\sqrt{2}}{3} \frac{n(n+1)}{2n+1} \left\{ \left[-j_n^2 e^{-j_n \alpha} + k_n^2 e^{-k_n \alpha} \right] - \frac{1}{\sinh^2\alpha} \left[e^{-j_n \alpha} - e^{-k_n \alpha} \right] \right.$$

$$\left. + \coth\alpha \left[-j_n e^{-j_n \alpha} + k_n e^{-k_n \alpha} \right] \right\}$$

with $j_n = n - 1/2$, $k_n = n + 3/2$, $P = \frac{j_n}{k_n}$

Q , R , S etc. refer to the names given to these expressions in the computer programme subroutine F2 .

The derivative of f_2 was determined analytically.

$$\frac{df_2}{dH} = \frac{Y^2 \frac{df_o}{dH} - 2Yf_o}{Y^4} \qquad (A.6.8)$$

Where $\frac{df_o}{dH} = \frac{df_o}{d\alpha} \times \frac{d\alpha}{dH}$

and

$$\frac{df_o}{d\alpha} = -2\sqrt{2}\cosh\alpha \sinh^2\alpha \sum_{n=1}^{\infty}\left(\frac{2n+1}{2n+3}\right)b_n - \frac{2\sqrt{2}}{3}\sinh^3\alpha \sum_{n=1}^{\infty}\frac{2n+1}{2n+3}\frac{db_n}{d\alpha}$$

Where

$$\frac{db_n}{d\alpha} = \frac{1}{(SR-TQ)}\left[\left[\frac{SdU_1}{d\alpha} - \frac{U_1 dS}{d\alpha}\right] - \left[\frac{QdU_2}{d\alpha} + \frac{U_2 dQ}{d\alpha}\right]\right] - \frac{(SU_1 - QU_2)}{(SR - TQ)^2}\left[\left[\frac{SdR}{d\alpha} + \frac{RdS}{d\alpha}\right] - \left[\frac{TdQ}{d\alpha} + \frac{QdT}{d\alpha}\right]\right]$$

$$\frac{dQ}{d\alpha} = S \quad , \quad \frac{dU_1}{d\alpha} = U_2 \quad , \quad \frac{dR}{d\alpha} = T$$

$$\frac{dS}{d\alpha} = j_n^2 \cosh(j_n\alpha) - k_n^2 \cosh(k_n\alpha)$$

$$\frac{dT}{d\alpha} = j^2 \sinh(j_n\alpha) - Pk_n^2 \sinh(k_n\alpha)$$

$$\frac{dU_2}{d\alpha} = \frac{-2\sqrt{2}}{3}\frac{n(n+1)}{(2n+1)}\left\{\left[j_n^3 e^{-j_n\alpha} - k_n^3 e^{-k_n\alpha}\right]\frac{-1}{\sinh^2\alpha}\left[-j_n e^{-j_n\alpha} + k_n e^{-k_n\alpha}\right]\right.$$

$$+\frac{2\cosh\alpha}{\sinh^3\alpha}\left[e^{-j_n\alpha} - e^{-k_n\alpha}\right] + \coth\alpha\left[j_n^2 e^{-j_n\alpha} - k_n e^{-k_n\alpha}\right]$$

$$\left.-\frac{1}{\sinh^2\alpha}\left[-j_n e^{-j_n\alpha} + k_n e^{-k_n\alpha}\right]\right\}$$

A.6.3 The factor $f_3(H)$

This factor corrects the ratio of the tangential particle velocity to the tangential fluid velocity in a linear shear flow tangent to a plane, H particle radii from the particle's surface. The factor was derived by Goldman et al. (1967). It was considered too difficult to obtain the factor analytically and initially it was found impossible to interpolate between the tabulated values presented by Goldman et al. The factor approaches

$1 - \frac{5}{16}\frac{1}{Y^3}$ as $Y \to \infty$ and the $\frac{1}{Y^3}$ term

caused the difficulty with the interpolation. The difficulty was removed when a new variable z was defined:

$$z = \frac{1}{Y^3}$$

After this transformation interpolation was satisfactory. Subroutine UCALC contained the means of generating f_3 .

A.6.4 The dimensionless radial particle velocity and its derivative

The radial velocity v^* was calculated from equation 6.14 .

$$v^* = -Y^2\left(\frac{3}{2} R + Y\right) \frac{f_1 f_2 \cos\theta}{(R + Y)^3} - \frac{4}{3} A_{kT} \frac{R}{Pe} \frac{f_1}{(Y^2 - 1)^2} \qquad (6.14)$$

The derivative $\frac{\partial v^*}{\partial H}$ was obtained by differentiation using the derivatives of f_1 and f_2 .

A.6.5 The dimensionless angular velocity and its derivative

The angular velocity u^* was calculated using equation 6.13

$$u^* = \left[\frac{3}{2} R^2 + Y\left(\frac{9}{4} R + Y\right)\right] \frac{Y f_3 \sin\theta}{(R + Y)^3} \qquad (6.13)$$

The derivative $\frac{\partial u^*}{\partial \theta}$ was given by:

$$\frac{\partial u^*}{\partial \theta} = u^* \cot\theta \qquad (A.6.9)$$

COMPUTER PROGRAMMES

Programme P 1 Calculation of rate constants from Coulter Counter data

```
      PROGRAM COULTA(INPUT,OUTPUT,TAPE5=INPUT,TAPE6=OUTPUT)
      DIMENSION G(20),S(20),AI(20),BL(20),T(20,20)
     1,TA(20,20),SIZE(20),DIF(20,20),ASIZE(20),DIFR(20,20),TIME(20)
     1,DIFLN(20,20),A(20)
      COMMON G,S,AI,BL,T,TA,SIZE,DIF,ASIZE,DIFR,TIME,DIFLN,A,M,N,
     1SUMSY,SUMY,SUMXY,SUMX,SUMSX,VAR,EROR,TOP,BOT,CALK,Z,B,C,D,R,J
C
C   READ IN THE DATA
C
      READ(5,1000) M,N
 1000 FORMAT(I3,I2)
      READ(5,1002)CALK
 1002 FORMAT(F5.2)
      READ(5,1015)(TIME(I),I=1,M)
 1015 FORMAT(6F5.2)
      READ(5,1003)(G(I),I=1,N)
 1003 FORMAT(11F7.3)
      READ(5,1004)(S(I),I=1,N)
 1004 FORMAT(11F4.1)
      READ(5,1005)(AI(I),I=1,N)
 1005 FORMAT(11F7.3)
      DO 100 I=1,N
      READ(5,1006)Z,B,C,D
 1006 FORMAT(4F7.0)
      BL(I)=0.
      IF(C.LT.0.5) BL(I)=(Z+B)/2.
C
C   AVERAGE THE BLANK COUNTS
C
      IF(C.GT.0.5)BL(I)=(Z+B+C+D)/4.
  100 CONTINUE
      DO 101 I=1,M
      DO 102 J=1,N
      READ(5,1007)Z,B,C,D
 1007 FORMAT(4F7.0)
      T(I,J)=0.
C
   AVERAGE THE RAW COUNTS
C
      IF(C.LT.0.5) T(I,J)=(Z+B)/2.
      IF(C.GT.0.5) T(I,J)=(Z+B+C+D)/4.
  102 CONTINUE
  101 CONTINUE
      DO 106 I=1,M
      DO 107 J=1,N
C
C   CORRECTED COUNTS ARE-
C
       TA(I,J) = T(I,J) - BL(J) + 2.5*(T(I,J)/1000.)**2.
  107 CONTINUE
  106 CONTINUE
      DO 108 I=1,N
      SIZE(I) = CALK*(S(I)*G(I)*AI(I))**0.3333
  108 CONTINUE
      DO 111 J = 1,10
      ASIZE(J) = (SIZE(J) + SIZE(J+1))/2.
  111 CONTINUE
      DO 109 I=1,M
      DIF(I,1)=TA(I,1)
      DO 110 J=2,N
      DIF(I,J)=TA(I,J)-TA(I,J-1)
```

```
 110 CONTINUE
 109 CONTINUE
     WRITE(6,1111)
1111 FORMAT(1X,*THE RESULTS OF THE BLANK SAMPLES*)
     DO 103 I=1,N
     WRITE(6,1009)G(I),S(I),AI(I),BL(I)
1009 FORMAT(1X,F10.3,F10.0,F10.3,F10.0/)
 103 CONTINUE
     DO 104 I=1,M
     WRITE(6,1009) TIME(I)
1009 FORMAT(1Y///1X,*THE RESULTS FOR TIME *,F6.2)
     DO 105 J=1,N
     WRITE(6,1010)G(J),S(J),AI(J),T(I,J),TA(I,J),SIZE(J),
    1DIF(I,J)
1010 FORMAT(1X,F10.3,F10.0,F10.3,2F10.0,F10.2,F10.0/)
 105 CONTINUE
 104 CONTINUE
     WRITE(6,1012)((DIF(I,J),I=1,M),J=1,N)
1012 FORMAT(9X,6F10.0/)
     DO 113 I=1,M
     DO 112 J=2,N
     IF(DIF(I,J).GT.0.) GO TO 2
     DIF(I,J)=1.
     WRITE(6,1021) ASIZE(J-1), TIME(I)
1021 FORMAT(1X,*INFINITE RATIO IN SIZE *,F6.2,* AT TIME *,F5.2)
   2 DIFR(I,J) = DIF(1,J)/DIF(I,J)
     IF(DIFR(I,J).GE.1.) GO TO 1
     WRITE(6,1016) ASIZE(J-1),TIME(I)
1016 FORMAT(1X,*ERROR IN DATA IN SIZE *,F6.2,* AT TIME *,F5.2)
     DIFR(I,J) = 1.
   1 DIFLN(I,J) = ALOG(DIFR(I,J))
 112 CONTINUE
 113 CONTINUE
     WRITE(6,1017)(TIME(I),I=1,M)
1017 FORMAT(1X,*TIME IN MINUTES*,6F10.2)
     DO 114 J = 1,10
     WRITE(6,1018) ASIZE(J)
1018 FORMAT(1X//F6.2)
     WRITE(6,1019)(DIFLN(I,J+1),I=1,M)
1019 FORMAT(16X,6F10.3)
 114 CONTINUE
     DO 118 J=2,11
     CALL GRAFIT(TIME,DIFLN(1,J),6,6,0,0)
     CALL LSQ(6,TIME,DIFLN(1,J),2,A)
     WRITE(6,1020)A(1),A(2)
1020 FORMAT(1X,*A(1)= *,F8.4,5X,*A(2)= *,F8.4)
     CALL ERROR
     WRITE(6,1040) ASIZE(J-1),A(2),R,EROR
1040 FORMAT(1X,*SIZE*,F6.2,*SLOPE*,F6.4,*CORRELATION COEFFICIENT *
    1,F3.2,*      STANDARD ERROR=  *,F6.4)
     PRINT,SUMY,SUMSY,SUMX,SUMSX,TOP,BOT,SUMXY
 118 CONTINUE
     STOP
     END
```

```
      SUBROUTINE ERROR
C    THIS ROUTINE CALCULATES THE STANDARD ERROR OF THE SLOPE
C   AND THE CORRELATION COEFICIENT
      DIMENSION G(20),S(20),AI(20),BL(20),T(20,20)
     1,TA(20,20),SIZE(20),DIF(20,20),ASIZE(20),DIFR(20,20),TIME(20)
     1,DIFLN(20,20),A(20)
      COMMON G,S,AI,BL,T,TA,SIZE,DIF,ASIZE,DIFR,TIME,DIFLN,A,M,N,
     1SUMSY,SUMY,SUMYY,SUMX,SUMSX,VAR,EROR,TOP,BOT,CALK,Z,B,C,D,R,J
      SUMX = 0.
      SUMSX= 0.
      DO 100 I=1,M
      SUMX = SUMX + TIME(I)
      SUMSX = SUMSX + TIME(I)**2.
  100 CONTINUE
      SUMSY = 0.
      SUMY  = 0.
      SUMXY = 0.
      DO 140 I=1,M
      SUMSY    =   SUMSY  +  DIFLN(I,J)**2.
      SUMY     = SUMY   +  DIFLN(I,J)
      SUMXY    =SUMXY   +  DIFLN(I,J)*TIME(I)
  140 CONTINUE
      VAR  =  ABS((SUMSY  -  A(1)*SUMY  -  A(2)*SUMXY)/4.)
      EROR       =     SQRT(VAR) /SQRT(ABS((SUMSX -(SUMX**2.)/6.)))
      TOP = SUMXY  -  (SUMX*SUMY)/6.
      BOT  =  (SUMSX -(SUMX**2.)/6.)*(SUMSY  -   (SUMY**2.)/6.)
      R    =  TOP   /SQRT(ABS(BOT))
      RETURN
      END
```

Programme P 2 Calculation of collision efficiency for a particle and a bubble

```
      PROGRAM CONT(INPUT,OUTPUT,TAPE5=INPUT,TAPE6=OUTPUT)
C
C     THIS PROGRAMME CALCULATES THE EFFICIENCY OF COLLECTION BY VISCOUS
C     AND ATTRACTIVE FORCES OF A PARTICLE BY A BUBBLE
C
      DIMENSION Y(201),YN(3),YO(3),F(201),F(201),G(201),Q(201),XB(201),H
     +B(201),UXO(4),UXN(4),CONC(21,201),NUML(21),DUDT(201),EFFIC(11)
      COMMON/MAIN/BE,THETA,V,U,DU,FF1,FF2,FF3,DFF1,DFF2,ALFA,FP,R,AKT,H,
     +DA,DETA,EL,TOR,BX,BY,M,AFF1(201),AFF2(201),ADFF1(201),ADFF2(201),N
     +PT,AALFA(201)
      COMMON W(3100)
      REAL M
C
C     READ IN THE CONTROL PARAMETERS AND PRINT THEM
C
      READ,AKT,R,FP,EL,TOR,BX,BY,M,NPT,IFLAG
      PRINT,AKT,R,FP,EL,TOR,BX,BY,M,NPT,IFLAG
      NA=20
      DETA=1./(FLOAT(NPT)-1.)
      DA=3.141592654/FLOAT(NA)
      TO=0.
C     THE BOUNDARY CONDITIONS FOR DP01A
      UXO(1)=0.
      UXO(2)=0.
      UXO(3)=1.
      UXO(4)=0.
      UXN(1)=0.
      UXN(2)=-1.
      UXN(3)=1.
      UXN(4)=0.
      UA    =0.001
      T  = 0.
      ETA=0.
      YA = UA
C     START CALCULATING THE COEFFICIENTS REQUIRED
      CALL FACT
      DO 1 I=1,NPT
      XB(I)=ETA
      IF(ETA-0.99999)2,3,3
    3 HB(I)=99
      GO TO 5
    2 HB(I)=-(1./BX)*ALOG(1.-ETA)-(1./BY)*ALOG(1.-ETA**M)
    5 CALL FUNCTS(A,B,C,D,T,ETA,IU,IDUDX)
      F(I) =B/A
      G(I)= C/A
      Q(I)=0.
    1 ETA=FLOAT(I)*DETA
      XO =0.
      XN =1.
C     BOUNDARY CONDITIONS FOR DD01A
      YO(1) =0.
      YO(2) =1.
      YO(3) =0.
      YN(1) =0.
      YN(2) =1.
      YN(3) =1.
      LIM=6
C     SOLVING THE PROBLEM AT THETA =0
      CALL DD01A(Y,XO,XN,NPT,YO,YN,F,G,Q,E,LIM,YA,NUM)
C     IS THAT ALL THATS REQUIRED ?
      IF(IFLAG.EQ.1) GO TO 6
```

```
      DO 7 I=1,NA
      DO 8 J=1,NPT
      CONC(I,J)=Y(J)
      NUML(I)=NUM
    8 CONTINUE
      NUM=0
C     SOLVE IT FOR ALL THETA
      CALL DPO1A(Y,X0,XN,NPT,TO,DA,UX0,UXN,DUDT,E,LIM,UA,NUM)
    7 CONTINUE
      DO 9 J=1,NPT
      CONC(NA+1,J)=Y(J)
    9 CONTINUE
      NUML(NA+1)=NUM
      NAP=NA/2+1
      WRITE(6,2040)(NUML(I),I=1,NAP)
      WRITE(6,2050)DA
      DO 10 J=1,NPT
      WRITE(6,2030) XB(J),HB(J),(CONC(I,J),I=1,NAP)
   10 CONTINUE
      WRITE(6,2060)DA
      WRITE(6,2040)(NUML(I),I=NAP,NA+1)
      DO 11 J=1,NPT
      WRITE(6,2030) XB(J),HB(J),(CONC(I,J),I=NAP,NA+1)
   11 CONTINUE
 2030 FORMAT(1X,/1X,13F10.4)
 2040 FORMAT(1X,*ERROR FLAGS*,8X,11I10//)
 2050 FORMAT(7X,*ETA*,8X,*H*,3X,*CONCENTRATIONS AT INTERVALS OF *,F5.2,*
     +RADIANS*)
 2060 FORMAT(7X,*ETA*,8X,*H*,3X,*CONCENTRATIONS AT INTERVALS OF *,F5.2,*
     +RADIANS, NOTE FIRST IS A REPEAT OF THE LAST ABOVE*)
      CALL HOPE(CONC,EFFIC,NA,IER)
      GO TO 14
    6 PRINT,NUM
      DO 12 J=1,NPT
      WRITE(6,2000) XB(J),HB(J),Y(J)
 2000 FORMAT(1X/1X,3F10.4)
   12 CONTINUE
   14 STOP
      END



      NOLIST
      SUBROUTINE HOPE(CONC,EFFIC,NA,IER)
C
C     THIS ROUTINE CALCULATES THE EFFICIENCY FROM THE CONCENTRATION DATA
C
      DIMENSION CONC(21,201),Y(10),Z(10),DCDE(21,11),ETAA(11),ARGI(21),V
     +ALI(21),EFFIC(11),ERROR(21)
      REAL M
      COMMON/MAIN/BE,THETA,V,U,DU,FF1,FF2,FF3,DFF1,DFF2,ALFA,FP,R,AKT,H,
     +DA,DETA,EL,TOR,BX,BY,M,AFF1(201),AFF2(201),ADFF1(201),ADFF2(201),N
     +PT,AALFA(201)
      TRPE = 2.*R/EP
      ETAA(1)=0.
      DO 1 I=2,10
      ETAA(I)=FLOAT(I-1)*DETA
    1 CONTINUE
      DO 2 I=1,20
      DO3 J=1,10
```

```
    3 Y(J) = CONC(I,J)
C   DIFFERENTIATE W.R.T. H
      CALL DET3(DETA,Y,Z,10,IER)
      DO 2 J=1,10
      DCDE(I,J)=Z(J)
      ERROR(I)=FLOAT(IER)
    2 CONTINUE
      DO 6 I=1,20
      WRITE(6,1000)(DCDE(I,J),J=1,10),ERROR(I)
 1000 FORMAT(1X/1X,10E10.4,E10.2)
    6 CONTINUE
      DO 4 J=2,10
      THETA =0.
      DO 5 I=1,20
      HB=-(1./BX)*ALOG(1.-ETAA(J))-(1./BY)*ALOG(1.-ETAA(J)**M)
      YB=HB+1.
      ALFA = ALOG(YB + SQRT((YB**2-1.)))
      CALL VCALC(YB)
      AA=BX*BY*(1.-ETAA(J))*(1.-ETAA(J)**M)
      BB=BY*(1.-ETAA(J)**M)+BX*M*(1.-ETAA(J))*ETAA(J)**(M-1.)
      DNDH=AA/BB
      ARGI(I)=(TRPE*EF1*DCDE(I,J)*DNDH - V*CONC(I,J))*SIN(THETA)
      THETA=FLOAT(I)*DA
    5 CONTINUE
C   INTEGRATE AROUND THE BUBBLE
      CALL SIMS(DA,ARGI,VALI,20)
      WRITE(6,1030)(VALI(I),I=1,11)
      WRITE(6,1030)(VALI(I),I=10,20)
 1030 FORMAT(1X//1X,11E10.6)
      EFFIC(J) = VALI(20)*2.*(1.+YB/R)**2
    4 CONTINUE
      WRITE(6,2020) BX,BY,M
 2020 FORMAT(1X//1X,*THE VALUES OF B1,B2 AND M ARE *,3F8.4)
      WRITE(6,1050) R,EP,AKT
 1050 FORMAT(1X//10X,*R=*,F10.4,5X,*PECLET NUMBER =*,F10.4,5X,*AKT =*,F1
     +0.4//)
      WRITE(6,1020)
 1020 FORMAT(1X//1X,*THE EFFICIENCY CALCULATED AT THE FIRST NINE AVAILAB
     +LE POSITIONS IS*,1X//)
      WRITE(6,1010)(EFFIC(J),J=2,10)
 1010 FORMAT(1X//1X,9E10.6)
      WRITE(6,1040)
 1040 FORMAT(1X,100(1H*),1X//)
      RETURN
      END
      SUBROUTINE SIMS(H,Y,Z,NDIM)
C     THIS SUBROUTINE COMPUTES THE VECTOR OF INTEGRAL VALUES FOR A
C     GIVEN EQUIDISTANT TABLE OF FUNCTIONAL VALUES.
C     IT BEGINS WITH Z(1)=0.0 EVALUATION OF VECTOR Z IS DONE BY MEANS
C     OF SIMPSONS RULE TOGETHER WITH NEWTONS 3/8 RULE OR A COMBINATION
C     OF THESE TWO RULES.  TRUNCATION ERRORS  OF THE ORDER H**5.
C     EXCEPT FOR Z(2) IT IS OF THE ORDER OF H**4.
C     PARAMETERS ARE AS FOLLOWS....
C     H       INCREMENT OF ARGUMENT VALUES
C     Y       INPUT VECTOR OF FUNTION VALUES
C     Z       RESULTING VECTOR OF INTEGRAL VALUES.NB. Z MAY BE IDENTICAL
C                     WITH Y
C     NDIM    DIMENSIONS OF VECTOR Z AND Y.  NO RESULT ARE POSSIBLE
C                     IF NDIM IS LESS THAN 3.....
C
C
```

```
      DIMENSION Y(21),Z(21)
      HT=0.3333333333*H
      IF(NDIM-5)7,8,1
C     IF DIMENSION IS GREATER THAN 5 PREPARE INTEGRATION LOOP
    1 SUM1=(Y(1)+4.0*Y(2)+Y(3))*HT
      AUX1=SUM1+HT*(Y(3)+4.0*Y(4)+Y(5))
      AUX2=HT*(Y(1)+3.875*(Y(2)+Y(5))+2.625*(Y(3)+Y(4))+Y(6))
      SUM2=AUX2-HT*(Y(4)+4.0*Y(5)+Y(6))
      Z(1)=0.0
      AUX=4.0*Y(3)
      Z(2)=SUM2-HT*(Y(2)+AUX+Y(4))
      Z(3)=SUM1
      Z(4)=SUM2
      IF(NDIM.LE.6) GO TO 5
      DO 4 I=7,NDIM,2
      SUM1=AUX1
      SUM2=AUX2
      AUX1=SUM1+HT*(Y(I-2)+4.0*Y(I-1)+Y(I))
      Z(I-2)=SUM1
      IF(I.GE.NDIM) GO TO 6
      AUX2=SUM2+HT*(Y(I-1)+4.0*Y(I)+Y(I+1))
    4 Z(I-1)=SUM2
    5 Z(NDIM-1)=AUX1
      Z(NDIM)=AUX2
      RETURN
    6 Z(NDIM-1)=SUM2
      Z(NDIM)=AUX1
      RETURN
C     THE END OF THE INTEGRATION LOOP
C
    7 IF(NDIM-3)12,11,8
C     SPECIAL CASE OF NDIM EQUAL TO 4 OR 5
    8 SUM2=1.125*HT*(Y(1)+3.0*(Y(2)+Y(3))+Y(4))
      SUM1=HT*(Y(1)+4.0*Y(2)+Y(3))
      Z(1)=0.0
      AUX1=4.0*Y(3)
      Z(2)=SUM2-HT*(Y(2)+AUX1+Y(4))
      IF(NDIM.LT.5) GO TO 10
      AUX1=4.0*Y(4)
      Z(5)=SUM1+HT*(Y(3)+AUX1+Y(5))
   10 Z(3)=SUM1
      Z(4)=SUM2
      RETURN
C     SPECIAL CASE OF NDIM EQUAL TO 3
C
   11 SUM1=HT*(1.25*Y(1)+2.0*Y(2)-0.25*Y(3))
      Z(1)=0.0
      Z(2)=SUM1
      Z(3)=HT*(Y(1)+4.0*Y(2)+Y(3))
   12 RETURN
      END



      SUBROUTINE FUNCTS(A,B,C,D,T,Z,IU,IDUDX)
C
C     THIS ROUTINE CALCULATES THE REQUIRED MATRIX.INDETERMINATE VALUES
C     ARE SET TO 1
C
      REAL M
```

```
      DO 1 I=2,NPT-1
      Z=FLOAT(I-1)/FLOAT(NPT-1)
      H=-(1./BX)*ALOG(1.-Z) - (1./BY)*ALOG(1.-Z**M)
      YB=H+1.
      ALFA = ALOG(YB + SQRT((YB**2-1.)))
      AALFA(I)=ALFA
      CALL F1(ALFA,FT1)
      CALL F2(ALFA,YB,FT2)
      CALL DF1(ALFA,YB,DFT1)
      CALL DF2H(ALFA,YB,DFT2)
      AFF1(I)=FT1
      AFF2(I) =FT2
      ADFF1(I)=DFT1
      ADFF2(I)=DFT2
    1 CONTINUE
      RETURN
      END



      SUBROUTINE UCALC(YA)
C
C   THIS ROUTINE CALCULATES THE ANGULAR VELOCITY AND ITS DERIVATIVE IN
C   THE ANGULAR DIRECTION
C   THE FACTOR F3 IS INTERPOLATED FROM GIVEN DATA
C   REF. A. J. GOLDMAN, ET AL., CHEM. ENG. SCI., 1967, 22, 653
C
      DIMENSION ARG(10),VAL(10),ARGP(10),VALP(10),ARGX(10)
      COMMON/MAIN/RE,THETA,V,U,DU,FF1,FF2,FF3,DFF1,DFF2,ALFA,FP,R,AKT,H,
     +DA,DETA,EL,TOR,BX,BY,M,AFF1(201),AFF2(201),ADFF1(201),ADFF2(201),N
     +PT,AALFA(201)
      DATA (ARGP(I),I=1,6)/3.7622,2.3524,1.5431,1.1276,1.0453,1.0050/
      DATA (VALP(I),I=1,6)/0.99436,0.97768,0.92185,0.76692,0.65375,0.478
     +61/
      RY = R+YA
      IF(YA-3.8)2,1,1
    1 FF3=  1.-(5./16.)/YA**3
      GO TO 4
    2 DO 3 I=1,6
      ARGX(I) = 1./(ARGP(I))**3
    3 CONTINUE
      NDIM=6
      NDIM2=6
      IROW=6
      ICOL =1
      EPS  =0.001
      Z=1./YA**3
      CALL ATSM(Z,ARGX,VALP,IROW,ICOL,ARG,VAL,NDIM2)
      CALL ALI(Z,ARG,VAL,FF3,NDIM,EPS,IER)
    4 UA =(1.5*R**2 +YA*(2.25*R + YA))
      UB = YA*FF3*SIN(THETA)/RY**3
      DUB= YA*FF3*COS(THETA)/RY**3
      U  = UA*UB
      DU = UA*DUB
      RETURN
      END
```

```
      COMMON/MAIN/BE,THETA,V,U,DU,FF1,FF2,FF3,DFF1,DFF2,ALFA,EP,R,AKT,H,
     +DA,DETA,EL,TOR,BX,BY,M,AFF1(201),AFF2(201),ADFF1(201),ADFF2(201),N
     +PT,AALFA(201)
      IF(Z.GT.0.99999) GO TO 1
    2 IF(Z.LT.0.00001) GO TO 1
      THETA=T
      H=-(1./BX)*ALOG(1.-Z)-(1./BY)*ALOG(1.-Z**M)
      YB=H+1.
      ALFA = ALOG(YB + SQRT((YB**2-1.)))
      RY=R+YB
      KNT=1
   38 KNT=KNT+1
      DIFF=ABS(AALFA(KNT)-ALFA)
      IF(DIFF.GT.1.E-9) GO TO 38
      FF1=AFF1(KNT)
      DFF1=ADFF1(KNT)
      CALL DVDH(ALFA,YB,DV)
      CALL VCALC(YB)
      CALL UCALC(YB)
C
C  FOR THE ORDINARY D.E.
C
      AA=BX*BY*(1.-Z)*(1.-Z**M)
      BB=BY*(1.-Z**M) + BX*M*(1.-Z)*Z**(M-1)
      DNDH=AA/BB
      DAADN=-BX*BY*(M*Z**(M-1)*(1.-Z) + (1.-Z**M))
      DBBDN= -M*BY*Z**(M-1) + BY*M*((M-1)*Z**(M-2)-M*Z**(M-1))
      SIMON=(BB*DAADN - AA*DBBDN)/BB**2
      CHRIS= 2.*R*FF1*SIMON*DNDH/EP
      A=(2.*R/EP)*FF1*DNDH**2
      B=((2.*R/EP)*(DFF1+ 2.*FF1/(R+YB)) -V)*DNDH + CHRIS
      C=-((2./RY)*(V+DU)+DV)
      D=0.
      IF(THETA.LT.0.00001) GO TO 3
C
C  FOR THE PARTIAL D.E.
C
      F=U/RY
      A=A/F
      B=B/F
      C=C/F
    3 RETURN
    1 A=1.
      B=1.
      C=1.
      D=0.
      RETURN
      END



      SUBROUTINE FACT
C
C   THIS ROUTINE CALCULATES THE FACTORS F1,F2, AND THEIR DERIVATIVES
C   AND STORES THE RESULTS IN LISTS
C
      REAL M
      COMMON/MAIN/BE,THETA,V,U,DU,FF1,FF2,FF3,DFF1,DFF2,ALFA,EP,R,AKT,H,
     +DA,DETA,EL,TOR,BX,BY,M,AFF1(201),AFF2(201),ADFF1(201),ADFF2(201),N
     +PT,AALFA(201)
```

```
      SUBROUTINE VCALC(YA)
      COMMON/MAIN/BE,THETA,V,U,DU,FF1,FF2,FF3,DFF1,DFF2,ALFA,EP,R,AKT,H,
     +DA,DETA,EL,TOR,BX,BY,M,AFF1(201),AFF2(201),ADFF1(201),ADFF2(201),N
     +PT,AALFA(201)
      A1 = -(YA**2*(1.5*R + YA))
      KNT=1
   38 KNT=KNT+1
      DIFF=ABS(AALFA(KNT)-ALFA)
      IF(DIFF.GT.1.E-9) GO TO 38
      FF1=AFF1(KNT)
      FF2=AFF2(KNT)
      B1=FF1*FF2*COS(THETA)/(R+YA)**3
      C1=(4./3.)*AKT*(R/EP)*FF1/(YA**2-1.)**2
      D1=FF1*(EL*TOR*R/EP)*EXP(-TOR*H)/(1.+EXP(-TOR*H))
      V=A1*B1-C1+D1
      RETURN
      END



      SUBROUTINE DVDH(A,YA,DV)
C
C  THIS ROUTINE CALCULATES THE DERIVATIVE OF THE RADIAL VELOCITY
C
      COMMON/MAIN/BE,THETA,V,U,DU,FF1,FF2,FF3,DFF1,DFF2,ALFA,EP,R,AKT,H,
     +DA,DETA,EL,TOR,BX,BY,M,AFF1(201),AFF2(201),ADFF1(201),ADFF2(201),N
     +PT,AALFA(201)
      KNT=1
   38 KNT=KNT+1
      DIFF=ABS(AALFA(KNT)-ALFA)
      IF(DIFF.GT.1.E-9) GO TO 38
      FF1=AFF1(KNT)
      FF2=AFF2(KNT)
      DFF1=ADFF1(KNT)
      DFF2=ADFF2(KNT)
      VA = -((3./2.)*YA**2*R + YA**3)
      VB = FF1
      VC=FF2*COS(THETA)
      DVADH = -(3.*YA*R +3.*YA**2)
      DVBDH = DFF1
      DVCDH = DFF2*COS(THETA)
      RY = (R+YA)
      FK = RY**3*(VA*VB*DVCDH +VB*VC*DVADH +VA*VC*DVBDH)
      FL = VA*VB*VC*3.*RY**2
      DV1=(FK -FL)/RY**6
      FM = -((4./3.)*AKT*R/EP)
      YB = (YA**2 - 1.)
      DV2 = FM*(YB**2*DFF1  - 4.*FF1*YB*YA)/YB**4
      DFEL=EL*TOR*(R/EP)*(DFF1*EXP(-TOR*H)/(1.+EXP(-TOR*H))-TOR*FF1*EXP(
     +        -TOR*H)/(1.+EXP(-TOR*H))**2)
      DV=DV1+DV2+DFEL
      RETURN
      END
```

```
      SUBROUTINE DF2H(A,YA,DF2DH)
C
C  THIS ROUTINE CALCULATES THE DERIVATIVE OF THE FACTOR F2
C
      Z=-(SQRT(8./9.))*SINH(A)**3
      EF2= 0.
      FI = 0.
      DADH = 1./(SQRT(YA**2 - 1.))
      N=0
    1 N=N+1
      AN = FLOAT(N)
      AJ = AN - .5
      AK = AN + 1.5
      P=AJ/AK
      B1 = -(SQRT(8./9.))*(AN*(AN + 1.)/(2.*AN+1.))
      COSHA = COSH(A)
      SINHA = SINH(A)
      EXPJA = EXP(-AJ*A)
      EXPKA = EXP(-AK*A)
      COSHJ = COSH(AJ*A)
      COSHK = COSH(AK*A)
      SINHJ = SINH(AJ*A)
      SINHK = SINH(AK*A)
      B2 = AJ*EXPJA - AK*EXPKA
      B3 = (COSHA/SINHA)*(EXPJA - EXPKA)
      U1=B1*(B2 + B3)
      C1 = -AJ**2*EXPJA + AK**2*EXPKA
      C2 = (EXPJA - EXPKA)/SINHA**2
      C3 = (-AJ*EXPJA + AK*EXPKA)*COSHA/SINHA
      U2= B1*(C1-C2 + C3)
      Q = COSHJ - COSHK
      R = SINHJ - P*SINHK
      S = AJ*SINHJ - AK*SINHK
      T = AJ*COSHJ - P*AK*COSHK
      BN = (S*U1 - Q*U2)/(S*R - T*Q)
      E = ((2.*AN + 1.)/(2.*AN + 3.))*BN
      FA = Z*E
      VDU = -SQRT(8.)*SINHA**2*COSHA*E
      DSDA = AJ**2*COSHJ - AK**2*COSHK
      DTDA = AJ**2*SINHJ - P*AK**2*SINHK
      DB1 = AJ**3*EXPJA - AK**3*EXPKA
      DB2 = 2.*(COSHA/SINHA**3)*(EXPJA - EXPKA)
      DB3 = (-AJ*EXPJA + AK*EXPKA)/SINHA**2
      DB4 = (-AJ*EXPJA + AK*EXPKA)/SINHA**2
      DB5 = (AJ**2*EXPJA - AK**2*EXPKA)*COSHA/SINHA
      DU2   = B1*(DB1 + DB2 - DB3 -DB4 +DB5)
      FF=((U1*DSDA + S*U2) -(U2*S + Q*DU2))*(S*R - T*Q)
      FH =Z*((2.*AN+1.)/(2.*AN+3.))/(S*R -T*Q)**2
      FG =(U1*S - U2*Q)*((S*T + R*DSDA)-(T*S + Q*DTDA))
      UDV = FH*(FF - FG)
      DF2 =VDU+UDV
      EF2 =EF2 +FA
      FI = FI +DF2
      IF(N - 500)2,2,3
    2 IF((FA.LT.0.00001).AND.(DF2.LT.0.00001)) GO TO 4
      GO TO 1
    3 WRITE(6,1000) N
 1000 FORMAT(1X,//1X,*THE REQUIRED ACCURACY FOR DF2DH COULD NOT BE REACH
     +ED AFTER*,I4,* TERMS*)
    4 DF2DH =(-2.*EF2/YA**3 +  FI*DADH/YA**2)
      RETURN
      END
```

```
      SUBROUTINE DF1(A,YA,DFDH)
C     THIS ROUTINE CALCULATES THE DERIVATIVE OF THE FACTOR F1 GIVEN THE
C     VALVE ALFA AND THE DISTANCE YA
      CALL F1(A,ATOT)
      DFDL = -(ATOT**2)
      N=0
      AA = 0.
      AB = 0.
C     START SUMMING THE TERMS
    1 N = N + 1
      AN = FLOAT(N)
      DADH  =1./(SQRT(YA**2 - 1.))
      W = AN*(AN + 1.)/((2.*AN - 1.)*(2.*AN + 3.))
      BINUM =2.*SINH((2.*AN+1.)*A) + (2.*AN+1.)*SINH(2.*A)
      BIDEN =4.*((SINH((AN + .5)*A))**2)-((2.*AN+1.)**2)*(SINH(A)**2)
      DNUM=(4.*AN+2.)*COSH((2.*AN + 1.)*A) +(4.*AN+2.)*COSH(2.*A)
      DDEN = (4.*AN+2.)*SINH((2.*AN+1.)*A) -((2.*AN+1.)**2)*SINH(2.*A)
      BI = BINUM/BIDEN -1.
      ABI = W*BI
      FB = ABI*(4./3.)*COSH(A)
      AA = AA + FB
      ABJ= W*(BIDEN*DNUM - BINUM*DDEN)/BIDEN**2
      FC = ABJ*(4./3.)*SINH(A)
      AB = AB +FC
      IF(500-N)3,3,2
C     CHECKING TO SEE THAT THE REQUIRED ACCURACY HAS BEEN REACHED
    2 IF((FB.LT.0.00001).AND.(FC.LT.0.00001)) GO TO 4
      GO TO 1
    3 WRITE(6,1000)N
 1000 FORMAT(1X,//1X,*MORE THAN *,I5,* TERMS WERE NEEDED*//1X,)
C     AFTER ADDING THE REQUIRED NUMBER OF TERMS THE FINAL RESULT IS
C     CALCULATED DF1DH = DFDL*FLOA*DADH
C     AA+AB IS EQUAL TO DLDA
    4 DFDH = DFDL*DADH*(AA + AB)
      RETURN
      END



      SUBROUTINE F1(A,ATOT)
C     ..................................................................
C         SUBROUTINE F1
C
C         PURPOSE
C           THIS ROUTINE CALCULATES THE FACTOR F1 WHICH CORRECTS THE
C           STOKES EQUATION NEAR A SOLID OBJECT
C
C         USAGE
C            CALL F1(A,ATOT)
C
C         DECRIPTION OF PARAMETERS
C           A      -THE FACTOR ALPHA =LN(YA + SQRT((YA)**2 -.))
C           ATOT   -THE FACTOR F1
C
C         METHOD
C           CALCULATED FROM BRENNER H.  CHEM.ENG.SCI. 16 +242
C           F1 IS CALCULATED FROM A SERIES.THE SERIES IS TERMINATED
C           WHEN THE CONTRIBUTION OF THE TERM IS LESS THAN 0.00001
```

```
C     ..................................................................
      ATOT = 0.
      N=0
C
C**** START TO CALCULATE TERMS
C
    1 N = N + 1
      AN = FLOAT(N)
      W = AN*(AN + 1.)/((2.*AN-1.)*(2.*AN+3.))
      BTNUM = 2.*SINH((2.*AN+1.)*A) + (2.*AN+1.)*SINH(2.*A)
      BIDEN = 4.*(SINH((AN+.5)*A))**2)-((2.*AN+1.)**2)*(SINH(A)**2)
      BI = BTNUM/BIDEN - 1.
      ABI = W*BI
      FA = ABI*(4./3.)*SINH(A)
      ATOT = ATOT + FA
C
CXXXX IS THE CONTRIBUTION OF THIS TERM LESS THAN 0.00001
C
      IF(500 - N)3,3,2
    2 IF(FA - 0.00001)4,1,1
    3 WRITE(6,1000)
 1000 FORMAT(1X//*THE NUMBER OF TERMS WAS GREATER THAN 500*//)
    4 ATOT = 1./ATOT
      RETURN
      END



      SUBROUTINE F2(A,YA,FE2)
C
C  THIS ROUTINE CALCULATES THE FACTOR F2
C  REF. S. L. GOREN AND M. E. ONEILL, CHEM. ENG. SCI., 1971, 26, 325
C  NOTE ERROR NEAR EQUN 3.14
C
      IF(YA.LT.1.001) GO TO 5
      Z=-(SQRT(8./9.))*SINH(A)**3
      N=0
      EF2=0.
    1 N=N+1
      AN = FLOAT(N)
      AJ = AN - .5
      AK = AN + 1.5
      P=AJ/AK
      B1 = -(SQRT(8./9.))*(AN*(AN + 1.)/(2.*AN+1.))
      COSHA = COSH(A)
      SINHK = SINH(AK*A)
      SINHJ = SINH(AJ*A)
      COSHK = COSH(AK*A)
      COSHJ = COSH(AJ*A)
      EXPKA = EXP(-AK*A)
      EXPJA = EXP(-AJ*A)
      SINHA = SINH(A)
      B2 = AJ*EXPJA - AK*EXPKA
      B3 = (COSHA/SINHA)*(EXPJA - EXPKA)
      U1=B1*(B2 + B3)
      C1 = -AJ**2*EXPJA + AK**2*EXPKA
      C2 = (EXPJA - EXPKA)/SINHA**2
      C3 = (-AJ*EXPJA + AK*EXPKA)*COSHA/SINHA
      U2= B1*(C1-C2 + C3)
      Q = COSHJ - COSHK
      R = SINHJ - P*SINHK
      S = AJ*SINHJ - AK*SINHK
      T = AJ*COSHJ - P*AK*COSHK
      BN = (S*U1 - Q*U2)/(S*R - T*Q)
      E = ((2.*AN + 1.)/(2.*AN + 3.))*BN
      FA = Z*E
      EF2 = EF2 + FA
      FE2 = EF2/(YA**2)
      IF(N-500)2,2,3
    2 IF(FA-0.00001)4,4,1
    3 WRITE(6,1002) N
 1002 FORMAT(1X/1X,*THE REQUIRED ACCURACY COULD NOT BE REACHED AFTER*,I4
     1,* ITERATIONS*)
      GO TO 4
    5 FE2 = 3.2295
    4 RETURN
      END
```

REFERENCES

Almond, J.K.,
"Possible applications of high frequency vibrations in froth flotation", Ph.D. Thesis, University of London, (1955)

Arbiter, N.,
Trans. A.I.M.E., 190, p791, (1954)

Bach, N., and Gilman, A.,
Acta Physicochimica U.R.S.S., 9, p27, (1938)

Bakker, C.A.P., van Buytenen, P.M., and Beek, W.J.,
Chem. Eng. Sci., 21, p1039, (1966)

Barry, A.I.,
Chemical Engineering, 58, p107, (1951)

Bird, R.B., Stewart, W.E., and Lightfoot, E.N.,
"Transport phenomena", Wiley, N.Y., (1960)

Blake, T.D., and Kitchener, J.A.,
J. Chem. Soc. Far. Trans., I, 68, p1435, (1972)

Bogdanov, O.S., Kizevalter, B.V., and Khayman, V.Ya.,
Non-ferr. Metals Moscow, 4, (1954)
(quoted by Klassen and Mokrousov)

Bratby, J., and Marais, G.V.R.,
Filtr. and Sep., Nov/Dec., p614, (1974)

Brenner, H.,
Chem. Eng. Sci., 16, p242, (1961)

Brown, D.J.,
In "Aerodynamic capture of particles",Ed. E.G. Richardson, Pergamon, London, (1960)

Burman, J.E.,
"Bubble growth in supersaturated solution", Ph.D. Thesis, University of London, (1974)

Bushell, C.H.G.,
Trans. A.I.M.E., 223, p266, (1962)

Cassell, E.A., Matijevic, E., Francis, J.M., and others,
A.I.Ch. E.J., 17, p1486, (1971)

CERN CERN Subroutine Library, (1975)

Chatfield, C.,
"Statistics for technology", Penguin, (1970)

Churaev, N.V.,
Coll. J. U.S.S.R., (trans), 34, p851, (1972)

Cichos, C.,
Freiberg Forschungsh, A, 513, p7, (1973)

Connor, P., and Ottewill, R.H.,
J. of Colloid and Interface Sci., 37(3), p642, (1971)

Cornish, R.J.,
Proc. Roy. Soc. London, Ser. A, 120, p691, (1928)

Coulter Counter ZB Manual,
"Instruction manual for Coulter Counter model ZB (industrial), Second edition, Coulter Electronics, (1973)

De Bruyn, H.J., and Modi, H.J.,
Trans. A.I.M.E., 205, p415, (1956)

Derjaguin, B.V., and Dukhin, S.S.,
Trans. I.M.M., 70, p221, (1961)

Derjaguin, B.V., and Shukakidse, N.D.,
Trans. I.M.M., 70, p569, (1961)

DeVivo, D.G., and Karger, B.L.,
Sep. Sci., 5, p145, (1970)

Dibbs, H.P., Sirois, L.L., and Bredin, R.,
"The role of gas bubbles in the flotation of quartz", Research report No. R248, Dept. of Energy, Mines and Resources, Mines Branch, Ottawa, Canada, Information Canada, (1972)

Dukhin, S.S., and Derjaguin, B.V.,
In "Surface and colloid science", John Wiley, New York, (1974)

Evans, L.F.,
Ind. Eng. Chem., 46, p2420, (1954)

Fitzpatrick, J.A., and Spielman, L.A.,
J. of Colloid and Interface Sci., 43, p350, (1973)

Flint, L.R.,
(1971) "Bubble column flotation", Ph.D. Thesis, University of Queensland, Australia, (1971)

Flint, L.R.,
(1973) Miner. Sci. Engng., 5, p232, (1973)

Flint, L.R., and Howarth, W.J.,
Chem. Eng. Sci., 26, p1155, (1971)

Fonda, A., and Herne, H.,
Mining Research Establishment Report, No. 2068, Scientific Dept., National Coal Board, (1957)

Fowkes, F.M.,
Adv. Chem. Ser., 43, p99, (1964)

Fox, L.,
Proc. Roy. Soc., A, 190, p31, (1947)

Gaudin, A.M., Schuhmann, R., and Schlechten, A.W.,
J. Phys. Chem., 46, p901, (1942)

Goldman, A.J., Cox, R.G., and Brenner, H.,
Chem. Eng. Sci.,22, p653, (1967)

Goren, S.L., and O'Neill, M.E.,
Chem. Eng. Sci., 26, p325, (1971)

Grieves, R.B., and Bewley, J.L.,
Can. J. Chem. Eng., 50, p261, (1972)

Hamaker, H.C.,
Physica, 4, p1058, (1937)

Harper, J.F.,
Adv. in Appl. Mech., 12, p59, (1972)

Hauser, E.A., and Niles, G.E.,
J. Phys. Chem., 45, p954, (1941)

Hocking, L.M.,
Intern. J. Air Pollution, 13, p154, (1960)

Hogg, R., Healey, T.W., and Fuerstenau, D.W.,
Trans. Faraday Soc., 62(1), p638, (1966)

Israelachvili, J.N., and Tabor, D.,
In "Progress in surface and membrane science", Vol 7,
Academic Press, London, (1973)

Ives, K.J., and Gregory, J.,
J. Proc. Soc. Water Treat. Exam., 15, p93, (1966)

Jaycock, M.J., and Ottewill, R.H.,
Trans. I.M.M., 72, p497, (1963)

Kalman, K.S.,
Ph.D. Thesis, McGill University, Montreal, Canada,
(quoted by Reay and Ratcliff (1974))

Kar, G., Chandler, S., and Mika, T.S.,
J. of Colloid and Interface Sci., 44, p347, (1973)

Kaufmann, K.M.,
M. Eng. Thesis, Clarkson College of Technology, N.Y.
(quoted by Reay and Ratcliff (1974))

Kitchener, J.A.,
(1974) Minerals Sci. Engng., 6, p27, (1974)

Kitchener, J.A.,
(1975) Private communication (1975)

Klassen, V.I., and Mokrousov, V.A.,
"An introduction to the theory of flotation",
Butterworths, London, (1963)

Krupp, H., Schnabel, W., and Walter, G.,
J. of Colloid and Interface Sci., 39, p421, (1972)

Kruyt, H.R.(ed),
"Colloid science", Vol 1, Elsevier, Amsterdam, (1952)

Kuhn, A.,
Chemical Processing, June and July, pp9, 5 resp,(1974)

Langbein, D.,
J. Adhes., 1, p237, (1969)

Laskowski, J., and Kitchener, J.A.,
J. of Colloid and Interface Sci., 29, p670, (1969)

Lemlich, R.,
(1966) Chem. Eng., 73, p7, (1966)

Lemlich, R.,
(1968) In "Progress in separation and purification", Ed. E.S. Perry, Interscience, N.Y., (1968)

Lemlich, R.(ed.),
(1972) "Adsorptive bubble separation techniques",Academic Press, London, (1972)

Levich, V.G.,
"Physicochemical hydrodynamics", Prentice-Hall, New Jersey, (1962)

Levy, H., and Baggott, E.A.,
"Numerical solutions of differential equations", Dover, (1950)

Lifshitz, E.M.,
Sov. Phys. J.E.T.P., 2, p73, (1956)

Lovell, V.M.,
Minerals Sci. Engng., 6, p176, (1974)

Lyman, G.J.,
"The gas bubble in flotation: a preliminary study of the Dorn effect for gas bubbles", M.E. Thesis, McGill University, Montreal, Canada, (1974)

McTaggart, H.A.,
Phil. Mag., 44, p386, (1922)

Morris, T.M.,
Trans. A.I.M.E., 193, p794, (1952)

Napper, D.H.,
Ind. Eng. Chem. Prod. Res. Devel., 9, p467, (1970)

Nilsson, G.,
J. Phys. Chem., 61, p1135, (1957)

O'Neill, M.E.,
Private communication (1975)

Ottewill, R.H., and Walker, T.,
Trans. Faraday Soc.,5(1), p917, (1974)

Parsegian, V.A., and Ninham, B.W.,
(1970) Biophys. J., 10, p664, (1970)

Parsegian, V.A., and Ninham, B.W.,
(1971) J. of Colloid and Interface Sci., 37, p332, (1971)

Perry, J.H.(ed.),
"Chemical engineer's handbook", 4th. Ed., McGraw-Hill, N.Y., (1963)

Pethica, B.A.,
Trans. Faraday Soc., 50, p413, (1954)

Prieve, D.C., and Ruckenstein, E.,
A.I.Ch.E.J., 20, p1178, (1974)

Rao, S.R.,
Minerals Sci. Engng., 6, p45, (1974)

Read, A.D., and Kitchener, J.A.,
(1967) Soc. Chem. Ind. Monograph No. 25, p300, London, (1967)

Read, A.D., and Kitchener, J.A.,
(1969) J. of Colloid and Interface Sci., 30, p391, (1969)

Reay, D.;
(1973) "Removal of fine particles from water by dispersed air flotation", Ph.D. Thesis, McGill University, Montreal, Canada, (1973)

Reay, D.,
(1974) Private communication (1974)

Reay, D., and Ratcliff, G.A.,
(1973) Can. J. Chem. Eng., 51, p178, (1973)

Reay, D., and Ratcliff, G.A.,
(1974) to be published.

Richards, W.N.,
"Aspects of flotation as a water treatment process", M.Phil. Thesis, University of London, (1975)

Rubin, A.J., and Johnson, J.D.,
Anal. Chem., 39, p298, (1967)

Rubin, E., and Jorne, J.,
J. Ind. Eng. Chem. Fund., 8, p474, (1969)

Samygin, V.D., Derjaguin, B.V., and Dukhin, S.S.,
Koll. Zh., 26, p424, (1964)

Scott, A.B., and Tatar, H.V.,
J. Am. Chem. Soc., 65, p692, (1943)

Shafrir, U., and Neiburger, N.,
"Collision efficiencies of two spheres falling in a viscous medium for Reynolds numbers up to 19.2", University of California Press, (1964)

Shaw, D.J.,
"Electrophoresis", Academic Press, London, (1969)

Sheiham, I.,
"A study of some aspects of the flotation of precipitates, colloids and collectors", Ph.D. Thesis, University of Witwatersrand, South Africa, (1970)

Sheiham, I., and Pinfold, T.A.,
Analyst, 94, p387, (1969)

Sheiham, I., and Pinfold, T.A.,
Sep. Sci., 7, p25, (1972)

Shelton, R.S., Van Campen, M.G., Tilford, C.H., and others,
J.Am. Chem. Soc., 68, p753, (1946)

Smith, G.D.,
"Numerical solution of partial differential equations", O.U.P., London, (1969)

Somasundaran, P.,
Sepn. and Purfn. Methods, 1, p117, (1972)

Spielman, L.A., and Cukor, P.M.,
J. of Colloid and Interface Sci., 43, p51, (1973)

Spielman, L.A., and Fitzpatrick, J.A.,
J. of Colloid and Interface Sci., 42, p607, (1973)

Spielman, L.A., and Goren, S.L.,
Environmental Sci. Tech., 4, p135, (1970)

Sutherland, K.L.,
J. Phys. Chem., 52, p394, (1948)

Sutherland, K.L., and Wark, I.W.,
"Principles of flotation", Australasian Institute of Mining and Metallurgy, Melbourne, (1955)

Taggart, A.F.,
"Handbook of mineral dressing", Wiley, N.Y., (1945)

Tomlinson, H.S., and Fleming, M.G.,
In "Mineral processing", A. Roberts Ed., Pergamon, London, (1963)

United Kingdom Atomic Energy Authority,
Harwell Subroutine Library,- a catalogue of subroutines (1973) HMSO/AERE R7477 .

Van Gils, G.E., and Kruyt, H.R.,
Kolloid Beihefte, 45, p60, (1936)

Visser, J.,
Advances in Colloid and Interface Science, 3, p331, (1972)

Watson, D., and Grainger-Allen, T.J.N.,
Trans. Instn. Min. Metal, Sec. C, 82, pC103, (1973)

Wiersema, P.H., Loeb, A.L., and Overbeek, J.T.G.,
J. of Colloid and Interface Sci., 22, p78, (1966)

Yao, M., Habibian, M.T., and O'Melia, C.R.,
Environmental Sci. Tech., 5, p1105, (1971)

LIST OF SYMBOLS

The following is a list of symbols used in the theoretical work of Chapter 6, including some of the more important symbols used elsewhere.

a	radius of sphere, cm
a_b	bubble radius, cm
a_p	particle radius, cm
A	Hamaker constant or effective Hamaker constant, ergs
A_{ijk}	Hamaker constant for interaction of media i and k through medium j, ergs
A_{kT}	A/kT
b, b_1 b_2, m	expansion parameter for the transformation of the radial coordinate
c	local concentration, particles/cm^3
c_∞	concentration of particles far from the bubble, particles/cm^3
C^*	c/c_∞
d_p	diameter of particle, cm
D	local diffusion coefficient, cm^2/sec
D_∞	diffusion coefficient far from the bubble, cm^2/sec
E	collection efficiency
E_a	adhesion efficiency
E_c	collision efficiency
f_1, f_2 f_3	hydrodynamic correction factors
h	minimum separation between particle and bubble surfaces, cm
H	h/a_p
I	rate of deposition, particles/sec
k	Boltzmann's constant, ergs/^{o}K
k_p	first order rate constant, min^{-1}

$m(H)$	local particle mobility coefficient, cm/dyne-sec
m_∞	mobility coefficient far from the bubble, cm/dyne-sec
N_r	radial particle flux, particles/cm^2-sec
N_t	No. of particles/experimental volume at time t
N_θ	angular particle flux, particles/cm^2-sec
Pe	Péclet number = $2a_b U/D_\infty$
r	radial coordinate
R	a_b/a_p
Re	Reynolds number $2a_b \rho_f U/\eta_f$
s_r	radial fluid velocity, cm/sec
s_θ	angular fluid velocity, cm/sec
t	time
T	absolute temperature ^oK
U	bubble terminal velocity, cm/sec
U_E	particle electromobility, microns/sec/Volt/cm
u*	v_θ/U
v_r	radial particle velocity, cm/sec
v_θ	angular particle velocity, cm/sec
v*	v_r/U
V_{DL}	potential of the double layer, ergs
V_v	potential due to van der Waals dispersion forces, ergs
y	minimum distance between particle centre and bubble surface,
Y	H + 1

Greek symbols

α	adsorption depth, cm
γ	surface tension, dynes/cm

Γ	surface excess, moles/cm^2
ε	dielectric constant
$\varepsilon(i\xi)$	dielectric permittivity of an interacting body at the imaginary frequency $i\xi$
ζ	zeta potential, mV
η	transformed radial coordinate
η_f	fluid viscosity, poise
θ	angular coordinate
κ	reciprocal double layer thickness, cm^{-1}
Π	disjoining pressure
Π_{DL}	double layer contribution to disjoining pressure
Π_V	van der Waals contribution to disjoining pressure
Π_S	specific surface contribution to disjoining pressure includes all interactions not accounted for by Π_{DL} or Π_V
ρ_f	fluid density, gms/cm^3
ρ_p	particle density gms/cm^3
Ψ	surface potential
